On optimal tests for rotational symmetry against new classes of hyperspherical distributions

Eduardo García-Portugués

Department of Statistics
Carlos III University of Madrid
Calle Madrid, 126
28903 Getafe (Madrid), Spain

Davy Paindaveine

Département de Mathématique and ECARES
Université Libre de Bruxelles
Avenue F.D. Roosevelt, 50
ECARES, CP114/04
B-1050 Bruxelles, Belgium

Thomas Verdebout

Département de Mathématique and ECARES
Université Libre de Bruxelles
Avenue F.D. Roosevelt, 50
ECARES, CP114/04
B-1050 Bruxelles, Belgium

Summary. Motivated by the central role played by rotationally symmetric distributions in directional statistics, we consider the problem of testing rotational symmetry on the hypersphere. We adopt a semiparametric approach and tackle the situations where the location of the symmetry axis is either specified or unspecified. For each problem, we define two tests and study their asymptotic properties under very mild conditions. We introduce two new classes of directional distributions that extend the rotationally symmetric class and are of independent interest. We prove that each test is locally asymptotically maximin, in the Le Cam sense, for one kind of the alternatives given by the new classes of distributions, both for specified and unspecified symmetry axis. The tests, aimed to detect location-like and scatter-like alternatives, are combined into a convenient hybrid test that is consistent against both alternatives. A Monte Carlo study illustrates the finite-sample performances of the tests and corroborates empirically the theoretical findings. Finally, we apply the tests for assessing rotational symmetry in two real data examples coming from geology and proteomics.

1. Introduction

Directional statistics deals with data belonging to the unit hypersphere $\mathcal{S}^{p-1} := \{\mathbf{x} \in \mathbb{R}^p : \|\mathbf{x}\|^2 = \mathbf{x}'\mathbf{x} = 1\}$ of $\mathbb{R}^p$. The most popular parametric model in directional statistics, which can be traced back to the beginning of the 20th century, is the von Mises–Fisher (vMF) model characterized by the density (densities on $\mathcal{S}^{p-1}$ throughout are with respect to the surface area measure σ_{p-1} on $\mathcal{S}^{p-1}$)

$$\mathbf{x} \mapsto c_{p,\kappa}^{\mathcal{M}} \exp(\kappa\, \mathbf{x}'\boldsymbol{\theta}),$$

where $\boldsymbol{\theta} \in \mathcal{S}^{p-1}$ is a location parameter (it is the modal location on the sphere), $\kappa > 0$ is a concentration parameter (the larger the value of κ, the more the probability mass is concentrated about $\boldsymbol{\theta}$), and $c_{p,\kappa}^{\mathcal{M}}$ is a normalizing constant to be specified later. The vMF model belongs to a much broader model comprised by *rotationally symmetric* densities of the form

$$\mathbf{x} \mapsto c_{p,g}\, g(\mathbf{x}'\boldsymbol{\theta}),$$

where $g : [-1, 1] \longrightarrow \mathbb{R}^+$ and $c_{p,g}$ is a normalizing constant. The rotationally symmetric model is indexed by the finite-dimensional parameter $\boldsymbol{\theta}$ and the infinite-dimensional parameter g, hence is of a semiparametric nature. Clearly, the (parametric) vMF submodel is obtained with $g(t) = \exp(\kappa t)$. Note that for axial distributions ($g(-t) = g(t)$ for any t), only the pair $\{\pm\boldsymbol{\theta}\}$ is identified, whereas non-axial distributions allow to identify $\boldsymbol{\theta}$ under mild conditions (identifiability of $\boldsymbol{\theta}$ is discussed later in the paper). Rotationally symmetric distributions are often regarded as the most natural (non-uniform) distributions on the sphere and tend to have more tractable normalizing constants than non-rotationally symmetric models. Yet, since these distributions impose a rather stringent symmetry on the hypersphere (as they are invariant under rotations fixing $\boldsymbol{\theta}$), it is natural to test for rotational symmetry prior to adopt any rotationally symmetric model to conduct inference.

The problem of testing rotational symmetry has mainly been considered in the circular case ($p = 2$), where rotational symmetry is referred to as *reflective symmetry*. Tests of reflective symmetry about a specified $\boldsymbol{\theta}$ have been considered by Schach (1969), using a linear rank test, and Mardia and Jupp (2000), using sign-based statistics, whereas Pewsey (2002) introduced a test based on second-order trigonometric moments for unspecified $\boldsymbol{\theta}$. Ley and Verdebout (2014) and Meintanis and Verdebout (2016) developed tests that are locally and asymptotically optimal against some specific alternatives, both for specified $\boldsymbol{\theta}$. For $p \geq 3$, however, the problem is more difficult, which explains that the corresponding literature is much sparser. To the best of our knowledge, for $p \geq 3$, only Jupp and Spurr (1983) and Ley and Verdebout (2017b) addressed the problem of testing rotational symmetry in a *semiparametric* way (that is, without specifying the function g). The former considered a test for symmetry in $p \geq 2$ using the Sobolev tests machinery of Giné (1975), whereas the latter established the efficiency of the Watson (1983)'s test against a new type of non-rotationally symmetric alternatives. Both papers considered only the specified-$\boldsymbol{\theta}$ situation. Goodness-of-fit tests within the directional framework (*i.e.*, tests for checking that the underlying distribution on the hypersphere belongs to a given parametric class of distributions) have received comparatively more attention in the literature. For instance, Boulerice and Ducharme (1997) proposed goodness-of-fit tests based on spherical harmonics for a class of rotationally symmetric distributions. More recently, Figueiredo (2012) considered goodness-of-fit tests for vMF distributions, while Boente et al. (2014) introduced goodness-of-fit tests based on kernel density estimation for any (possibly non-rotationally symmetric) distribution.

In this paper, we consider the problem of testing rotational symmetry on the sphere or hypersphere ($p \geq 3$). The contributions are three-fold. Firstly, we tackle the specified-$\boldsymbol{\theta}$ case and propose two tests aimed to detect *scatter*-like and *location*-like departures from the null. Secondly, we introduce two new classes $\mathcal{C}_1$ and $\mathcal{C}_2$ of distributions on $\mathcal{S}^{p-1}$ that are of independent interest and may serve as natural alternatives to rotational symmetry. In particular, the class $\mathcal{C}_1$ is an "elliptical" extension of the class of rotationally symmetric distributions based on the angular Gaussian distributions from Tyler (1987). We prove that the proposed scatter and location tests are locally asymptotically maximin against alternatives in $\mathcal{C}_1$ and $\mathcal{C}_2$, respectively. Thirdly, we address the more challenging unspecified-$\boldsymbol{\theta}$ case. The scatter test is seen to be unaffected asymptotically by the estimation of $\boldsymbol{\theta}$ under the null (and therefore under contiguous alternatives), whereas the location test presents a more involved asymptotic behaviour affected by the estimation of $\boldsymbol{\theta}$. We therefore propose corrected versions of the location tests that keep optimality properties against alternatives in $\mathcal{C}_2$. Finally, using the asymptotic independence between the location and scatter test statistics, we introduce hybrid tests for the specified and unspecified-$\boldsymbol{\theta}$ problems that enjoy appealing asymptotic power properties against both types of alternatives (in $\mathcal{C}_1$ and $\mathcal{C}_2$) without being optimal neither against alternatives in $\mathcal{C}_1$ nor in $\mathcal{C}_2$.

The outline of the paper is as follows. In Section 2 we address the testing for rotational symmetry with $\boldsymbol{\theta}$ specified. The asymptotic distributions of two tests proposed for that aim are provided in Section 2.1. Section 2.2 gives two non-rotationally symmetric extensions of the class of rotationally symmetric distributions, used in Sections 2.3–2.4 to investigate the non-null asymptotic behaviour of the proposed tests. In Section 3, we extend the proposed tests to the problem of testing rotational symmetry about an unspecified location and investigate their non-null asymptotic behaviour. Hybrid tests are introduced in Section 4. In Section 5, we conduct Monte Carlo experiments to study how well the finite-sample behaviour of the proposed tests agrees with our asymptotic results. We treat two real data examples in Section 6 and discuss perspectives for future research in Section 7. Appendix A collects the proofs of the main results, whereas Appendix B provides useful lemmas.

2. Testing rotational symmetry about a specified θ

A random vector $\mathbf{X}$, with values in $\mathcal{S}^{p-1}$, is said to be *rotationally symmetric* about $\boldsymbol{\theta} \in \mathcal{S}^{p-1}$ if and only if $\mathbf{OX} \stackrel{\mathcal{D}}{=} \mathbf{X}$ for any $p \times p$ orthogonal matrix $\mathbf{O}$ satisfying $\mathbf{O}\boldsymbol{\theta} = \boldsymbol{\theta}$ (throughout, $\stackrel{\mathcal{D}}{=}$ denotes equality in distribution). For any $\mathbf{x} \in \mathcal{S}^{p-1}$, write

$$v_{\boldsymbol{\theta}}(\mathbf{x}) := \mathbf{x}'\boldsymbol{\theta} \qquad \text{and} \qquad \mathbf{u}_{\boldsymbol{\theta}}(\mathbf{x}) := \frac{\boldsymbol{\Gamma}'_{\boldsymbol{\theta}}\mathbf{x}}{\|\boldsymbol{\Gamma}'_{\boldsymbol{\theta}}\mathbf{x}\|} = \frac{\boldsymbol{\Gamma}'_{\boldsymbol{\theta}}\mathbf{x}}{(1 - v^2_{\boldsymbol{\theta}}(\mathbf{x}))^{1/2}}, \tag{2.1}$$

where $\boldsymbol{\Gamma}_{\boldsymbol{\theta}}$ denotes an arbitrary $p \times (p-1)$ matrix whose columns form an orthonormal basis of the orthogonal complement to $\boldsymbol{\theta}$ (so that $\boldsymbol{\Gamma}'_{\boldsymbol{\theta}}\boldsymbol{\Gamma}_{\boldsymbol{\theta}} = \mathbf{I}_{p-1}$ and $\boldsymbol{\Gamma}_{\boldsymbol{\theta}}\boldsymbol{\Gamma}'_{\boldsymbol{\theta}} = \mathbf{I}_p - \boldsymbol{\theta}\boldsymbol{\theta}'$). This allows to consider the *tangent-normal* decomposition

$$\mathbf{x} = v_{\boldsymbol{\theta}}(\mathbf{x})\boldsymbol{\theta} + (\mathbf{I}_p - \boldsymbol{\theta}\boldsymbol{\theta}')\mathbf{x} = v_{\boldsymbol{\theta}}(\mathbf{x})\boldsymbol{\theta} + (1 - v^2_{\boldsymbol{\theta}}(\mathbf{x}))^{1/2}\,\boldsymbol{\Gamma}_{\boldsymbol{\theta}}\mathbf{u}_{\boldsymbol{\theta}}(\mathbf{x}). \tag{2.2}$$

If $\mathbf{X}$ is rotationally symmetric about $\boldsymbol{\theta}$, then the distribution of the random $(p-1)$-vector $\boldsymbol{\Gamma}'_{\boldsymbol{\theta}}\mathbf{X}$ is spherically symmetric about the origin of $\mathbb{R}^{p-1}$, so that the *multivariate sign* $\mathbf{u}_{\boldsymbol{\theta}}(\mathbf{X})$ is uniformly distributed over $\mathcal{S}^{p-2}$, hence satisfying the moment conditions

$$\mathrm{E}[\mathbf{u}_{\boldsymbol{\theta}}(\mathbf{X})] = \mathbf{0} \tag{2.3}$$

and

$$\mathrm{E}[\mathbf{u}_{\boldsymbol{\theta}}(\mathbf{X})\mathbf{u}'_{\boldsymbol{\theta}}(\mathbf{X})] = \frac{1}{p-1}\,\mathbf{I}_{p-1}. \tag{2.4}$$

Note also that $\mathbf{u}_{\boldsymbol{\theta}}(\mathbf{X})$ and the cosine $v_{\boldsymbol{\theta}}(\mathbf{X})$ are mutually independent. This multivariate sign is therefore a quantity that is more appealing than the "projection" $\boldsymbol{\Gamma}'_{\boldsymbol{\theta}}\mathbf{X}$, that is neither distribution-free nor independent of $v_{\boldsymbol{\theta}}(\mathbf{X})$. If $\mathbf{X}$ admits a density, then this density is of the form

$$\mathbf{x} \mapsto f_{\boldsymbol{\theta},g}(\mathbf{x}) = c_{p,g}\, g(\mathbf{x}'\boldsymbol{\theta}),$$

where $c_{p,g}(>0)$ is a normalizing constant and $g : [-1, 1] \longrightarrow \mathbb{R}^+$ is referred to as an *angular function* in the sequel. Then, $v_{\boldsymbol{\theta}}(\mathbf{X})$ is absolutely continuous with respect to the Lebesgue measure on $[-1, 1]$ and the corresponding density is

$$v \mapsto \tilde{g}_p(v) := \omega_{p-1} c_{p,g} (1 - v^2)^{(p-3)/2} g(v), \tag{2.5}$$

where $\omega_{p-1} := 2\pi^{\frac{p-1}{2}}/\Gamma(\frac{p-1}{2})$ is the surface area of $\mathcal{S}^{p-2}$. Application of (2.5) to the vMF with location $\boldsymbol{\theta}$ and concentration κ (notation: $\mathcal{M}_p(\boldsymbol{\theta}, \kappa)$), gives $c^{\mathcal{M}}_{p,\kappa} = \kappa^{\frac{p-2}{2}}/((2\pi)^{\frac{p}{2}} I_{\frac{p-2}{2}}(\kappa))$, where I_ν is the order-ν modified Bessel function of the first kind.

2.1. The proposed tests

In view of the above considerations, it is natural to test the null of rotational symmetry about $\boldsymbol{\theta}$ by testing that $\mathbf{u}_{\boldsymbol{\theta}}(\mathbf{X})$ is uniformly distributed over $\mathcal{S}^{p-2}$. Since there are extremely diverse alternatives to uniformity on $\mathcal{S}^{p-2}$, one may first want to consider *location* alternatives and *scatter* alternatives, the ones associated with violations of the expectation (2.3) and the covariance (2.4), respectively. The tests we propose in this paper are designed to detect such alternatives.

Let $\mathbf{X}_1, \ldots, \mathbf{X}_n$ be a random sample from a distribution on $\mathcal{S}^{p-1}$ and consider the problem of testing the null $\mathcal{H}_{0,\boldsymbol{\theta}}$ that $\mathbf{X}_1$ is rotationally symmetric about a given location $\boldsymbol{\theta}$. Writing $\mathbf{U}_{i,\boldsymbol{\theta}} := \mathbf{u}_{\boldsymbol{\theta}}(\mathbf{X}_i)$, $i = 1, \ldots, n$, the first test we propose rejects the null for large values of

$$Q^{\mathrm{loc}}_{\boldsymbol{\theta}} := \frac{p-1}{n} \sum_{i,j=1}^{n} \mathbf{U}'_{i,\boldsymbol{\theta}} \mathbf{U}_{j,\boldsymbol{\theta}} = n(p-1)\|\bar{\mathbf{U}}_{\boldsymbol{\theta}}\|^2,$$

where $\bar{\mathbf{U}}_{\boldsymbol{\theta}} := \frac{1}{n}\sum_{i=1}^n \mathbf{U}_{i,\boldsymbol{\theta}}$. As for the uniformity of the $\mathbf{U}_{i,\boldsymbol{\theta}}$'s on $\mathcal{S}^{p-2}$, this test is simply the celebrated Rayleigh (1919)'s test. Alternatively, if it is assumed that the $\mathbf{X}_i$'s are sampled from a rotationally symmetric distribution (about an unspecified location), then the test also coincides with the Paindaveine and Verdebout (2015) *sign* test for the null that the unknown location is equal to $\boldsymbol{\theta}$. Since, under the null $\mathcal{H}_{0,\boldsymbol{\theta}}$, the $\mathbf{U}_{i,\boldsymbol{\theta}}$'s form a random sample from the uniform distribution over $\mathcal{S}^{p-2}$, the Central Limit Theorem (CLT) readily entails that $\sqrt{n}\bar{\mathbf{U}}_{\boldsymbol{\theta}} \overset{\mathcal{D}}{\rightsquigarrow} \mathcal{N}(\mathbf{0}, \frac{1}{p-1}\mathbf{I}_{p-1})$, and hence that $Q^{\mathrm{loc}}_{\boldsymbol{\theta}} \overset{\mathcal{D}}{\rightsquigarrow} \chi^2_{p-1}$ under $\mathcal{H}_{0,\boldsymbol{\theta}}$, where $\overset{\mathcal{D}}{\rightsquigarrow}$ denotes convergence in distribution. The resulting test, $\phi^{\mathrm{loc}}_{\boldsymbol{\theta}}$ say, then rejects the null $\mathcal{H}_{0,\boldsymbol{\theta}}$ at asymptotic level α whenever $Q^{\mathrm{loc}}_{\boldsymbol{\theta}} > \chi^2_{p-1,1-\alpha}$, where $\chi^2_{\ell,1-\alpha}$ denotes the α-upper quantile of the chi-square distribution with ℓ degrees of freedom. As we will show, this test typically detects the location alternatives violating the expectation condition (2.3).

In contrast, the second test we propose is designed to show power against the scatter alternatives that violate the covariance condition (2.4). This second test rejects $\mathcal{H}_{0,\boldsymbol{\theta}}$ for large values of

$$Q^{\mathrm{sc}}_{\boldsymbol{\theta}} := \frac{p^2-1}{2n} \sum_{i,j=1}^{n} \left((\mathbf{U}'_{i,\boldsymbol{\theta}} \mathbf{U}_{j,\boldsymbol{\theta}})^2 - \frac{1}{p-1} \right) = \frac{n(p^2-1)}{2} \left(\mathrm{tr}\big[\mathbf{S}^2_{\boldsymbol{\theta}}\big] - \frac{1}{p-1} \right),$$

where we let $\mathbf{S}_{\boldsymbol{\theta}} := \frac{1}{n}\sum_{i=1}^n \mathbf{U}_{i,\boldsymbol{\theta}}\mathbf{U}'_{i,\boldsymbol{\theta}}$. Using again the fact that, under $\mathcal{H}_{0,\boldsymbol{\theta}}$, the $\mathbf{U}_{i,\boldsymbol{\theta}}$'s form a random sample from the uniform distribution over $\mathcal{S}^{p-2}$, it readily follows from Hallin and Paindaveine (2006b) that $Q^{\mathrm{sc}}_{\boldsymbol{\theta}} \overset{\mathcal{D}}{\rightsquigarrow} \chi^2_{(p-2)(p+1)/2}$ under $\mathcal{H}_{0,\boldsymbol{\theta}}$. The resulting test, $\phi^{\mathrm{sc}}_{\boldsymbol{\theta}}$ say, then rejects the null $\mathcal{H}_{0,\boldsymbol{\theta}}$ at asymptotic level α whenever $Q^{\mathrm{sc}}_{\boldsymbol{\theta}} > \chi^2_{(p-2)(p+1)/2,1-\alpha}$.

For each test, thus, the asymptotic distribution of the test statistic, under the null of rotational symmetry about a *specified* location $\boldsymbol{\theta}$, follows from results available in the literature. Yet, two important questions remain open at this stage: (i) do $\phi^{\rm loc}_{\boldsymbol\theta}$ and $\phi^{\rm sc}_{\boldsymbol\theta}$ behave well under non-null distributions? In particular, are there alternatives to $\mathcal{H}_{0,\boldsymbol\theta}$ against which these tests would enjoy some power optimality? (ii) To test rotational symmetry about an unspecified $\boldsymbol\theta$, can one use the tests $\phi^{\rm loc}_{\hat{\boldsymbol\theta}}$ and $\phi^{\rm sc}_{\hat{\boldsymbol\theta}}$ obtained by replacing $\boldsymbol\theta$ with an appropriate estimator $\hat{\boldsymbol\theta}$ in $\phi^{\rm loc}_{\boldsymbol\theta}$ and $\phi^{\rm sc}_{\boldsymbol\theta}$? We address (i) in Sections 2.3 and 2.4 (for appropriate scatter and location alternatives, respectively), and (ii) in Section 3.

2.2. Non-rotationally symmetric tangent distributions

As explained in the previous section, if $\mathbf{X}$ is rotationally symmetric about $\boldsymbol\theta$, then the sign $\mathbf{U} := \mathbf{u}_{\boldsymbol\theta}(\mathbf{X})$ (see (2.1)) is uniformly distributed over $\mathcal{S}^{p-2}$ and is independent of the cosine $V := v_{\boldsymbol\theta}(\mathbf{X})$. Vice versa, it directly follows from the tangent-normal decomposition in (2.2) that any rotational distribution on $\mathcal{S}^{p-1}$ can be obtained as the distribution of

$$V\boldsymbol\theta + \sqrt{1-V^2}\,\boldsymbol\Gamma_{\boldsymbol\theta}\mathbf{U}, \tag{2.6}$$

where $\mathbf{U}$ is a random vector that is uniformly distributed over $\mathcal{S}^{p-2}$ and where the random variable V with values in $[-1,1]$ is independent of $\mathbf{U}$. In this section, we introduce natural alternatives to rotational symmetry by relaxing some of the distributional constraints on $\mathbf{U}$ in (2.6). Rather than assuming that $\mathbf{U}$ is uniformly distributed over $\mathcal{S}^{p-2}$, we construct two families of non-rotationally symmetric distributions for which $\mathbf{U}$ follows an *angular central Gaussian distribution* (see, e.g., Tyler (1987)) and a vMF distribution.

For the first family, recall that the random $(p-1)$-vector $\mathbf{U}$ has an angular central Gaussian distribution on $\mathcal{S}^{p-2}$ with shape parameter $\boldsymbol\Lambda$ (notation: $\mathbf{U}\sim\mathcal{A}_{p-1}(\boldsymbol\Lambda)$) if it admits the density

$$\mathbf{u}\mapsto c^{\mathcal{A}}_{p-1,\boldsymbol\Lambda}(\mathbf{u}'\boldsymbol\Lambda^{-1}\mathbf{u})^{-(p-1)/2}$$

with respect to the surface area measure σ_{p-2} on $\mathcal{S}^{p-2}$, where $c^{\mathcal{A}}_{p-1,\boldsymbol\Lambda} := \big(\omega_{p-1}(\det\boldsymbol\Lambda)^{1/2}\big)^{-1}$ is a normalizing constant. Here, the scatter parameter $\boldsymbol\Lambda$ is a $(p-1)\times(p-1)$ symmetric and positive-definite matrix that is normalized into a shape matrix in the sense that $\mathrm{tr}[\boldsymbol\Lambda]=p-1$ (without this normalization, $\boldsymbol\Lambda$ would be identified up to a positive scalar factor only). Denoting by $\mathcal{L}_{p-1}$ the collection of shape matrices $\boldsymbol\Lambda$, and by $\mathcal{G}$ the set of all cumulative distribution functions G over $[-1,1]$, we then introduce the family of *tangent elliptical distributions*.

Definition 2.1. *Let $\boldsymbol\theta\in\mathcal{S}^{p-1}$, $\boldsymbol\Lambda\in\mathcal{L}_{p-1}$, and $G\in\mathcal{G}$. Then the random vector $\mathbf{X}$ has a* tangent elliptical distribution *on $\mathcal{S}^{p-1}$ with location $\boldsymbol\theta$, shape $\boldsymbol\Lambda$, and angular distribution function G if and only if $\mathbf{X}\stackrel{\mathcal{D}}{=}V\boldsymbol\theta+\sqrt{1-V^2}\,\boldsymbol\Gamma_{\boldsymbol\theta}\mathbf{U}$, where $V\sim G$ and $\mathbf{U}\sim\mathcal{A}_{p-1}(\boldsymbol\Lambda)$ are mutually independent. If V admits the density (2.5) involving the angular function g, then we will write $\mathbf{X}\sim\mathcal{TE}_p(\boldsymbol\theta,g,\boldsymbol\Lambda)$.*

Clearly, rotationally symmetric distributions are obtained for $\boldsymbol\Lambda=\mathbf{I}_{p-1}$. Since $\mathcal{A}_{p-1}(\boldsymbol\Lambda)$ can be obtained by projecting radially on $\mathcal{S}^{p-2}$ a $(p-1)$-dimensional elliptical distribution with location $\mathbf{0}$ and scatter $\boldsymbol\Lambda$, the distributions in Definition 2.1 form an *elliptical extension* of the class of the (by nature, spherical) rotationally symmetric distributions, which justifies the terminology. In the absolutely continuous case, the following result provides the density of a tangent elliptical distribution.

Theorem 2.1. *If $\mathbf{X}\sim\mathcal{TE}_p(\boldsymbol\theta,g,\boldsymbol\Lambda)$, then $\mathbf{X}$ is absolutely continuous and the corresponding density is $\mathbf{x}\mapsto f^{\mathcal{TE}}_{\boldsymbol\theta,g,\boldsymbol\Lambda}(\mathbf{x})=\omega_{p-1}c_{p,g}c^{\mathcal{A}}_{p-1,\boldsymbol\Lambda}g(v_{\boldsymbol\theta}(\mathbf{x}))(\mathbf{u}'_{\boldsymbol\theta}(\mathbf{x})\boldsymbol\Lambda^{-1}\mathbf{u}_{\boldsymbol\theta}(\mathbf{x}))^{-(p-1)/2}$.*

As mentioned above, tangent elliptical distributions provide an elliptical extension of the class of rotationally symmetric distributions, hence in particular of vMF distributions. Another elliptical extension of vMF distributions is Kent (1982)'s class of Fisher–Bingham distributions. In addition to the immediate generalization to $p \geq 3$, the tangent elliptical distributions show several advantages with respect to the latter: (i) they form a semiparametric class of distributions that contains *all* rotationally symmetric distributions; (ii) the densities of tangent elliptical distributions involve normalizing constants that are simple to compute (see, e.g., Kume and Wood (2005) for the delicate problem of approximating normalizing constants in the Fisher–Bingham model); (iii) simulation is straightforward, since it reduces to simulating independently a univariate variable V and a $\mathcal{N}(\mathbf{0}, \mathbf{\Lambda})$.

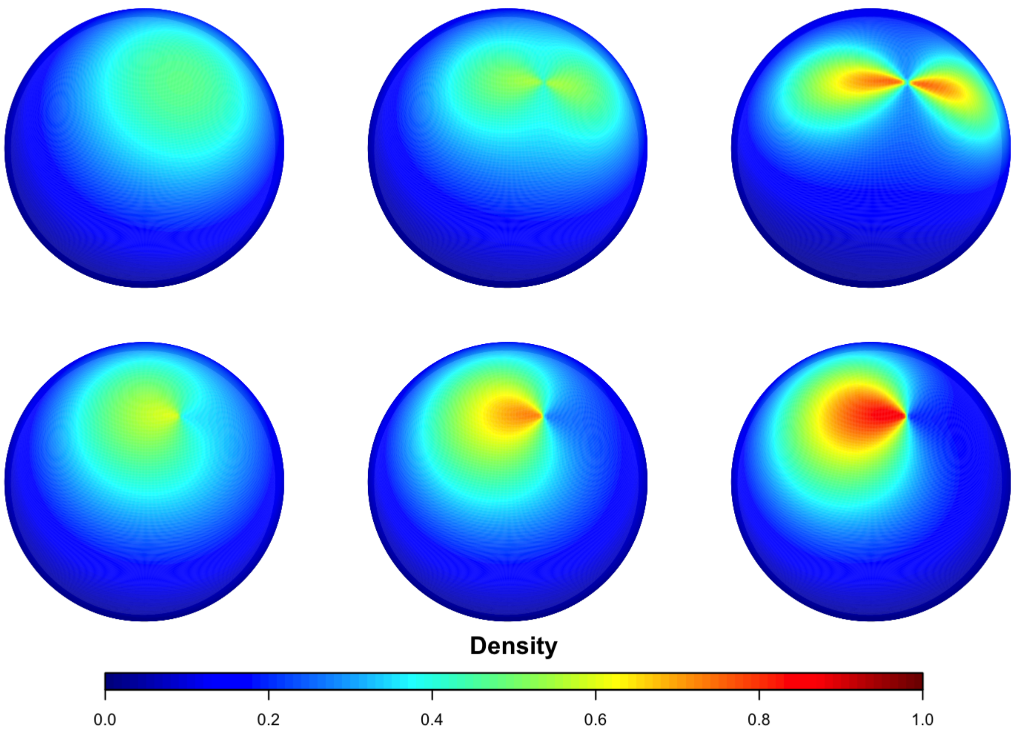

Fig. 1. Contour plots of tangent elliptical and tangent vMF densities, both with $g(z) = \exp(3z)$. Top row: from left to right, tangent elliptical with shape matrices $\mathbf{\Lambda} = \left(\begin{smallmatrix} 1+a & 0 \\ 0 & 1-a \end{smallmatrix}\right)$, $a = 0$ (rotationally symmetric) and $a = 0.15, 0.45$. Bottom row: from left to right, tangent vMF densities with skewness intensities $\kappa = 0.25, 0.50, 0.75$.

The second class of distributions we introduce, namely the class of *tangent vMF distributions*, is obtained by assuming that $\mathbf{U} \sim \mathcal{M}_{p-1}(\boldsymbol{\mu}, \kappa)$. Unlike the tangent elliptical distributions, under which $\mathbf{U}$ assumes an axial distribution on $\mathcal{S}^{p-2}$, the unimodality of $\mathcal{M}_{p-1}(\boldsymbol{\mu}, \kappa)$ in the tangent space provides a skewed distribution for $\mathbf{X}$ around $\boldsymbol{\theta}$ (see bottom row of Figure 1).

Definition 2.2. *Let $\boldsymbol{\theta} \in \mathcal{S}^{p-1}$, $\boldsymbol{\mu} \in \mathcal{S}^{p-2}$, $\kappa \geq 0$, and $G \in \mathcal{G}$. Then the random vector $\mathbf{X}$ has a* tangent vMF distribution *on $\mathcal{S}^{p-1}$ with location $\boldsymbol{\theta}$, skewness direction $\boldsymbol{\mu}$, skewness intensity κ, and angular distribution function G if and only if $\mathbf{X} \stackrel{\mathcal{D}}{=} V\boldsymbol{\theta} + \sqrt{1-V^2}\,\mathbf{\Gamma}_{\boldsymbol{\theta}}\mathbf{U}$, where $V \sim G$ and $\mathbf{U} \sim \mathcal{M}_{p-1}(\boldsymbol{\mu}, \kappa)$ are mutually independent. If V admits the density (2.5) involving the angular function g, then we will write $\mathbf{X} \sim \mathcal{TM}_p(\boldsymbol{\theta}, g, \boldsymbol{\mu}, \kappa)$.*

The following result provides the density of the tangent vMF distributions in the absolutely continuous case. Its proof is along the same lines as the proof of Theorem 2.1, hence is omitted.

THEOREM 2.2. *If* $\mathbf{X} \sim \mathcal{TM}_p(\boldsymbol{\theta}, g, \boldsymbol{\mu}, \kappa)$*, then* $\mathbf{X}$ *is absolutely continuous and the corresponding density is* $\mathbf{x} \mapsto f^{\mathcal{TM}}_{\boldsymbol{\theta},g,\boldsymbol{\mu},\kappa}(\mathbf{x}) = \omega_{p-1} c_{p,g} c^{\mathcal{M}}_{p-1,\kappa} g(v_{\boldsymbol{\theta}}(\mathbf{x})) \exp(\kappa \boldsymbol{\mu}' \mathbf{u}_{\boldsymbol{\theta}}(\mathbf{x}))$.

Note that, albeit our framework is $p \geq 3$, the distributions are also properly defined for $p = 2$. In that case, the signs $\mathbf{U}$ belong to $\mathcal{S}^0 = \{-1, 1\}$, $\omega_1 = 2$, and, since σ_0 is the counting measure, the angular central Gaussian and the vMF densities become probability mass functions. The former, since it is an axial distribution, puts equal mass in ± 1. The vMF, since $I_{-\frac{1}{2}}(\kappa) = \sqrt{2/(\pi\kappa)}\cosh(\kappa)$, assigns probabilities $\exp(\pm\mu\kappa)/(\exp(-\mu\kappa) + \exp(\mu\kappa))$ to ± 1, respectively, with $\mu \in \mathcal{S}^0$. In view of these considerations, it becomes apparent that only the tangent vMF distributions are non-rotationally symmetric extensions of the rotationally symmetric class when $p = 2$. This is coherent with the fact that $Q^{\mathrm{sc}}_{\boldsymbol{\theta}}$ is constant when $p = 2$ and therefore does not provide any reasonable test. In order to deal with non-degenerate tests, we restrict to $p \geq 3$ in the sequel.

2.3. Non-null results for tangent elliptical alternatives

In this section, we will investigate the performances of the tests $\phi^{\mathrm{loc}}_{\boldsymbol{\theta}}$ and $\phi^{\mathrm{sc}}_{\boldsymbol{\theta}}$ under the tangent elliptical alternatives to rotational symmetry introduced above. To do so, we will need the following notation: we write $\mathrm{vech}\,(\mathbf{A})$ for the $(p(p+1)/2)$-dimensional vector stacking the upper-triangular elements of a $p \times p$ symmetric matrix $\mathbf{A} = (A_{ij})$, $\overset{\circ}{\mathrm{vech}}\,(\mathbf{A})$ for $\mathrm{vech}\,(\mathbf{A})$ with the first element (A_{11}) excluded, $\mathbf{M}_p$ for the matrix satisfying $\mathbf{M}_p' \overset{\circ}{\mathrm{vech}}\,(\mathbf{A}) = \mathrm{vec}\,(\mathbf{A})$ for any $p \times p$ symmetric matrix $\mathbf{A}$ with $\mathrm{tr}[\mathbf{A}] = 0$, $\mathbf{J}_p := \sum_{i,j=1}^p (\mathbf{e}_{p,i}\mathbf{e}_{p,j}') \otimes (\mathbf{e}_{p,i}\mathbf{e}_{p,j}') = (\mathrm{vec}\,\mathbf{I}_p)(\mathrm{vec}\,\mathbf{I}_p)'$, and $\mathbf{K}_p = \sum_{i,j=1}^p (\mathbf{e}_{p,i}\mathbf{e}_{p,j}') \otimes (\mathbf{e}_{p,j}\mathbf{e}_{p,i}')$ (the *commutation matrix*), where $\mathbf{e}_{p,\ell}$ denotes the ℓ-th vector of the canonical basis of $\mathbb{R}^p$. Since the shape matrix $\boldsymbol{\Lambda}$ of a tangent elliptical distribution is symmetric and satisfies $\mathrm{tr}[\boldsymbol{\Lambda}] = p - 1$, it is completely characterized by $\overset{\circ}{\mathrm{vech}}\,(\boldsymbol{\Lambda})$. Throughout, we let $V_{i,\boldsymbol{\theta}} := v_{\boldsymbol{\theta}}(\mathbf{X}_i) = \mathbf{X}_i'\boldsymbol{\theta}$ and we denote as $\chi^2_\nu(\lambda)$ the chi-square distribution with ν degrees of freedom and non-centrality parameter λ (so that $\chi^2_\nu(0) \overset{\mathcal{D}}{=} \chi^2_\nu$).

In order to examine log-likelihood ratios involving the angular functions g, we need to assume some regularity conditions on g. More precisely, we will restrict to the collection $\mathcal{G}_a$ of non-constant angular functions $g : [-1, 1] \longrightarrow \mathbb{R}^+_0$ that are absolutely continuous and for which $\mathcal{J}_p(g) := \int_{-1}^1 \varphi_g^2(t)(1-t^2)\tilde{g}_p(t)dt$ is finite, where $\varphi_g := \dot{g}/g$ involves the almost everywhere derivative $\dot{g}$ of g.

Consider then the semiparametric model $\{\mathrm{P}^{\mathcal{TE}(n)}_{\boldsymbol{\theta},g,\boldsymbol{\Lambda}} : \boldsymbol{\theta} \in \mathcal{S}^{p-1}, g \in \mathcal{G}_a, \boldsymbol{\Lambda} \in \mathcal{L}^{p-1}\}$, where $\mathrm{P}^{\mathcal{TE}(n)}_{\boldsymbol{\theta},g,\boldsymbol{\Lambda}}$ denotes the probability measure associated with observations $\mathbf{X}_1, \ldots, \mathbf{X}_n$ that are randomly sampled from the tangent elliptical distribution $\mathcal{TE}_p(\boldsymbol{\theta}, g, \boldsymbol{\Lambda})$. In the rotationally symmetric case, that is, for $\boldsymbol{\Lambda} = \mathbf{I}_{p-1}$, we will simply write $\mathrm{P}^{(n)}_{\boldsymbol{\theta},g}$ instead of $\mathrm{P}^{\mathcal{TE}(n)}_{\boldsymbol{\theta},g,\mathbf{I}_{p-1}}$. Investigating the optimality of tests of rotational symmetry against tangent elliptical alternatives requires studying the asymptotic behaviour of tangent elliptical log-likelihood ratios associated with local deviations from $\boldsymbol{\Lambda} = \mathbf{I}_{p-1}$. This leads to the following *Local Asymptotic Normality (LAN)* result.

THEOREM 2.3. *Fix* $\boldsymbol{\theta} \in \mathcal{S}^{p-1}$ *and* $g \in \mathcal{G}_a$*. Let* $\boldsymbol{\tau}_n := (\mathbf{t}_n', \overset{\circ}{\mathrm{vech}}\,(\mathbf{L}_n)')'$*, where* $(\mathbf{t}_n)$ *is a bounded sequence in* $\mathbb{R}^p$ *such that* $\boldsymbol{\theta}_n := \boldsymbol{\theta} + n^{-1/2}\mathbf{t}_n \in \mathcal{S}^{p-1}$ *for any* n*, and where* $(\mathbf{L}_n)$ *is a bounded sequence of* $(p-1) \times (p-1)$ *matrices such that* $\boldsymbol{\Lambda}_n := \mathbf{I}_{p-1} + n^{-1/2}\mathbf{L}_n \in \mathcal{L}_{p-1}$ *for any* n*. Then, the tangent elliptical* *log-likelihood ratio associated to local deviations* $\mathbf{\Lambda}_n$ *from* $\mathbf{\Lambda} = \mathbf{I}_{p-1}$ *satisfies*

$$\log \frac{d\mathrm{P}^{\mathcal{TE}(n)}_{\boldsymbol{\theta}_n,g,\mathbf{\Lambda}_n}}{d\mathrm{P}^{(n)}_{\boldsymbol{\theta},g}} = \boldsymbol{\tau}'_n \mathbf{\Delta}^{\mathcal{TE}(n)}_{\boldsymbol{\theta},g} - \frac{1}{2}\boldsymbol{\tau}'_n \mathbf{\Gamma}^{\mathcal{TE}}_{\boldsymbol{\theta},g}\boldsymbol{\tau}_n + o_{\mathrm{P}}(1) \tag{2.7}$$

as $n \to \infty$ *under* $\mathrm{P}^{(n)}_{\boldsymbol{\theta},g}$*, where the central sequence*

$$\mathbf{\Delta}^{\mathcal{TE}(n)}_{\boldsymbol{\theta},g} := \begin{pmatrix} \mathbf{\Delta}^{(n)}_{\boldsymbol{\theta},g;1} \\ \mathbf{\Delta}^{\mathcal{TE}(n)}_{\boldsymbol{\theta};2} \end{pmatrix} := \begin{pmatrix} \frac{1}{\sqrt{n}}\sum_{i=1}^n \varphi_g(V_{i,\boldsymbol{\theta}})(1-V^2_{i,\boldsymbol{\theta}})^{1/2}\,\mathbf{\Gamma}_{\boldsymbol{\theta}}\mathbf{U}_{i,\boldsymbol{\theta}} \\ \frac{p-1}{2\sqrt{n}}\,\mathbf{M}_p \sum_{i=1}^n \mathrm{vec}\left(\mathbf{U}_{i,\boldsymbol{\theta}}\mathbf{U}'_{i,\boldsymbol{\theta}} - \frac{1}{p-1}\,\mathbf{I}_{p-1}\right) \end{pmatrix}$$

is, still under $\mathrm{P}^{(n)}_{\boldsymbol{\theta},g}$*, asymptotically normal with mean zero and covariance matrix*

$$\mathbf{\Gamma}^{\mathcal{TE}}_{\boldsymbol{\theta},g} := \begin{pmatrix} \mathbf{\Gamma}_{\boldsymbol{\theta},g;11} & \mathbf{0} \\ \mathbf{0} & \mathbf{\Gamma}^{\mathcal{TE}}_{\boldsymbol{\theta};22} \end{pmatrix} := \begin{pmatrix} \frac{\mathcal{J}_p(g)}{p-1}(\mathbf{I}_p - \boldsymbol{\theta}\boldsymbol{\theta}') & \mathbf{0} \\ \mathbf{0} & \frac{p-1}{4(p+1)}\mathbf{M}_p\left(\mathbf{I}_{(p-1)^2} + \mathbf{K}_{p-1}\right)\mathbf{M}'_p \end{pmatrix}.$$

The restriction that $g \in \mathcal{G}_a$ in particular guarantees that the g-parametric submodel of the tangent elliptical model has a finite Fisher information for $\boldsymbol{\theta}$ in the vicinity of rotational symmetry. Any LAN result requires a finite Fisher information condition of this sort (along with a smoothness condition that allows to define Fisher information). The LAN result in Theorem 2.3 easily provides the following corollary.

Corollary 2.1. *Fix* $\boldsymbol{\theta} \in \mathcal{S}^{p-1}$ *and* $g \in \mathcal{G}_a$*. Let* $\mathbf{\Lambda}_n$ *and* $(\mathbf{L}_n)$ *be as in Theorem 2.3, now with* $\mathbf{L}_n \to \mathbf{L} \neq \mathbf{0}$*. Then, under* $\mathrm{P}^{\mathcal{TE}(n)}_{\boldsymbol{\theta},g,\mathbf{\Lambda}_n}$*: (i)* $Q^{\mathrm{loc}}_{\boldsymbol{\theta}} \overset{\mathcal{D}}{\rightsquigarrow} \chi^2_{p-1}$*; (ii)* $Q^{\mathrm{sc}}_{\boldsymbol{\theta}} \overset{\mathcal{D}}{\rightsquigarrow} \chi^2_{(p-2)(p+1)/2}(\lambda)$*, with* $\lambda = (p-1)\mathrm{tr}[\mathbf{L}^2]/(2(p+1))$*.*

First note that (i) implies that, for the local alternatives considered, the null and non-null asymptotic distributions of $Q^{\mathrm{loc}}_{\boldsymbol{\theta}}$ do coincide, so that the test $\phi^{\mathrm{loc}}_{\boldsymbol{\theta}}$ has asymptotic power α against such alternatives. On the contrary, (ii) shows that the test $\phi^{\mathrm{sc}}_{\boldsymbol{\theta}}$ exhibits non-trivial asymptotic powers against any alternatives associated with $\mathbf{\Lambda}_n = \mathbf{I}_{p-1} + n^{-1/2}\mathbf{L}_n$, $\mathbf{L}_n \to \mathbf{L} \neq \mathbf{0}$ (note indeed that $\mathrm{tr}[\mathbf{L}^2]$ is the squared Frobenius norm of $\mathbf{L}$). Note also that, since $\mathbf{L}$ has trace zero by construction, the non-centrality parameter $(p-1)\mathrm{tr}[\mathbf{L}^2]/(2(p+1))$ above is proportional to the variance of the eigenvalues of $\mathbf{L}$, which is line with the fact that $\phi^{\mathrm{sc}}_{\boldsymbol{\theta}}$ has the nature of a sphericity test.

While Corollary 2.1 shows that the test $\phi^{\mathrm{sc}}_{\boldsymbol{\theta}}$ can detect local alternatives of a tangent elliptical nature, it does not provide information on the possible optimality of this test. General results on the Le Cam theory (see, e.g., Chapter 5 of Ley and Verdebout (2017a)) together with Theorem 2.3 directly entail that a locally asymptotically maximin test, at asymptotic level α, when testing $\{\mathrm{P}^{(n)}_{\boldsymbol{\theta},g}\}$ against $\bigcup_{\mathbf{\Lambda}\in\mathcal{L}_{p-1}\setminus\{\mathbf{I}_p\}}\{\mathrm{P}^{\mathcal{TE}(n)}_{\boldsymbol{\theta},g,\mathbf{\Lambda}}\}$ rejects the null whenever

$$Q^{\mathrm{sc}}_{\boldsymbol{\theta}} = \left(\mathbf{\Delta}^{\mathcal{TE}(n)}_{\boldsymbol{\theta};2}\right)'\left(\mathbf{\Gamma}^{\mathcal{TE}}_{\boldsymbol{\theta};22}\right)^{-1}\mathbf{\Delta}^{\mathcal{TE}(n)}_{\boldsymbol{\theta};2} > \chi^2_{(p-2)(p+1)/2,1-\alpha}. \tag{2.8}$$

Now, using the closed form for the inverse of $\mathbf{\Gamma}^{\mathcal{TE}}_{\boldsymbol{\theta};22}$ in Lemma 5.2 from Hallin and Paindaveine (2006a), it is easy to show that the test statistic in (2.8) coincides with $Q^{\mathrm{sc}}_{\boldsymbol{\theta}}$. Since this holds at *any* angular function g in $\mathcal{G}_a$, we proved the following result.

Corollary 2.2. *When testing* $\bigcup_{g\in\mathcal{G}_a}\{\mathrm{P}^{(n)}_{\boldsymbol{\theta},g}\}$ *against* $\bigcup_{g\in\mathcal{G}_a}\bigcup_{\mathbf{\Lambda}\in\mathcal{L}_{p-1}\setminus\{\mathbf{I}_p\}}\{\mathrm{P}^{\mathcal{TE}(n)}_{\boldsymbol{\theta},g,\mathbf{\Lambda}}\}$*, the test* $\phi^{\mathrm{sc}}_{\boldsymbol{\theta}}$ *is locally asymptotically maximin at asymptotic level* α*.*

We conclude that, when testing rotational symmetry about a specified location $\boldsymbol{\theta}$ against tangent elliptical alternatives, the location test $Q^{\mathrm{loc}}_{\boldsymbol{\theta}}$ *does not show any power*, while the scatter test $Q^{\mathrm{sc}}_{\boldsymbol{\theta}}$ is *optimal* in the Le Cam sense, uniformly in the angular function $g \in \mathcal{G}_a$.

2.4. Non-null results under tangent vMF alternatives

To investigate the non-null behaviour of the proposed tests under tangent vMF alternatives, we consider the semiparametric model $\{\mathrm{P}^{\mathcal{TM}(n)}_{\boldsymbol{\theta},g,\boldsymbol{\mu},\kappa} : \boldsymbol{\theta} \in \mathcal{S}^{p-1}, g \in \mathcal{G}_a, \boldsymbol{\mu} \in \mathcal{S}^{p-2}, \kappa \geq 0\}$, where $\mathrm{P}^{\mathcal{TM}(n)}_{\boldsymbol{\theta},g,\boldsymbol{\mu},\kappa}$ denotes the probability measure associated with observations $\mathbf{X}_1, \ldots, \mathbf{X}_n$ that are randomly sampled from the tangent vMF distribution $\mathcal{TM}_p(\boldsymbol{\theta}, g, \boldsymbol{\mu}, \kappa)$; for $\kappa = 0$, $\mathrm{P}^{\mathcal{TM}(n)}_{\boldsymbol{\theta},g,\boldsymbol{\mu},\kappa}$ is defined as the rotationally symmetric hypothesis $\mathrm{P}^{(n)}_{\boldsymbol{\theta},g}$ (see the notation introduced in Section 2.3). To investigate optimality properties of tests of rotational symmetry against such alternatives, it is convenient to parametrize this model with $\boldsymbol{\theta}$, $\boldsymbol{\delta}$, and g, where we let $\boldsymbol{\delta} := \kappa\boldsymbol{\mu}$; obviously, we will then use the notation $\mathrm{P}^{\mathcal{TM}(n)}_{\boldsymbol{\theta},g,\boldsymbol{\delta}}$. In this new parametrization, the null hypothesis of rotational symmetry coincides with $\mathcal{H}_0 : \boldsymbol{\delta} = \mathbf{0}$. The main advantage of the parametrization in $\boldsymbol{\delta} \in \mathbb{R}^{p-1}$ over the original one in $(\kappa, \boldsymbol{\mu}) \in \mathbb{R}^+ \times \mathcal{S}^{p-2}$ is that the $\boldsymbol{\delta}$-parameter space is standard (it is the Euclidean space $\mathbb{R}^{p-1}$), while the $(\kappa, \boldsymbol{\mu})$-one is curved.

As for tangent elliptical distributions, our investigation of optimality issues will then be based on a LAN result, that takes here the following form (see Appendix A for the proof).

THEOREM 2.4. *Fix $\boldsymbol{\theta} \in \mathcal{S}^{p-1}$ and $g \in \mathcal{G}_a$. Let $\boldsymbol{\tau}_n := (\mathbf{t}_n', \mathbf{d}_n')'$, where $(\mathbf{t}_n)$ is a bounded sequence in $\mathbb{R}^p$ such that $\boldsymbol{\theta}_n := \boldsymbol{\theta} + n^{-1/2}\mathbf{t}_n \in \mathcal{S}^{p-1}$ for any n, and $\boldsymbol{\delta}_n := n^{-1/2}\mathbf{d}_n$ with $(\mathbf{d}_n)$ a bounded sequence in $\mathbb{R}^{p-1}$. Then, the tangent vMF log-likelihood ratio associated to local deviations $\boldsymbol{\delta}_n$ from $\boldsymbol{\delta} = \mathbf{0}$ is*

$$\log \frac{d\mathrm{P}^{\mathcal{TM}(n)}_{\boldsymbol{\theta}_n,g,\boldsymbol{\delta}_n}}{d\mathrm{P}^{(n)}_{\boldsymbol{\theta},g}} = \boldsymbol{\tau}_n' \boldsymbol{\Delta}^{\mathcal{TM}(n)}_{\boldsymbol{\theta},g} - \frac{1}{2}\boldsymbol{\tau}_n' \boldsymbol{\Gamma}^{\mathcal{TM}}_{\boldsymbol{\theta},g} \boldsymbol{\tau}_n + o_{\mathrm{P}}(1),$$

as $n \to \infty$ under $\mathrm{P}^{(n)}_{\boldsymbol{\theta},g}$, where the central sequence

$$\boldsymbol{\Delta}^{\mathcal{TM}(n)}_{\boldsymbol{\theta},g} := \begin{pmatrix} \boldsymbol{\Delta}^{(n)}_{\boldsymbol{\theta},g;1} \\ \boldsymbol{\Delta}^{\mathcal{TM}(n)}_{\boldsymbol{\theta};2} \end{pmatrix} := \begin{pmatrix} \frac{1}{\sqrt{n}} \sum_{i=1}^n \varphi_g(V_{i,\boldsymbol{\theta}})(1 - V_{i,\boldsymbol{\theta}}^2)^{1/2}\, \boldsymbol{\Gamma}_{\boldsymbol{\theta}} \mathbf{U}_{i,\boldsymbol{\theta}} \\ \frac{1}{\sqrt{n}} \sum_{i=1}^n \mathbf{U}_{i,\boldsymbol{\theta}} \end{pmatrix}$$

is, still under $\mathrm{P}^{(n)}_{\boldsymbol{\theta},g}$, asymptotically normal with mean zero and covariance matrix

$$\boldsymbol{\Gamma}^{\mathcal{TM}}_{\boldsymbol{\theta},g} := \begin{pmatrix} \boldsymbol{\Gamma}_{\boldsymbol{\theta},g;11} & \boldsymbol{\Gamma}^{\mathcal{TM}}_{\boldsymbol{\theta},g;12} \\ \boldsymbol{\Gamma}^{\mathcal{TM}}_{\boldsymbol{\theta},g;21} & \boldsymbol{\Gamma}^{\mathcal{TM}}_{22} \end{pmatrix} := \begin{pmatrix} \frac{\mathcal{J}_p(g)}{p-1}(\mathbf{I}_p - \boldsymbol{\theta}\boldsymbol{\theta}') & \frac{\mathcal{I}_p(g)}{p-1}\boldsymbol{\Gamma}_{\boldsymbol{\theta}} \\ \frac{\mathcal{I}_p(g)}{p-1}\boldsymbol{\Gamma}_{\boldsymbol{\theta}}' & \frac{1}{p-1}\mathbf{I}_{p-1} \end{pmatrix},$$

with $\mathcal{I}_p(g) := \int_{-1}^1 \varphi_g(t)\sqrt{1-t^2}\, \tilde{g}_p(t) dt$.

Unlike for the LAN property in Theorem 2.3, the Fisher information matrix associated with the LAN property above, namely $\boldsymbol{\Gamma}^{\mathcal{TM}}_{\boldsymbol{\theta},g}$, is in not block-diagonal. Note also that Jensen's inequality ensures that $\mathcal{J}_p(g) \geq \mathcal{I}_p^2(g)$, which confirms the finiteness of $\mathcal{I}_p(g)$ and the positive semidefiniteness of $\boldsymbol{\Gamma}^{\mathcal{TM}}_{\boldsymbol{\theta},g}$. It is also easy to check that the *only* angular functions for which Jensen's inequality is actually an equality (hence, for which $\boldsymbol{\Gamma}^{\mathcal{TM}}_{\boldsymbol{\theta},g}$ is singular) are of the form $g(t) = C\exp(\kappa \arcsin(t))$ for some real constants C and κ.

COROLLARY 2.3. *Fix $\boldsymbol{\theta} \in \mathcal{S}^{p-1}$ and $g \in \mathcal{G}_a$. Let $(\boldsymbol{\mu}_n)$ be a sequence in $\mathcal{S}^{p-2}$ that converges to $\boldsymbol{\mu}$. Let $\kappa_n := n^{-1/2}k_n$, where (k_n) is a sequence in $\mathbb{R}_0^+$ that converges to $k > 0$. Then, under $\mathrm{P}^{\mathcal{TM}(n)}_{\boldsymbol{\theta},g,\boldsymbol{\mu}_n,\kappa_n}$: (i) $Q^{\mathrm{loc}}_{\boldsymbol{\theta}} \overset{\mathcal{D}}{\rightsquigarrow} \chi^2_{p-1}(\lambda)$, with $\lambda = k^2/(p-1)$; (ii) $Q^{\mathrm{sc}}_{\boldsymbol{\theta}} \overset{\mathcal{D}}{\rightsquigarrow} \chi^2_{(p-2)(p+1)/2}$.*

The location test $\phi^{\mathrm{loc}}_{\boldsymbol{\theta}}$ and the scatter test $\phi^{\mathrm{sc}}_{\boldsymbol{\theta}}$ therefore exhibit opposite non-null behaviours under tangent vMF alternatives, compared to what occurs under tangent elliptical alternatives in Section 2.3:

under tangent vMF alternatives, $\phi_{\boldsymbol{\theta}}^{\mathrm{sc}}$ has asymptotic power equal to the nominal level α, whereas $\phi_{\boldsymbol{\theta}}^{\mathrm{loc}}$ shows non-trivial asymptotic powers. Since the latter test is the test rejecting the null hypothesis of rotational symmetry about $\boldsymbol{\theta}$ whenever

$$Q_{\boldsymbol{\theta}}^{\mathrm{loc}} = \big(\boldsymbol{\Delta}_{\boldsymbol{\theta};2}^{\mathcal{TM}(n)}\big)'\big(\boldsymbol{\Gamma}_{22}^{\mathcal{TM}}\big)^{-1}\boldsymbol{\Delta}_{\boldsymbol{\theta};2}^{\mathcal{TM}(n)} > \chi^2_{p-1,1-\alpha},$$

it is actually locally asymptotically maximin when testing $\{\mathrm{P}_{\boldsymbol{\theta},g}^{(n)}\}$ against $\bigcup_{\boldsymbol{\mu}\in\mathcal{S}^{p-2}}\bigcup_{\kappa>0}\{\mathrm{P}_{\boldsymbol{\theta},g,\boldsymbol{\mu},\kappa}^{\mathcal{TM}(n)}\}$ at asymptotic level α. Moreover, since $Q_{\boldsymbol{\theta}}^{\mathrm{loc}}$ does not depend on g, we have the following result.

Corollary 2.4. *When testing $\bigcup_{g\in\mathcal{G}_a}\{\mathrm{P}_{\boldsymbol{\theta},g}^{(n)}\}$ against $\bigcup_{g\in\mathcal{G}_a}\bigcup_{\boldsymbol{\mu}\in\mathcal{S}^{p-2}}\bigcup_{\kappa>0}\{\mathrm{P}_{\boldsymbol{\theta},g,\boldsymbol{\mu},\kappa}^{\mathcal{TM}(n)}\}$, the test $Q_{\boldsymbol{\theta}}^{\mathrm{loc}}$ is locally asymptotically maximin at asymptotic level α.*

We conclude that the location test $\phi_{\boldsymbol{\theta}}^{\mathrm{loc}}$ and the scatter test $\phi_{\boldsymbol{\theta}}^{\mathrm{sc}}$ are optimal in the Le Cam sense, uniformly in $g \in \mathcal{G}_a$, against tangent vMF alternatives and tangent elliptical alternatives, respectively.

3. Testing rotational symmetry about an unspecified $\boldsymbol{\theta}$

The tests $\phi_{\boldsymbol{\theta}}^{\mathrm{loc}}$ and $\phi_{\boldsymbol{\theta}}^{\mathrm{sc}}$ studied in the previous section allow to test for rotational symmetry about a given location $\boldsymbol{\theta}$. Often, however, it is desirable to rather test for rotational symmetry about an unspecified $\boldsymbol{\theta}$. Natural tests for this unspecified-$\boldsymbol{\theta}$ problem are obtained by substituting an appropriate estimator $\hat{\boldsymbol{\theta}}$ for $\boldsymbol{\theta}$ in $\phi_{\boldsymbol{\theta}}^{\mathrm{loc}}$ and $\phi_{\boldsymbol{\theta}}^{\mathrm{sc}}$. In this section, we investigate whether or not this approach provides tests that are valid (in the sense that they meet asymptotically the nominal level) or even optimal.

3.1. Scatter tests

We start by considering the test $\phi_{\boldsymbol{\theta}}^{\mathrm{sc}}$, which was showed in Section 2.3 to be optimal in the Le Cam sense against tangent elliptical alternatives. First note that it is easy to show that the local asymptotic normality results in Theorems 2.3–2.4 can be strengthened into *Uniform Local Asymptotic Normality* (ULAN) ones. In such a ULAN setup, it is customary to use an estimator $\hat{\boldsymbol{\theta}}$ satisfying the following assumptions:

$\mathrm{A}_{\mathcal{G}'}$ The estimator $\hat{\boldsymbol{\theta}}$ (with values in $\mathcal{S}^{p-1}$) is part of a sequence that is: (i) *root-n consistent* under any $g \in \mathcal{G}'$, *i.e.*, $\sqrt{n}(\hat{\boldsymbol{\theta}} - \boldsymbol{\theta}) = O_{\mathrm{P}}(1)$ under $\bigcup_{g\in\mathcal{G}'}\{\mathrm{P}_{\boldsymbol{\theta},g}^{(n)}\}$; (ii) *locally and asymptotically discrete*, *i.e.*, for all $\boldsymbol{\theta}$ and for all $C > 0$, there exists a positive integer $M = M(C)$ such that the number of possible values of $\hat{\boldsymbol{\theta}}$ in balls of the form $\{\mathbf{t} \in \mathcal{S}^{p-1} : \sqrt{n}\,\|\mathbf{t} - \boldsymbol{\theta}\| \leq C\}$ is bounded by M, uniformly as $n \to \infty$.

Part (i) of Assumption $\mathrm{A}_{\mathcal{G}'}$ requires that the preliminary estimator is root-n consistent under the null hypothesis of rotational symmetry for a broad range $\mathcal{G}'$ of angular functions g. The restriction to a proper subclass $\mathcal{G}'$ of the full set of angular functions is explained by the fact that classical estimators of $\boldsymbol{\theta}$ typically address either monotone rotationally symmetric distributions (g is monotone increasing) or axial ones ($g(-t) = g(t)$ for any t), but cannot deal with mixed types, such as girdle-like distributions. Practitioners are thus expected to take $\mathcal{G}'$ as the collection of monotone or even angular functions, depending on the types of directional data (unimodal or axial data) they are facing. In the unimodal case, the most classical estimator that is root-n consistent under any (non-constant) monotone angular function is the *spherical mean* $\hat{\boldsymbol{\theta}} = \bar{\mathbf{X}}/\|\bar{\mathbf{X}}\|$, with $\bar{\mathbf{X}} := \frac{1}{n}\sum_{i=1}^n \mathbf{X}_i$. In the axial case, estimators of the location $\boldsymbol{\theta}$ are typically based on the eigenvectors of the sample covariance matrix.

Part (ii) is a purely technical requirement (see, e.g., Ley et al. (2013)) with little practical implications in the sense that, for fixed n, any estimate can be considered part of a locally and asymptotically discrete sequence of estimators. This is because the precision in the (in principle, required) discretization of a non-discrete estimator can be arbitrarily large; see, e.g., page 2467 in Ilmonen and Paindaveine (2011) for a discussion.

Now, the block-diagonality of the Fisher information matrix in the LAN property of Theorem 2.3 entails that the replacement in $Q_{\boldsymbol{\theta}}^{\rm sc}$ of $\boldsymbol{\theta}$ with an estimator $\hat{\boldsymbol{\theta}}$ satisfying $\mathrm{A}_{\mathcal{G}'}$ has no asymptotic impact under the null. More precisely, we have the following result.

PROPOSITION 3.1. *Let $\hat{\boldsymbol{\theta}}$ satisfy $A_{\mathcal{G}'}$. Then, for any $\boldsymbol{\theta} \in \mathcal{S}^{p-1}$ and any $g \in \mathcal{G}_a \cap \mathcal{G}'$, $Q_{\hat{\boldsymbol{\theta}}}^{\rm sc} - Q_{\boldsymbol{\theta}}^{\rm sc} = o_{\rm P}(1)$ as $n \to \infty$ under $\mathrm{P}_{\boldsymbol{\theta},g}^{(n)}$.*

From contiguity, the null asymptotic equivalence in this proposition extends to local alternatives of the form $\mathrm{P}_{\boldsymbol{\theta},g,\boldsymbol{\Lambda}_n}^{\mathcal{TE}(n)}$, with $\boldsymbol{\Lambda}_n = \mathbf{I}_{p-1} + n^{-1/2}\mathbf{L}_n$ as in Theorem 2.3. Therefore, the test, $\phi_{\dagger}^{\rm sc}$ say, that rejects the null of rotational symmetry about an unspecified location $\boldsymbol{\theta}$ when $Q_{\hat{\boldsymbol{\theta}}}^{\rm sc} > \chi^2_{(p-2)(p+1)/2,1-\alpha}$ remains optimal in the Le Cam sense against the tangent elliptical alternatives introduced in Section 2.2. More precisely, this test is locally asymptotically maximin at asymptotic level α when testing $\bigcup_{\boldsymbol{\theta}\in\mathcal{S}^{p-1}} \bigcup_{g\in\mathcal{G}_a\cap\mathcal{G}'} \{\mathrm{P}_{\boldsymbol{\theta},g}^{(n)}\}$ against $\bigcup_{\boldsymbol{\theta}\in\mathcal{S}^{p-1}} \bigcup_{g\in\mathcal{G}_a\cap\mathcal{G}'} \bigcup_{\boldsymbol{\Lambda}\in\mathcal{L}_{p-1}\setminus\{\mathbf{I}_p\}} \{\mathrm{P}_{\boldsymbol{\theta},g,\boldsymbol{\Lambda}}^{\mathcal{TE}(n)}\}$. Of course, the same contiguity argument also implies that $\phi_{\dagger}^{\rm sc}$ has asymptotic power α against the local tangent vMF alternatives considered in Corollary 2.3.

3.2. Location tests: the parametric case

Under the null of rotational symmetry, as well as under local tangent vMF/elliptical alternatives, the replacement of $\boldsymbol{\theta}$ with a suitable estimator $\hat{\boldsymbol{\theta}}$ in $Q_{\boldsymbol{\theta}}^{\rm sc}$ has no asymptotic impact due to the block-diagonality of the Fisher information matrix. The story is very different for $Q_{\boldsymbol{\theta}}^{\rm loc}$: the ULAN extension of Theorem 2.4 yields that, if $\hat{\boldsymbol{\theta}}$ is an estimator of $\boldsymbol{\theta}$ satisfying $\mathrm{A}_{\mathcal{G}'}$, then

$$\boldsymbol{\Delta}_{\hat{\boldsymbol{\theta}};2}^{\mathcal{TM}(n)} - \boldsymbol{\Delta}_{\boldsymbol{\theta};2}^{\mathcal{TM}(n)} = -\boldsymbol{\Gamma}_{\boldsymbol{\theta},g;21}^{\mathcal{TM}} \sqrt{n}(\hat{\boldsymbol{\theta}} - \boldsymbol{\theta}) + o_{\rm P}(1) \tag{3.9}$$

as $n \to \infty$ under $\mathrm{P}_{\boldsymbol{\theta},g}^{(n)}$, with $g \in \mathcal{G}_a \cap \mathcal{G}'$, so that $Q_{\hat{\boldsymbol{\theta}}}^{\rm loc}$ is no more asymptotically chi-square distributed under the same sequence of (null) hypotheses. Unlike for $Q_{\boldsymbol{\theta}}^{\rm sc}$, thus, the substitution of $\hat{\boldsymbol{\theta}}$ for $\boldsymbol{\theta}$ in $Q_{\boldsymbol{\theta}}^{\rm loc}$ has a non-negligible asymptotic impact. In order to examine this impact, we first focus on the parametric case (specified g) and explore in the next section the semiparametric situation (unspecified g).

When the Fisher information matrix is not block-diagonal, it is well-known that inference on $\boldsymbol{\delta}$ (we consider the model and parametrization from Section 2.4) under unspecified $\boldsymbol{\theta}$ is to be based on the *efficient central sequence*

$$\boldsymbol{\Delta}_{\boldsymbol{\theta},g;2*}^{\mathcal{TM}(n)} := \boldsymbol{\Delta}_{\boldsymbol{\theta};2}^{\mathcal{TM}(n)} - \boldsymbol{\Gamma}_{\boldsymbol{\theta},g;21}^{\mathcal{TM}} \boldsymbol{\Gamma}_{\boldsymbol{\theta},g;11}^{-} \boldsymbol{\Delta}_{\boldsymbol{\theta},g;1}^{(n)} = \frac{1}{\sqrt{n}} \sum_{i=1}^{n} \bigg(1 - \frac{\mathcal{I}_p(g)}{\mathcal{J}_p(g)}\, \varphi_g(V_{i,\boldsymbol{\theta}})(1 - V_{i,\boldsymbol{\theta}}^2)^{1/2}\bigg) \mathbf{U}_{i,\boldsymbol{\theta}} \tag{3.10}$$

(throughout, $\mathbf{A}^-$ stands for the Moore-Penrose inverse of $\mathbf{A}$). Under $\mathrm{P}_{\boldsymbol{\theta},g}^{(n)}$,

$$\boldsymbol{\Delta}_{\boldsymbol{\theta},g;2*}^{\mathcal{TM}(n)} \overset{\mathcal{D}}{\rightsquigarrow} \mathcal{N}\big(\mathbf{0}, \boldsymbol{\Gamma}_{g,22*}^{\mathcal{TM}}\big), \qquad \text{with } \boldsymbol{\Gamma}_{g,22*}^{\mathcal{TM}} := \frac{1}{p-1}\bigg(1 - \frac{\mathcal{I}_p^2(g)}{\mathcal{J}_p(g)}\bigg)\mathbf{I}_{p-1},$$

and the corresponding test, $\phi_{\boldsymbol{\theta},g*}^{\rm loc}$ say, consists in rejecting the null of rotational symmetry ($\mathcal{H}_0 : \boldsymbol{\delta} = \mathbf{0}$) at asymptotic level α whenever

$$Q_{\boldsymbol{\theta},g*}^{\rm loc} := \big(\boldsymbol{\Delta}_{\boldsymbol{\theta},g;2*}^{\mathcal{TM}(n)}\big)' \big(\boldsymbol{\Gamma}_{g,22*}^{\mathcal{TM}}\big)^{-1} \boldsymbol{\Delta}_{\boldsymbol{\theta},g;2*}^{\mathcal{TM}(n)} > \chi^2_{p-1,1-\alpha}.$$

This test has asymptotic level α under $\mathrm{P}^{(n)}_{\boldsymbol{\theta},g}$ and is locally asymptotically maximin, under angular function $g \in \mathcal{G}_a$, in the unspecified-$\boldsymbol{\theta}$ problem. A direct application of Le Cam's third lemma yields that, under the same sequence of alternatives as the one considered in Corollary 2.3,

$$\boldsymbol{\Delta}^{\mathcal{TM}(n)}_{\boldsymbol{\theta},g;2*} \overset{\mathcal{D}}{\rightsquigarrow} \mathcal{N}\big(\mathbf{m}_g, \boldsymbol{\Gamma}^{\mathcal{TM}}_{g,22*}\big), \quad \text{with } \mathbf{m}_g := \lim_{n\to\infty} \mathrm{E}_{\boldsymbol{\theta},g}\big[\boldsymbol{\Delta}^{\mathcal{TM}(n)}_{\boldsymbol{\theta},g;2*}\big(\boldsymbol{\Delta}^{\mathcal{TM}(n)}_{\boldsymbol{\theta};2}\big)'\big]\mathbf{d}_n = \frac{1}{p-1}\bigg(1 - \frac{\mathcal{I}^2_p(g)}{\mathcal{J}_p(g)}\bigg)k\boldsymbol{\mu},$$

so that $Q^{\mathrm{loc}}_{\boldsymbol{\theta},g*} \overset{\mathcal{D}}{\rightsquigarrow} \chi^2_{p-1}(\lambda)$ with non-centrality parameter

$$\lambda = \mathbf{m}'_g\big(\boldsymbol{\Gamma}^{\mathcal{TM}}_{g,22*}\big)^{-1}\mathbf{m}_g = \frac{k^2}{p-1}\bigg(1 - \frac{\mathcal{I}^2_p(g)}{\mathcal{J}_p(g)}\bigg).$$

Note that this non-centrality parameter is smaller than or equal to the one in Corollary 2.3. The comments below Theorem 2.4 imply that the non-centrality parameter is larger than or equal to zero, with equality if and only if g is of the form $g(t) = C\exp(\kappa \arcsin(t))$. In other words, it is only for angular densities of the form $g(t) = C\exp(\kappa \arcsin(t))$ that the g-optimal unspecified-$\boldsymbol{\theta}$ test has asymptotic power α.

Now, even if we are after the construction of a parametric (g-fixed) test, the test $\phi^{\mathrm{loc}}_{\boldsymbol{\theta},g*}$ is unfortunately infeasible because $\boldsymbol{\theta}$ in practice is unknown. Proposition 3.1 of Ley et al. (2013) directly implies that if $\hat{\boldsymbol{\theta}}$ satisfies $\mathrm{A}_{\mathcal{G}'}$, then

$$\boldsymbol{\Delta}^{(n)}_{\hat{\boldsymbol{\theta}},g;1} = \boldsymbol{\Delta}^{(n)}_{\boldsymbol{\theta},g;1} - \boldsymbol{\Gamma}_{\boldsymbol{\theta},g;11}\sqrt{n}(\hat{\boldsymbol{\theta}} - \boldsymbol{\theta}) + o_{\mathrm{P}}(1) \tag{3.11}$$

as $n \to \infty$ under $\mathrm{P}^{(n)}_{\boldsymbol{\theta},g}$. Using this and (3.9), we then obtain that, again as $n \to \infty$ under $\mathrm{P}^{(n)}_{\boldsymbol{\theta},g}$,

$$\begin{aligned}
\boldsymbol{\Delta}^{\mathcal{TM}(n)}_{\hat{\boldsymbol{\theta}},g;2*} &= \boldsymbol{\Delta}^{\mathcal{TM}(n)}_{\hat{\boldsymbol{\theta}};2} - \boldsymbol{\Gamma}^{\mathcal{TM}}_{\hat{\boldsymbol{\theta}},g;21}\boldsymbol{\Gamma}^{-}_{\hat{\boldsymbol{\theta}},g;11}\boldsymbol{\Delta}^{(n)}_{\hat{\boldsymbol{\theta}},g;1}\\
&= \big(\boldsymbol{\Delta}^{\mathcal{TM}(n)}_{\boldsymbol{\theta};2} - \boldsymbol{\Gamma}^{\mathcal{TM}}_{\boldsymbol{\theta},g;21}\sqrt{n}(\hat{\boldsymbol{\theta}} - \boldsymbol{\theta})\big) - \boldsymbol{\Gamma}^{\mathcal{TM}}_{\hat{\boldsymbol{\theta}},g;21}\boldsymbol{\Gamma}^{-}_{\hat{\boldsymbol{\theta}},g;11}\big(\boldsymbol{\Delta}^{(n)}_{\boldsymbol{\theta},g;1} - \boldsymbol{\Gamma}_{\boldsymbol{\theta},g;11}\sqrt{n}(\hat{\boldsymbol{\theta}} - \boldsymbol{\theta})\big) + o_{\mathrm{P}}(1)\\
&= \boldsymbol{\Delta}^{\mathcal{TM}(n)}_{\boldsymbol{\theta},g;2*} - \boldsymbol{\Gamma}^{\mathcal{TM}}_{\boldsymbol{\theta},g;21}\sqrt{n}(\hat{\boldsymbol{\theta}} - \boldsymbol{\theta}) + \boldsymbol{\Gamma}^{\mathcal{TM}}_{\hat{\boldsymbol{\theta}},g;21}\boldsymbol{\Gamma}^{-}_{\hat{\boldsymbol{\theta}},g;11}\boldsymbol{\Gamma}_{\boldsymbol{\theta},g;11}\sqrt{n}(\hat{\boldsymbol{\theta}} - \boldsymbol{\theta}) + o_{\mathrm{P}}(1)\\
&= \boldsymbol{\Delta}^{\mathcal{TM}(n)}_{\boldsymbol{\theta},g;2*} - \boldsymbol{\Gamma}^{\mathcal{TM}}_{\boldsymbol{\theta},g;21}\sqrt{n}(\hat{\boldsymbol{\theta}} - \boldsymbol{\theta}) + \boldsymbol{\Gamma}^{\mathcal{TM}}_{\boldsymbol{\theta},g;21}\boldsymbol{\Gamma}^{-}_{\boldsymbol{\theta},g;11}\boldsymbol{\Gamma}_{\boldsymbol{\theta},g;11}\sqrt{n}(\hat{\boldsymbol{\theta}} - \boldsymbol{\theta}) + o_{\mathrm{P}}(1)\\
&= \boldsymbol{\Delta}^{\mathcal{TM}(n)}_{\boldsymbol{\theta},g;2*} + o_{\mathrm{P}}(1),
\end{aligned}$$

where the last equality follows from the fact that $(\mathbf{I}_p - \boldsymbol{\theta}\boldsymbol{\theta}')\sqrt{n}(\hat{\boldsymbol{\theta}} - \boldsymbol{\theta}) = \sqrt{n}(\hat{\boldsymbol{\theta}} - \boldsymbol{\theta}) + o_{\mathrm{P}}(1)$ as $n \to \infty$ under $\mathrm{P}^{(n)}_{\boldsymbol{\theta},g}$. Consequently, under the same sequence of hypotheses (as well as under contiguous tangent vMF alternatives),

$$Q^{\mathrm{loc}}_{\hat{\boldsymbol{\theta}},g*} = Q^{\mathrm{loc}}_{\boldsymbol{\theta},g*} + o_{\mathrm{P}}(1), \tag{3.12}$$

so that the g-parametric test ϕ^{loc}_{g*} that rejects the null at asymptotic level α whenever $Q^{\mathrm{loc}}_{\hat{\boldsymbol{\theta}},g*} > \chi^2_{p-1,1-\alpha}$ has the exact same asymptotic properties as the infeasible test $\phi^{\mathrm{loc}}_{\boldsymbol{\theta},g*}$ above. In particular, like $\phi^{\mathrm{loc}}_{\boldsymbol{\theta},g*}$, the test ϕ^{loc}_{g*} is locally asymptotically maximin at asymptotic level α when testing $\bigcup_{\boldsymbol{\theta}\in\mathcal{S}^{p-1}}\big\{\mathrm{P}^{(n)}_{\boldsymbol{\theta},g}\big\}$ against $\bigcup_{\boldsymbol{\theta}\in\mathcal{S}^{p-1}}\bigcup_{\boldsymbol{\mu}\in\mathcal{S}^{p-2}}\bigcup_{\kappa>0}\big\{\mathrm{P}^{\mathcal{TM}(n)}_{\boldsymbol{\theta},g,\boldsymbol{\mu},\kappa}\big\}$. From contiguity, (3.12) also holds under the sequence of local tangent elliptical alternatives considered in Corollary 2.1, which implies that ϕ^{loc}_{g*} has asymptotic power α under such alternatives.

3.3. Location tests: the semiparametric case

The test ϕ^{loc}_{g*} constructed above is a purely parametric test: it requires the knowledge of the underlying angular function g. In practice, of course, g may hardly be assumed to be known and it is therefore desirable to define a location test that would be valid (in the sense that is meets asymptotically the nominal level constraint) under a broad range of angular functions g. Two options are possible here. The first one aims at uniform optimality in g by reconstructing, at any g, the test statistic $Q^{\rm loc}_{\hat{\boldsymbol\theta},g*}$ above. The form of the g-efficient central sequence in (3.10) makes it clear that this requires estimating nonparametrically the optimal score function φ_g, which typically requires large sample sizes and which makes it hard to control the replacement of $\boldsymbol\theta$ with $\hat{\boldsymbol\theta}$. We therefore favour the second approach, that consists in robustifying the parametric test $\phi^{\rm loc}_{g*}$ in such a way that it remains *valid* away from the target angular function at which power optimality is to be achieved (of course, in general, the resulting test will not be *optimal* away from the selected target density).

To be more specific, assume that we target optimality at the fixed angular function f. Our goal is to define a test statistic that: (i) is asymptotically equivalent to $Q^{\rm loc}_{\hat{\boldsymbol\theta},f*}$ whenever f is the true angular function (which will ensure asymptotic optimality of the resulting test at angular function f); (ii) remains χ^2_{p-1} under the null with angular function $g\neq f$ (which will guarantee the validity away from angular function f). With these objectives in mind, consider the alternative efficient central sequence

$$\boldsymbol\Delta^{\mathcal{TM}(n)}_{\boldsymbol\theta,f;g;2*} := \boldsymbol\Delta^{\mathcal{TM}(n)}_{\boldsymbol\theta;2} - \boldsymbol\Gamma^{\mathcal{TM}}_{\boldsymbol\theta,g;21}\boldsymbol\Gamma^{-}_{\boldsymbol\theta,f;g;11}\boldsymbol\Delta^{(n)}_{\boldsymbol\theta,f;1} = \frac{1}{\sqrt{n}}\sum_{i=1}^{n}\left(1-\frac{\mathcal{I}_p(g)}{\mathcal{J}_p(f;g)}\,\varphi_f(V_{i,\boldsymbol\theta})(1-V^2_{i,\boldsymbol\theta})^{1/2}\right)\mathbf{U}_{i,\boldsymbol\theta}, \quad (3.13)$$

where $\boldsymbol\Gamma_{\boldsymbol\theta,f;g;11} := (\mathcal{J}_p(f;g)/(p-1))(\mathbf{I}_p-\boldsymbol\theta\boldsymbol\theta')$ involves the "cross-information" quantity

$$\mathcal{J}_p(f;g) := \int_{-1}^{1}\varphi_f(t)\varphi_g(t)(1-t^2)\tilde{g}_p(t)dt.$$

First note that, for $g=f$, this alternative efficient central sequence $\boldsymbol\Delta^{\mathcal{TM}(n)}_{\boldsymbol\theta,f;g;2*}$ coincides with the f-version of the efficient central sequence in (3.10), so that a test based on (3.13) will meet the objective (i) above. As for the objective (ii), Proposition 3.1 of Ley et al. (2013) actually shows that the asymptotic linearity property in (3.11) generalizes into

$$\boldsymbol\Delta^{(n)}_{\hat{\boldsymbol\theta},f;1} = \boldsymbol\Delta^{(n)}_{\boldsymbol\theta,f;1} - \boldsymbol\Gamma_{\boldsymbol\theta,f;g;11}\sqrt{n}(\hat{\boldsymbol\theta}-\boldsymbol\theta) + o_{\rm P}(1)$$

as $n\to\infty$ under ${\rm P}^{(n)}_{\boldsymbol\theta,g}$, which, jointly with (3.9), provides

$$\begin{aligned}
\boldsymbol\Delta^{\mathcal{TM}(n)}_{\hat{\boldsymbol\theta},f;g;2*} &= \boldsymbol\Delta^{\mathcal{TM}(n)}_{\hat{\boldsymbol\theta};2} - \boldsymbol\Gamma^{\mathcal{TM}}_{\hat{\boldsymbol\theta},g;21}\boldsymbol\Gamma^{-}_{\hat{\boldsymbol\theta},f;g;11}\boldsymbol\Delta^{(n)}_{\hat{\boldsymbol\theta},f;1}\\
&= \big(\boldsymbol\Delta^{\mathcal{TM}(n)}_{\boldsymbol\theta;2} - \boldsymbol\Gamma^{\mathcal{TM}}_{\boldsymbol\theta,g;21}\sqrt{n}(\hat{\boldsymbol\theta}-\boldsymbol\theta)\big) - \boldsymbol\Gamma^{\mathcal{TM}}_{\hat{\boldsymbol\theta},g;21}\boldsymbol\Gamma^{-}_{\hat{\boldsymbol\theta},f;g;11}(\boldsymbol\Delta^{(n)}_{\boldsymbol\theta,f;1} - \boldsymbol\Gamma_{\boldsymbol\theta,f;g;11}\sqrt{n}(\hat{\boldsymbol\theta}-\boldsymbol\theta)) + o_{\rm P}(1)\\
&= \boldsymbol\Delta^{\mathcal{TM}(n)}_{\boldsymbol\theta,f;g;2*} - \boldsymbol\Gamma^{\mathcal{TM}}_{\boldsymbol\theta,g;21}\sqrt{n}(\hat{\boldsymbol\theta}-\boldsymbol\theta) + \boldsymbol\Gamma^{\mathcal{TM}}_{\hat{\boldsymbol\theta},g;21}\boldsymbol\Gamma^{-}_{\hat{\boldsymbol\theta},f;g;11}\boldsymbol\Gamma_{\boldsymbol\theta,f;g;11}\sqrt{n}(\hat{\boldsymbol\theta}-\boldsymbol\theta) + o_{\rm P}(1)\\
&= \boldsymbol\Delta^{\mathcal{TM}(n)}_{\boldsymbol\theta,f;g;2*} + o_{\rm P}(1)
\end{aligned}$$

as $n\to\infty$ under ${\rm P}^{(n)}_{\boldsymbol\theta,g}$. This confirms that the alternative efficient central sequence above is defined in such a way that the replacement of $\boldsymbol\theta$ with $\hat{\boldsymbol\theta}$ has no asymptotic impact also under $g\neq f$.

Since, under ${\rm P}^{(n)}_{\boldsymbol\theta,g}$,

$$\boldsymbol\Delta^{\mathcal{TM}(n)}_{\boldsymbol\theta,f;g;2*} \overset{\mathcal{D}}{\rightsquigarrow} \mathcal{N}\big(\mathbf{0},\boldsymbol\Gamma^{\mathcal{TM}}_{f;g;22*}\big), \quad \text{with } \boldsymbol\Gamma^{\mathcal{TM}}_{f;g;22*} := \frac{1}{p-1}\left(1-\frac{2\mathcal{I}_p(g)\mathcal{H}_p(f;g)}{\mathcal{J}_p(f;g)}+\frac{\mathcal{I}^2_p(g)\mathcal{K}_p(f;g)}{\mathcal{J}^2_p(f;g)}\right)\mathbf{I}_{p-1},$$

where we let

$$\mathcal{H}_p(f;g) := \int_{-1}^{1}\varphi_f(t)(1-t^2)^{1/2}\tilde{g}_p(t)dt \quad\text{and}\quad \mathcal{K}_p(f;g) := \int_{-1}^{1}\varphi^2_f(t)(1-t^2)\tilde{g}_p(t)dt,$$

the resulting test rejects the null at asymptotic level α whenever

$$Q^{\rm loc}_{\hat{\boldsymbol\theta},f;g*} := \big(\boldsymbol\Delta^{\mathcal{TM}(n)}_{\hat{\boldsymbol\theta},f;g;2*}\big)'\big(\boldsymbol\Gamma^{\mathcal{TM}}_{f;g;22*}\big)^{-1}\boldsymbol\Delta^{\mathcal{TM}(n)}_{\hat{\boldsymbol\theta},f;g;2*} > \chi^2_{p-1,1-\alpha}. \tag{3.14}$$

Le Cam's third lemma allows to show that, under the sequence of alternatives considered in Corollary 2.3, $\boldsymbol\Delta^{\mathcal{TM}(n)}_{\boldsymbol\theta,f;g;2*}$ is asymptotically normal with covariance $\boldsymbol\Gamma^{\mathcal{TM}}_{f;g;22*}$ and mean

$$\mathbf{m}_{f;g} := \lim_{n\to\infty} \mathrm{E}_{\boldsymbol\theta,g}\big[\boldsymbol\Delta^{\mathcal{TM}(n)}_{\boldsymbol\theta,f;g;2*}\big(\boldsymbol\Delta^{\mathcal{TM}(n)}_{\boldsymbol\theta;2}\big)'\big]k_n\boldsymbol\mu = \frac{1}{p-1}\left(1-\frac{\mathcal{I}_p(f)\mathcal{H}_p(f;g)}{\mathcal{J}_p(f;g)}\right)k\boldsymbol\mu,$$

so that $Q^{\rm loc}_{\boldsymbol\theta;f;g*}$ (hence also, $Q^{\rm loc}_{\hat{\boldsymbol\theta};f;g*}$) is asymptotically $\chi^2_{p-1}(\lambda)$ with non-centrality parameter λ given by

$$\mathbf{m}'_{f;g}\big(\boldsymbol\Gamma^{\mathcal{TM}}_{f;g;22*}\big)^{-1}\mathbf{m}_{f;g} = \frac{k^2}{p-1}\left(1-\frac{\mathcal{I}_p(g)\mathcal{H}_p(f;g)}{\mathcal{J}_p(f;g)}\right)^2\Bigg/\left(1-\frac{2\mathcal{I}_p(g)\mathcal{H}_p(f;g)}{\mathcal{J}_p(f;g)}+\frac{\mathcal{I}^2_p(g)\mathcal{K}_p(f;g)}{\mathcal{J}^2_p(f;g)}\right). \tag{3.15}$$

Now, since the test statistic (3.14) still depends on the unknown underlying angular function g, turning this pseudo-test into a genuine test requires estimating consistently the quantities $\mathcal{I}_p(g)$, $\mathcal{J}_p(f;g)$, $\mathcal{H}_p(f;g)$, and $\mathcal{K}_p(f;g)$. To that aim, we express them as

$$\mathcal{I}_p(g) = (p-2)\,\mathrm{E}_{\boldsymbol\theta,g}\left[\frac{V_{1,\boldsymbol\theta}}{(1-V^2_{1,\boldsymbol\theta})^{1/2}}\right],\quad \mathcal{J}_p(f;g) = (p-1)\,\mathrm{E}_{\boldsymbol\theta,g}[\varphi_f(V_{1,\boldsymbol\theta})V_{1,\boldsymbol\theta}] - \mathrm{E}_{\boldsymbol\theta,g}[\varphi'_f(V_{1,\boldsymbol\theta})(1-V^2_{1,\boldsymbol\theta})],$$

$$\mathcal{H}_p(f;g) := \mathrm{E}_{\boldsymbol\theta,g}[\varphi_f(V_{1,\boldsymbol\theta})(1-V^2_{1,\boldsymbol\theta})^{1/2}],\quad \mathcal{K}_p(f;g) := \mathrm{E}_{\boldsymbol\theta,g}[\varphi^2_f(V_{1,\boldsymbol\theta})(1-V^2_{1,\boldsymbol\theta})]$$

(the fist two identities are obtained from integration by parts, assuming that φ_f is differentiable). Natural estimators of these quantities are

$$\hat{\mathcal{I}}_p(g) := \frac{p-2}{n}\sum_{i=1}^n \frac{V_{i,\hat{\boldsymbol\theta}}}{(1-V^2_{i,\hat{\boldsymbol\theta}})^{1/2}},\qquad \hat{\mathcal{J}}_p(f;g) := \frac{p-1}{n}\sum_{i=1}^n \varphi_f(V_{i,\hat{\boldsymbol\theta}})V_{i,\hat{\boldsymbol\theta}} - \frac{1}{n}\sum_{i=1}\varphi'_f(V_{i,\hat{\boldsymbol\theta}})(1-V^2_{i,\hat{\boldsymbol\theta}}),$$

$$\hat{\mathcal{H}}_p(f;g) := \frac{1}{n}\sum_{i=1}^n \varphi_f(V_{i,\hat{\boldsymbol\theta}})(1-V^2_{i,\hat{\boldsymbol\theta}})^{1/2},\quad \hat{\mathcal{K}}_p(f;g) := \frac{1}{n}\sum_{i=1}^n \varphi^2_f(V_{i,\hat{\boldsymbol\theta}})(1-V^2_{i,\hat{\boldsymbol\theta}}),$$

at any g for which $\mathcal{I}_p(g)$, $\mathcal{J}_p(f;g)$, $\mathcal{H}_p(f;g)$, and $\mathcal{K}_p(f;g)$ are finite. Consistency follows by successively applying the weak law of large numbers, under $\mathrm{P}^{(n)}_{\boldsymbol\theta+n^{1/2}\mathbf{t}_n,g}$, with $\boldsymbol\theta+n^{1/2}\mathbf{t}_n\in\mathcal{S}^{p-1}$, to random variables of the form $n^{-1}\sum_{i=1}^n H_f(V_{i,\boldsymbol\theta+n^{1/2}\mathbf{t}_n})$ (with H_f a suitable function), the general version of the Le Cam's third lemma (see, e.g., Theorem 6.6 in van der Vaart (1998)), and then Lemma 4.4 from Kreiss (1987).

We consider now the important particular case $f_\eta(r) = \exp(\eta r)$ and derive an applicable version of (3.14). Since $f_\eta\in\mathcal{G}_a$ is the vMF angular function with concentration parameter η (we avoid using the standard notation κ, as this notation was used to denote the skewness intensity in the tangent vMF model), we have $\varphi_{f_\eta}(r)=\eta$. Letting

$$D_{p,g} := \frac{(p-2)\,\mathrm{E}_{\boldsymbol\theta,g}[V_{1,\boldsymbol\theta}(1-V^2_{1,\boldsymbol\theta})^{-1/2}]}{(p-1)\,\mathrm{E}_{\boldsymbol\theta,g}[V_{1,\boldsymbol\theta}]},$$

we have

$$\boldsymbol\Delta^{\mathcal{TM}(n)}_{\boldsymbol\theta,\mathrm{vMF},g;2*} := \boldsymbol\Delta^{\mathcal{TM}(n)}_{\boldsymbol\theta,f_\eta;g;2*} = \frac{1}{\sqrt{n}}\sum_{i=1}^n\Big(1-D_{p,g}\,(1-V^2_{i,\boldsymbol\theta})^{1/2}\Big)\mathbf{U}_{i,\boldsymbol\theta}$$

and

$$\boldsymbol\Gamma^{\mathcal{TM}(n)}_{\mathrm{vMF},g;22*} := \boldsymbol\Gamma^{\mathcal{TM}}_{f_\eta;g;22*} = \frac{1}{p-1}\left(1-2D_{p,g}\mathrm{E}_{\boldsymbol\theta,g}[(1-V^2_{1,\boldsymbol\theta})^{1/2}]+D^2_{p,g}(1-\mathrm{E}_{\boldsymbol\theta,g}[V^2_{1,\boldsymbol\theta}])\right)\mathbf{I}_{p-1},$$

where the notation is justified by the fact that, quite nicely, the f_η-efficient central sequence and corresponding Fisher information matrix do not depend on η. In the present case, the quantities to be estimated consistently are therefore

$$\mathrm{E}_{\boldsymbol{\theta},g}[V_{1,\boldsymbol{\theta}}(1-V_{1,\boldsymbol{\theta}}^2)^{-1/2}], \qquad \mathrm{E}_{\boldsymbol{\theta},g}[(1-V_{1,\boldsymbol{\theta}}^2)^{1/2}], \qquad \mathrm{E}_{\boldsymbol{\theta},g}[V_{1,\boldsymbol{\theta}}], \quad \text{and} \quad \mathrm{E}_{\boldsymbol{\theta},g}[V_{1,\boldsymbol{\theta}}^2], \tag{3.16}$$

and the corresponding estimators are

$$\frac{1}{n}\sum_{i=1}^n V_{i,\hat{\boldsymbol{\theta}}}(1-V_{i,\hat{\boldsymbol{\theta}}}^2)^{-1/2}, \qquad \frac{1}{n}\sum_{i=1}^n (1-V_{i,\hat{\boldsymbol{\theta}}}^2)^{1/2}, \qquad \frac{1}{n}\sum_{i=1}^n V_{i,\hat{\boldsymbol{\theta}}}, \quad \text{and} \quad \frac{1}{n}\sum_{i=1}^n V_{i,\hat{\boldsymbol{\theta}}}^2, \tag{3.17}$$

respectively. The same argument as above proves consistency of these estimators at any g in the collection $\mathcal{G}_b$ of angular functions for which (the rest of expectations in (3.16) are trivially finite for any g)

$$\mathrm{E}_{\boldsymbol{\theta},g}[V_{1,\boldsymbol{\theta}}(1-V_{1,\boldsymbol{\theta}}^2)^{-1/2}] = \int_{-1}^1 t(1-t^2)^{-1/2}\,\tilde{g}_p(t)\,dt < \infty. \tag{3.18}$$

The resulting test, $\phi_{\mathrm{vMF}}^{\mathrm{loc}}$ say, rejects the null whenever

$$Q_{\mathrm{vMF}}^{\mathrm{loc}} := \big(\widehat{\boldsymbol{\Delta}}_{\hat{\boldsymbol{\theta}},\mathrm{vMF};g;2*}^{\mathcal{TM}(n)}\big)'\big(\widehat{\boldsymbol{\Gamma}}_{\mathrm{vMF};g;22*}^{\mathcal{TM}(n)}\big)^{-1}\widehat{\boldsymbol{\Delta}}_{\hat{\boldsymbol{\theta}},\mathrm{vMF};g;2*}^{\mathcal{TM}(n)} > \chi^2_{p-1,1-\alpha},$$

where $\widehat{\boldsymbol{\Delta}}_{\boldsymbol{\theta},\mathrm{vMF};g;2*}^{\mathcal{TM}(n)}$ and $\widehat{\boldsymbol{\Gamma}}_{\boldsymbol{\theta},\mathrm{vMF};g;22*}^{\mathcal{TM}(n)}$ result from $\boldsymbol{\Delta}_{\boldsymbol{\theta},\mathrm{vMF};g;2*}^{\mathcal{TM}(n)}$ and $\boldsymbol{\Gamma}_{\mathrm{vMF};g;22*}^{\mathcal{TM}(n)}$, respectively, by replacing $\boldsymbol{\theta}$ with $\hat{\boldsymbol{\theta}}$ and the quantities in (3.16) with their consistent estimators in (3.17). This test was built to be locally asymptotically maximin at asymptotic level α when testing

$$\bigcup_{\boldsymbol{\theta}\in\mathcal{S}^{p-1}}\ \bigcup_{g\in\mathcal{G}_a\cap\mathcal{G}_b\cap\mathcal{G}'}\{\mathrm{P}_{\boldsymbol{\theta},g}^{(n)}\} \quad \text{against} \quad \bigcup_{\boldsymbol{\theta}\in\mathcal{S}^{p-1}}\ \bigcup_{\boldsymbol{\mu}\in\mathcal{S}^{p-2}}\ \bigcup_{\kappa>0}\{\mathrm{P}_{\boldsymbol{\theta},f_\eta,\boldsymbol{\mu},\kappa}^{\mathcal{TM}(n)}\}.$$

Note that, for $p\geq 3$, the finiteness condition in (3.18) holds as soon as the angular function g is bounded in a neighbourhood of 1. Remarkably, $Q_{\mathrm{vMF}}^{\mathrm{loc}}$ does not depend on η, so that $\phi_{\mathrm{vMF}}^{\mathrm{loc}}$ is locally asymptotically maximin at asymptotic level α when testing

$$\bigcup_{\boldsymbol{\theta}\in\mathcal{S}^{p-1}}\ \bigcup_{g\in\mathcal{G}_a\cap\mathcal{G}_b\cap\mathcal{G}'}\{\mathrm{P}_{\boldsymbol{\theta},g}^{(n)}\} \quad \text{against} \quad \bigcup_{\boldsymbol{\theta}\in\mathcal{S}^{p-1}}\ \bigcup_{\eta>0}\ \bigcup_{\boldsymbol{\mu}\in\mathcal{S}^{p-2}}\ \bigcup_{\kappa>0}\{\mathrm{P}_{\boldsymbol{\theta},f_\eta,\boldsymbol{\mu},\kappa}^{\mathcal{TM}(n)}\}$$

(in other words, when testing rotational symmetry with $(\boldsymbol{\theta},g)$ unspecified against $\mathcal{TM}_p(\boldsymbol{\theta},f_\eta,\kappa)$ distributions, with $(\boldsymbol{\theta},\eta,\kappa)$ unspecified), that is, it is optimal in the Le Cam sense as soon as the underlying angular function g is vMF, irrespectively of the corresponding concentration η. It is easy to show, however, that this vMF location test still has asymptotic power α against the local tangent elliptical alternatives considered in Corollary 2.1.

4. Hybrid tests

The location and scatter tests, either in the $\boldsymbol{\theta}$-specified or $\boldsymbol{\theta}$-unspecified situations, are based on the empirical checking of the moment conditions (2.3) and (2.4). Both are necessary conditions for the uniformity of the sign vector $\mathbf{u}_{\boldsymbol{\theta}}(\mathbf{X})$ over $\mathcal{S}^{p-2}$, and hence for rotational symmetry. For the families of alternatives introduced in Section 2.2, the tests present rather extreme behaviours: either they are optimal in the Le Cam sense, or they are *blind* to the alternatives. While this antithesis is desirable for testing against a specific kind of alternative, it is also a double-edged sword, since knowing the alternative on which rotational symmetry might be violated is sometimes hard in practice, specially for high dimensional settings. As we explain below, a possible way out is to construct *hybrid* tests that show non-trivial asymptotic powers against both types of alternatives considered (without being optimal against any of them).

Consider first the problem of testing rotational symmetry about a specified location $\boldsymbol{\theta}$. Since $\mathrm{vec}\,(\mathbf{U}_{i,\boldsymbol{\theta}}\mathbf{U}'_{i,\boldsymbol{\theta}})$ and $\mathbf{U}_{i,\boldsymbol{\theta}}$ are uncorrelated, then $\boldsymbol{\Delta}^{\mathcal{TE}(n)}_{\boldsymbol{\theta};2}$ and $\boldsymbol{\Delta}^{\mathcal{TM}(n)}_{\boldsymbol{\theta};2}$ are uncorrelated, too. The CLT then readily entails that, under $\mathrm{P}^{(n)}_{\boldsymbol{\theta},g}$,

$$\begin{pmatrix} \boldsymbol{\Delta}^{\mathcal{TM}(n)}_{\boldsymbol{\theta};2} \\ \boldsymbol{\Delta}^{\mathcal{TE}(n)}_{\boldsymbol{\theta};2} \end{pmatrix} \overset{\mathcal{D}}{\rightsquigarrow} \mathcal{N}\left(\begin{pmatrix} \mathbf{0} \\ \mathbf{0} \end{pmatrix}, \begin{pmatrix} \boldsymbol{\Gamma}^{\mathcal{TM}}_{22} & \mathbf{0} \\ \mathbf{0} & \boldsymbol{\Gamma}^{\mathcal{TE}}_{\boldsymbol{\theta};22} \end{pmatrix} \right), \tag{4.19}$$

which implies that, under $\mathcal{H}_{0,\boldsymbol{\theta}}$,

$$Q^{\mathrm{hyb}}_{\boldsymbol{\theta}} := Q^{\mathrm{loc}}_{\boldsymbol{\theta}} + Q^{\mathrm{sc}}_{\boldsymbol{\theta}} = \big(\boldsymbol{\Delta}^{\mathcal{TM}(n)}_{\boldsymbol{\theta};2}\big)'\big(\boldsymbol{\Gamma}^{\mathcal{TM}}_{22}\big)^{-1}\boldsymbol{\Delta}^{\mathcal{TM}(n)}_{\boldsymbol{\theta};2} + \big(\boldsymbol{\Delta}^{\mathcal{TE}(n)}_{\boldsymbol{\theta};2}\big)'\big(\boldsymbol{\Gamma}^{\mathcal{TE}}_{\boldsymbol{\theta};22}\big)^{-1}\boldsymbol{\Delta}^{\mathcal{TE}(n)}_{\boldsymbol{\theta};2} \overset{\mathcal{D}}{\rightsquigarrow} \chi^2_{(p-1)+(p-2)(p+1)/2}.$$

The resulting hybrid test, $\phi^{\mathrm{hyb}}_{\boldsymbol{\theta}}$ say, then rejects the null at asymptotic level α whenever

$$Q^{\mathrm{hyb}}_{\boldsymbol{\theta}} > \chi^2_{(p-1)+(p-2)(p+1)/2,1-\alpha}. \tag{4.20}$$

As announced, this test can detect both contiguous tangent elliptical and tangent vMF alternatives. More precisely, we have the following result.

COROLLARY 4.1. *Fix $\boldsymbol{\theta} \in \mathcal{S}^{p-1}$ and $g \in \mathcal{G}_a$. Let $\boldsymbol{\Lambda}_n$, $(\mathbf{L}_n)$, κ_n, and (k_n) be as in Corollaries 2.1 and 2.3. Then: (i) under $\mathrm{P}^{\mathcal{TE}(n)}_{\boldsymbol{\theta},g,\boldsymbol{\Lambda}_n}$, $Q^{\mathrm{hyb}}_{\boldsymbol{\theta}} \overset{\mathcal{D}}{\rightsquigarrow} \chi^2_{(p-1)+(p-2)(p+1)/2}(\lambda)$, with $\lambda = (p-1)\mathrm{tr}[\mathbf{L}^2]/(2(p+1))$; (ii) under $\mathrm{P}^{\mathcal{TM}(n)}_{\boldsymbol{\theta},g,\boldsymbol{\mu}_n,\kappa_n}$, $Q^{\mathrm{hyb}}_{\boldsymbol{\theta}} \overset{\mathcal{D}}{\rightsquigarrow} \chi^2_{(p-1)+(p-2)(p+1)/2}(\lambda)$, with $\lambda = k^2/(p-1)$.*

Let us then turn to the $\boldsymbol{\theta}$-unspecified problem. In the parametric case considered in Section 3.2, $\boldsymbol{\Delta}^{\mathcal{TM}(n)}_{\boldsymbol{\theta},g;2*}$ and $\boldsymbol{\Delta}^{\mathcal{TE}(n)}_{\boldsymbol{\theta};2}$ are still asymptotically normal with a block diagonal asymptotic covariance matrix, which leads to considering the hybrid test statistic $Q^{\mathrm{hyb}}_{\boldsymbol{\theta},g*} := Q^{\mathrm{loc}}_{\boldsymbol{\theta},g*} + Q^{\mathrm{sc}}_{\boldsymbol{\theta}}$. This test statistic, hence also (in view of (3.12)) its feasible version $Q^{\mathrm{hyb}}_{\hat{\boldsymbol{\theta}},g*}$, is asymptotically $\chi^2_{(p-1)+(p-2)(p+1)/2}$ under $\mathrm{P}^{(n)}_{\boldsymbol{\theta},g}$, so that the resulting parametric hybrid test rejects the null at asymptotic level α if $Q^{\mathrm{hyb}}_{\hat{\boldsymbol{\theta}},g*}$ exceeds the same critical value as in (4.20). The same argument entails that, for the semiparametric case of Section 3.3, $Q^{\mathrm{hyb}}_{\hat{\boldsymbol{\theta}},f;g*} := Q^{\mathrm{loc}}_{\hat{\boldsymbol{\theta}},f;g*} + Q^{\mathrm{sc}}_{\hat{\boldsymbol{\theta}}}$ and $Q^{\mathrm{hyb}}_{\mathrm{vMF}} := Q^{\mathrm{sc}}_{\mathrm{vMF}} + Q^{\mathrm{sc}}_{\hat{\boldsymbol{\theta}}}$ converge in law to a $\chi^2_{(p-1)+(p-2)(p+1)/2}$ under $\mathrm{P}^{(n)}_{\boldsymbol{\theta},g}$; in the sequel, we denote as $\phi^{\mathrm{hyb}}_{\mathrm{vMF}}$ the test rejecting the null at asymptotic level α when $Q^{\mathrm{hyb}}_{\mathrm{vMF}} > \chi^2_{(p-1)+(p-2)(p+1)/2,1-\alpha}$. It is easy to check that, like their $\boldsymbol{\theta}$-specified counterpart $\phi^{\mathrm{hyb}}_{\boldsymbol{\theta}}$, these hybrid $\boldsymbol{\theta}$-unspecified tests can detect both types of alternatives considered. This fact is of key practical importance in data applications for which the alternative to rotational symmetry is unknown, as evidenced by the real data examples given in Section 6.

5. Simulations

In this section, we investigate the finite-sample performances of the proposed tests through Monte Carlo studies. In the specified-$\boldsymbol{\theta}$ problem, we will consider the tests $\phi^{\mathrm{loc}}_{\boldsymbol{\theta}}$ and $\phi^{\mathrm{sc}}_{\boldsymbol{\theta}}$ from Section 2.1, as well as the hybrid test $\phi^{\mathrm{hyb}}_{\boldsymbol{\theta}}$ from Section 4. As explained in Section 2.1, these tests look for possible departures from rotational symmetry about $\boldsymbol{\theta}$ by checking whether or not the sign vector is uniformly distributed over $\mathcal{S}^{p-2}$. Clearly, competing tests for rotational symmetry about $\boldsymbol{\theta}$ can be obtained by applying other tests of uniformity over $\mathcal{S}^{p-2}$, such as (for $p = 3$) the well-known Kuiper's test or (for $p > 3$) the Giné's test; see pages 99 and 209 of Mardia and Jupp (2000), respectively. This generates a Kuiper test $\phi_{\boldsymbol{\theta}}^{\mathrm{Kui}}$ of rotational symmetry on $\mathcal{S}^2$ and a Giné test $\phi_{\boldsymbol{\theta}}^{\mathrm{Gin}}$ of rotational symmetry on $\mathcal{S}^{p-1}$ with $p > 3$, both about a specified $\boldsymbol{\theta}$. Since they are based on omnibus tests of uniformity over $\mathcal{S}^{p-2}$, both $\phi_{\boldsymbol{\theta}}^{\mathrm{Kui}}$, and $\phi_{\boldsymbol{\theta}}^{\mathrm{Gin}}$ are expected to show some power against both tangent vMF and tangent elliptical alternatives. Still for the specified-$\boldsymbol{\theta}$ problem, we will also consider the semiparametric test from Ley and Verdebout (2017b), denoted as $\phi_{\boldsymbol{\theta}}^{\mathrm{LV}}$. Now, for the $\boldsymbol{\theta}$-unspecified problem, we will restrict to the proposed semiparametric tests $\phi_{\dagger}^{\mathrm{sc}}$, $\phi_{\mathrm{vMF}}^{\mathrm{loc}}$, and $\phi_{\mathrm{vMF}}^{\mathrm{hyb}}$, from Sections 3.1, 3.3, and 4, respectively. To the best of our knowledge, indeed, these unspecified-$\boldsymbol{\theta}$ tests have no competitors in the literature. In particular, it is unclear how to turn the omnibus specified-$\boldsymbol{\theta}$ tests $\phi_{\boldsymbol{\theta}}^{\mathrm{Kui}}$ and $\phi_{\boldsymbol{\theta}}^{\mathrm{Gin}}$ into unspecified-$\boldsymbol{\theta}$ ones.

5.1. The unspecified-$\boldsymbol{\theta}$ problem on $\mathcal{S}^2$

The first simulation exercise focuses on the unspecified-$\boldsymbol{\theta}$ problem and intends to show, in particular, that using specified-$\boldsymbol{\theta}$ tests with a misspecified value of $\boldsymbol{\theta}$ leads to violation of the nominal level constraint. For two sample sizes ($n = 100, 200$) and two types of alternatives to rotational symmetry ($r = 1, 2$), we generated $N = 5000$ mutually independent random samples of the form

$$\mathbf{X}_{i;\ell}^{(r)}, \quad i = 1, \ldots, n, \quad \ell = 0, \ldots, 5, \quad r = 1, 2,$$

with values in $\mathcal{S}^2$. The $\mathbf{X}_{i;\ell}^{(1)}$'s follow a $\mathcal{TE}_3(\boldsymbol{\theta}_0, g_1, \boldsymbol{\Lambda}_\ell)$ with location $\boldsymbol{\theta}_0 := (1/\sqrt{2}, -1/\sqrt{2}, 0)'$, angular function $t \mapsto g_1(t) := \exp(2t)$, and shape $\boldsymbol{\Lambda}_\ell := \mathrm{diag}(1 + \ell/2, 1)/(2 + \ell/2)$. The $\mathbf{X}_{i;\ell}^{(2)}$'s follow a $\mathcal{TM}_3(\boldsymbol{\theta}_0, g_1, \boldsymbol{\mu}, \kappa_\ell)$ with skewness direction $\boldsymbol{\mu} := (1, 0)'$ and skewness intensity $\kappa_\ell := \ell$. In both cases, $\ell = 0$ corresponds to the null of rotational symmetry, whereas $\ell = 1, \ldots, 5$ provide increasingly severe alternatives. For each replication, we performed, at asymptotic level $\alpha = 5\%$, the specified-$\boldsymbol{\theta}$ tests $\phi_{\boldsymbol{\theta}}^{\mathrm{loc}}$, $\phi_{\boldsymbol{\theta}}^{\mathrm{sc}}$, $\phi_{\boldsymbol{\theta}}^{\mathrm{hyb}}$, $\phi_{\boldsymbol{\theta}}^{\mathrm{LV}}$, and $\phi_{\boldsymbol{\theta}}^{\mathrm{Kui}}$, all based on the *misspecified* location value $\boldsymbol{\theta} := (1, 0, 0)'$, and the unspecified-$\boldsymbol{\theta}$ tests $\phi_{\dagger}^{\mathrm{sc}}$, $\phi_{\mathrm{vMF}}^{\mathrm{loc}}$, and $\phi_{\mathrm{vMF}}^{\mathrm{hyb}}$, all computed with the spherical mean to estimate $\boldsymbol{\theta}$.

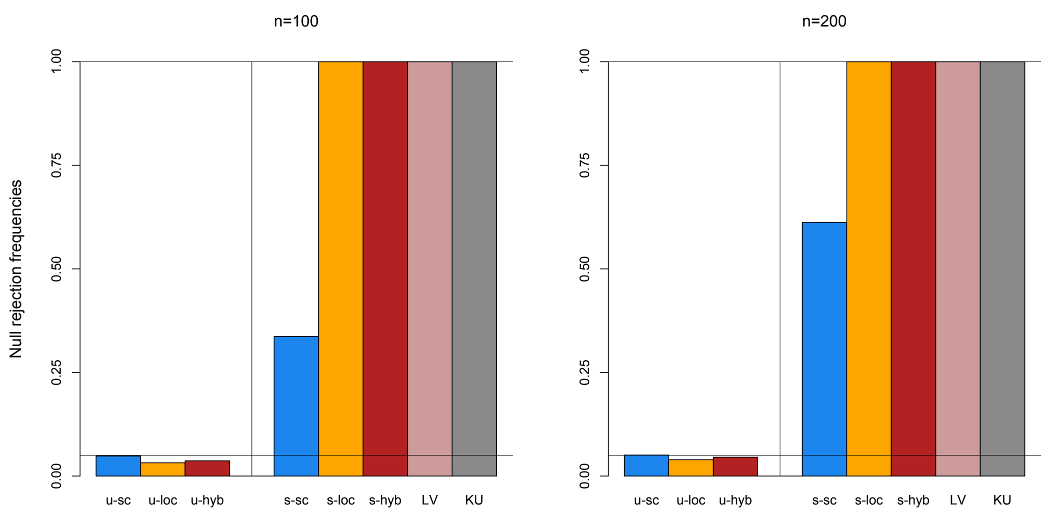

Fig. 2. Null rejection frequencies, for sample sizes $n = 100$ and $n = 200$, of the unspecified-$\boldsymbol{\theta}$ tests $\phi_{\dagger}^{\mathrm{sc}}$ (u-sc), $\phi_{\mathrm{vMF}}^{\mathrm{loc}}$ (u-loc), and $\phi_{\mathrm{vMF}}^{\mathrm{hyb}}$ (u-hyb), as well as the (mis)specified-$\boldsymbol{\theta}$ tests $\phi_{\boldsymbol{\theta}}^{\mathrm{sc}}$ (s-sc), $\phi_{\boldsymbol{\theta}}^{\mathrm{loc}}$ (s-loc), $\phi_{\boldsymbol{\theta}}^{\mathrm{hyb}}$ (s-hyb), $\phi_{\boldsymbol{\theta}}^{\mathrm{LV}}$ (LV), and $\phi_{\boldsymbol{\theta}}^{\mathrm{Kui}}$ (KU). All tests are performed at asymptotic level 5%; see Section 5.1 for details.

Due to misspecification, it is expected that only the unspecified-$\boldsymbol{\theta}$ tests will exhibit null rejection frequencies close to 5%. This is confirmed in Figure 2, that shows that all (mis)specified-$\boldsymbol{\theta}$ tests are severely liberal. For the two samples sizes and the two types of alternatives considered, Figure 3 plots the empirical powers of the three unspecified-$\boldsymbol{\theta}$ tests (a power comparison involving the specified-$\boldsymbol{\theta}$ tests would be meaningless since these tests do not meet the level constraint). Inspection of Figure 3 reveals that: (i) as expected, $\phi_{\dagger}^{\rm sc}$ dominates $\phi_{\dagger}^{\rm loc}$ under tangent elliptical alternatives while the opposite occurs under tangent vMF alternatives; (ii) the hybrid test detects both types of alternatives and performs particularly well against tangent vMF ones.

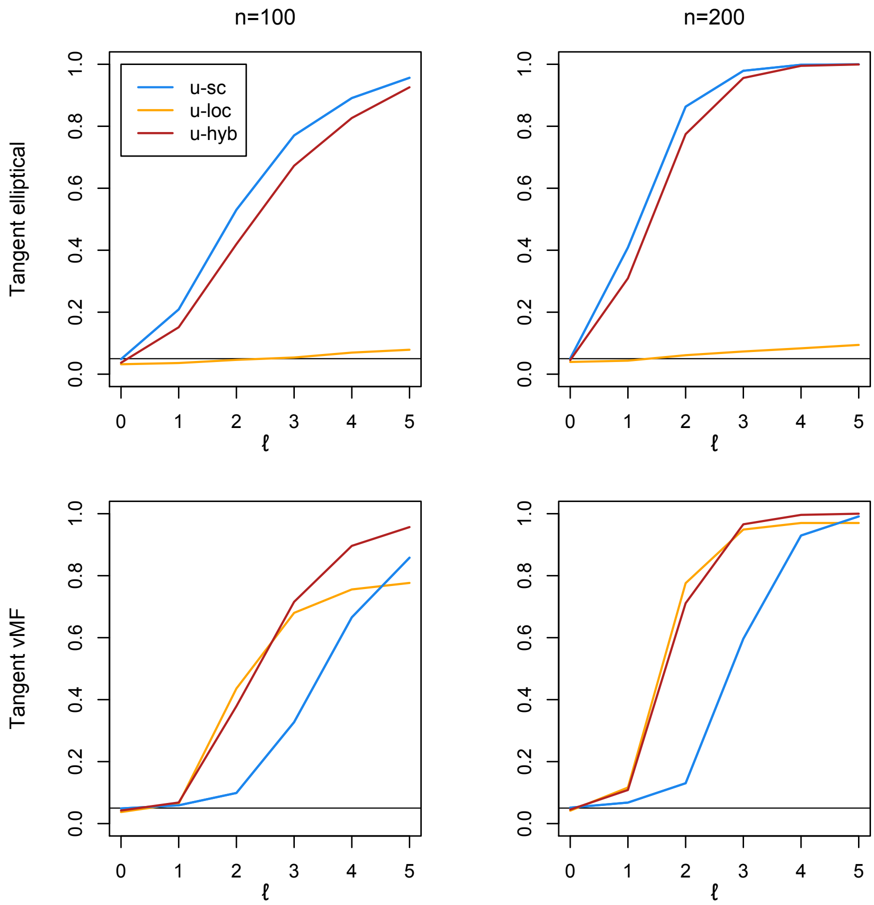

Fig. 3. Rejection frequencies, under tangent elliptical alternatives (top row) and tangent vMF ones (bottom row), of the unspecified-$\boldsymbol{\theta}$ tests $\phi_{\dagger}^{\rm sc}$, $\phi_{\rm vMF}^{\rm loc}$, and $\phi_{\rm vMF}^{\rm hyb}$ for $n = 100$ (left column) and $n = 200$ (right column). Both tests are performed at asymptotic level 5%; see Section 5.1 for details.

5.2. The specified-$\boldsymbol{\theta}$ problem on $\mathcal{S}^2$

The second simulation exercise focuses on the specified-$\boldsymbol{\theta}$ problem on $\mathcal{S}^2$. We generated $N = 5000$ mutually independent random samples of the form

$$\mathbf{X}_{i;\ell}^{(r)}, \quad i = 1, \ldots, n, \quad \ell = 0, \ldots, 5, \quad r = 1, 2, 3,$$

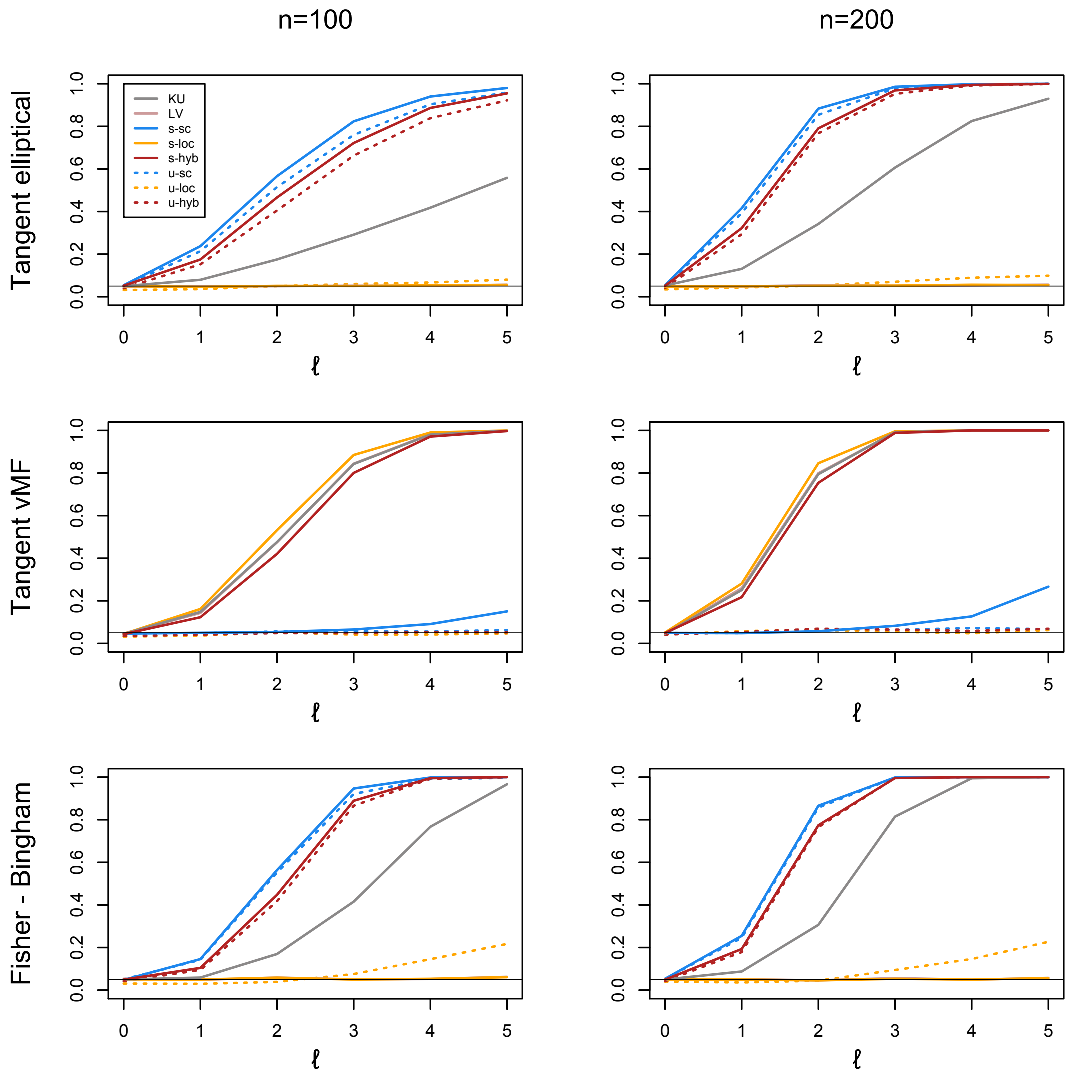

Fig. 4. Rejection frequencies, under tangent elliptical alternatives (top row), tangent vMF alternatives (middle row), and Fisher-Bingham alternatives (bottom row), of the specified-$\boldsymbol{\theta}$ tests $\phi_{\boldsymbol{\theta}}^{\rm sc}$ (s-sc), $\phi_{\boldsymbol{\theta}}^{\rm loc}$ (s-loc), $\phi_{\boldsymbol{\theta}}^{\rm hyb}$ (s-hyb), $\phi_{\boldsymbol{\theta}}^{\rm LV}$ (LV), and $\phi_{\boldsymbol{\theta}}^{\rm Kui}$ (KU), as well as the unspecified-$\boldsymbol{\theta}$ tests $\phi_{\dagger}^{\rm sc}$ (u-sc), $\phi_{\rm vMF}^{\rm loc}$ (u-loc), and $\phi_{\dagger}^{\rm hyb}$ (u-hyb). Sample sizes are $n = 100$ (left column) and $n = 200$ (right column). All tests are performed at asymptotic level 5%; see Section 5.2 for details.

with values in $\mathcal{S}^2$. The $\mathbf{X}_{i;\ell}^{(1)}$'s follow a $\mathcal{TE}_3(\boldsymbol{\theta}, g_2, \boldsymbol{\Lambda}_\ell)$, whereas the $\mathbf{X}_{i;\ell}^{(2)}$'s follow a $\mathcal{TM}_3(\boldsymbol{\theta}, g_2, \boldsymbol{\mu}, \kappa_\ell)$ with angular function $t \mapsto g_2(t) := \exp(5t)$ and skewness intensity $\kappa_\ell := \ell/6$. The $\mathbf{X}_{i;\ell}^{(3)}$'s have a Fisher-Bingham distribution with location $\boldsymbol{\theta}$, concentration 2, and shape matrix $\mathbf{A}_\ell := {\rm diag}(0, \ell/2, -\ell/2)$; we refer to Mardia and Jupp (2000) for details on Fisher-Bingham distributions, which, for the zero shape matrix, reduce to a vMF distribution. For $r = 1, 2, 3$, thus, the value $\ell = 0$ corresponds to the null of rotational symmetry about $\boldsymbol{\theta}$, whereas $\ell = 1, \ldots, 5$ provide increasingly severe alternatives. For each replication, we performed, at asymptotic level $\alpha = 5\%$, the specified-$\boldsymbol{\theta}$ tests $\phi_{\boldsymbol{\theta}}^{\rm loc}$, $\phi_{\boldsymbol{\theta}}^{\rm sc}$, $\phi_{\boldsymbol{\theta}}^{\rm hyb}$, $\phi_{\boldsymbol{\theta}}^{\rm LV}$, and $\phi_{\boldsymbol{\theta}}^{\rm Kui}$ (based on the true value of $\boldsymbol{\theta}$). For the sake of comparison, we also considered the unspecified-$\boldsymbol{\theta}$ tests $\phi_{\dagger}^{\rm sc}$,

$\phi^{\rm loc}_{\rm vMF}$, and $\phi^{\rm hyb}_{\rm vMF}$, based on the spherical mean.

Figure 4 plots the resulting empirical power curves for sample sizes $n = 100$ and $n = 200$. Inspection of the figure confirms the theoretical results: (i) $\phi^{\rm sc}_{\boldsymbol\theta}$ dominates the other tests under tangent elliptical alternatives, whereas $\phi^{\rm loc}_{\boldsymbol\theta}$ dominates the other tests under tangent vMF alternatives (even if the latter dominance is less prominent); (ii) $\phi^{\rm sc}_{\boldsymbol\theta}$ and $\phi^{\rm sc}_{\dagger}$ exhibit extremely similar performances, which is in line with their asymptotic equivalence (see Proposition 3.1 and the comments below that result); (iii) the tests $\phi^{\rm hyb}_{\boldsymbol\theta}$ and $\phi^{\rm Kui}_{\boldsymbol\theta}$ show non-trivial powers against each type of alternatives but are always dominated by some other test. Moreover, it should be noted that $\phi^{\rm sc}_{\boldsymbol\theta}$ and $\phi^{\rm hyb}_{\boldsymbol\theta}$ perform well under Fisher-Bingham alternatives, which was expected since, parallel to tangent elliptical alternatives, Fisher-Bingham alternatives are of an elliptical nature.

It may be surprising at first that, under tangent vMF alternatives, the (optimal) unspecified-$\boldsymbol\theta$ test $\phi^{\rm loc}_{\rm vMF}$ shows little power compared to the specified-$\boldsymbol\theta$ test $\phi^{\rm loc}_{\boldsymbol\theta}$. This, however, only reflects the fact that the cost of the unspecification of $\boldsymbol\theta$ is high for the (vMF) angular function considered. Actually, the results of the previous sections allow to quantify this cost theoretically. Under the sequence of alternatives considered in Corollary 2.3, the Asymptotic Relative Efficiency (ARE) of the unspecified-$\boldsymbol\theta$ test $\phi^{\rm loc}_{\rm vMF}$ with respect to the specified-$\boldsymbol\theta$ test $\phi^{\rm loc}_{\boldsymbol\theta}$ is as usual obtained as the ratio of the corresponding non-centrality parameters in the asymptotic non-null chi-square distributions of the corresponding statistics. If follows from (3.15) and Corollary 2.3 that, at the vMF with concentration η, $\mathrm{ARE}(\eta) = 1 - \mathcal{I}^2_p(g_\eta)/\mathcal{J}_p(g_\eta) = 1 - \big(2\Gamma\left(\frac{p}{2}\right)^2 I_{\frac{p-1}{2}}(\eta)^2\big)/\big((p-1)\Gamma\left(\frac{p-1}{2}\right)^2 I_{\frac{p-2}{2}}(\eta) I_{\frac{p}{2}}(\eta)\big)$, where $g_\eta(r) = \exp(\eta r)$ is the angular function of the vMF distribution with concentration η. Figure 5 provides plots of this ARE as a function of η, for various values of p. For the tangent vMF alternatives considered in the present simulation exercise (for which $\eta = 5$ and $p = 3$), the ARE is equal about 0.171, which explains the relatively poor performance of $\phi^{\rm loc}_{\rm vMF}$ compared to $\phi^{\rm loc}_{\boldsymbol\theta}$. This, of course, is not incompatible with the fact that $\phi^{\rm loc}_{\rm vMF}$ is optimal in the unspecified-$\boldsymbol\theta$ problem.

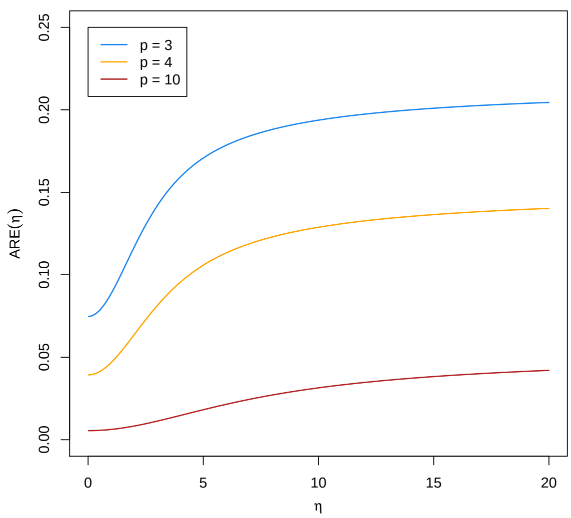

Fig. 5. Plots, for several dimensions p, of the asymptotic relative efficiency, as a function of η, of the unspecified-$\boldsymbol\theta$ test $\phi^{\rm loc}_{\rm vMF}$ with respect to the specified-$\boldsymbol\theta$ test $\phi^{\rm loc}_{\boldsymbol\theta}$ under the sequence of alternatives considered in Corollary 2.3 at the vMF with concentration η.

5.3. The specified-$\boldsymbol{\theta}$ problem on $\mathcal{S}^3$

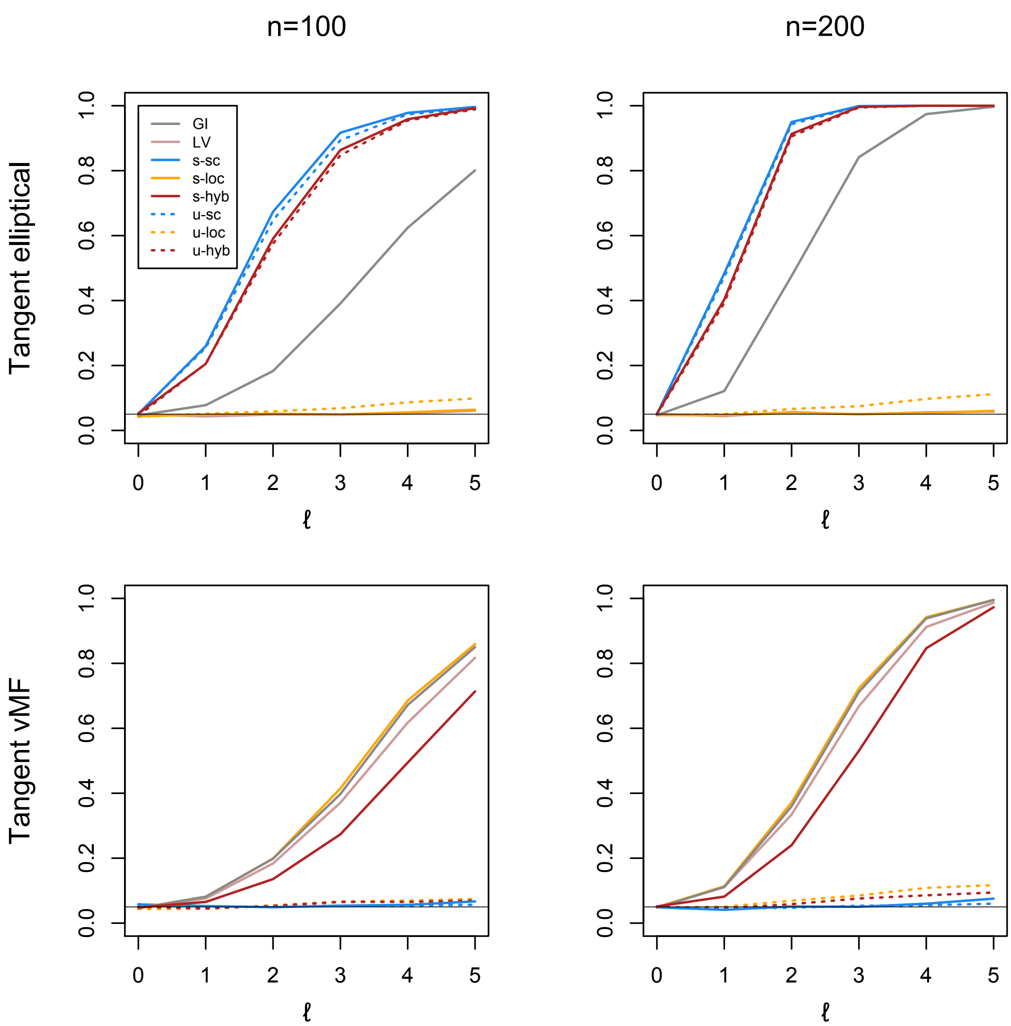

Fig. 6. Rejection frequencies, under tangent elliptical alternatives (top row) and tangent vMF alternatives (bottom row), of the specified-$\boldsymbol{\theta}$ tests $\phi_{\boldsymbol{\theta}}^{\mathrm{sc}}$ (s-sc), $\phi_{\boldsymbol{\theta}}^{\mathrm{loc}}$ (s-loc), $\phi_{\boldsymbol{\theta}}^{\mathrm{hyb}}$ (s-hyb), $\phi_{\boldsymbol{\theta}}^{\mathrm{LV}}$ (LV), and $\phi_{\boldsymbol{\theta}}^{\mathrm{Gin}}$ (GI), as well as the unspecified-$\boldsymbol{\theta}$ tests $\phi_{\dagger}^{\mathrm{sc}}$ (u-sc), $\phi_{\mathrm{vMF}}^{\mathrm{loc}}$ (u-loc), and $\phi_{\mathrm{vMF}}^{\mathrm{hyb}}$ (u-loc). Sample sizes are $n = 100$ (left column) and $n = 200$ (right column). All tests are performed at asymptotic level 5%; see Section 5.3 for details.

The third and last simulation exercise essentially replicates the second one on $\mathcal{S}^3$. Since the Kuiper test $\phi_{\boldsymbol{\theta}}^{\mathrm{Kui}}$ only applies for data on $\mathcal{S}^2$, we replaced it with the Giné test $\phi_{\boldsymbol{\theta}}^{\mathrm{Gin}}$, that, as the Kuiper test, is an omnibus test addressing the specified-$\boldsymbol{\theta}$ problem. For sample sizes $n = 100$ and $n = 200$ and for two types of alternatives to rotational symmetry ($r = 1, 2$), we generated $N = 5000$ mutually independent random samples of the form

$$\mathbf{X}_{i;\ell}^{(r)}, \quad i = 1, \ldots, n, \quad \ell = 0, \ldots, 5, \quad r = 1, 2,$$

with values in $\mathcal{S}^3$. The $\mathbf{X}_{i;\ell}^{(1)}$'s follow a $\mathcal{TE}_4(\boldsymbol{\theta}, g_2, \boldsymbol{\Lambda}_\ell)$ with location $\boldsymbol{\theta} := (1, 0, 0, 0)'$ and shape $\boldsymbol{\Lambda}_\ell :=$

$\mathrm{diag}(1+\ell/2,1,1)/(3+\ell/2)$. The $\mathbf{X}_{i;\ell}^{(2)}$'s follow a $\mathcal{TM}_4(\boldsymbol{\theta}, g_2, \boldsymbol{\mu}, \kappa_\ell)$ with skewness direction $\boldsymbol{\mu} = (1,0,0)'$ and skewness intensity $\kappa_\ell := \ell/8$. As in the previous simulation exercises, $\ell = 0$ corresponds to the null of rotational symmetry about $\boldsymbol{\theta}$ and $\ell = 1,\ldots,5$ provide increasingly severe alternatives. For each replication, we performed, at asymptotic level 5%, the specified-$\boldsymbol{\theta}$ tests $\phi_{\boldsymbol{\theta}}^{\mathrm{loc}}$, $\phi_{\boldsymbol{\theta}}^{\mathrm{sc}}$, $\phi_{\boldsymbol{\theta}}^{\mathrm{hyb}}$, $\phi_{\boldsymbol{\theta}}^{\mathrm{LV}}$, and the Giné test $\phi_{\boldsymbol{\theta}}^{\mathrm{Gin}}$, as well as the unspecified-$\boldsymbol{\theta}$ tests $\phi_{\dagger}^{\mathrm{sc}}$, $\phi_{\mathrm{vMF}}^{\mathrm{loc}}$, and $\phi_{\mathrm{vMF}}^{\mathrm{hyb}}$ (still based on the spherical mean). The resulting empirical power curves, that are provided in Figure 6, lead to conclusions that are very similar to those reported in the simulation exercise conducted in Section 5.2.

6. Real data applications

6.1. Paleozoic red-beds data

We consider magnetic remanence measurements made on samples collected from Paleozoic red-beds in Argentina. The data, that consists in $n = 26$ observations on $\mathcal{S}^2$, is showed in Figure 7. In line with the fact that the location $\boldsymbol{\theta}$ is unknown a priori, Ley et al. (2013) considered the problem of estimating $\boldsymbol{\theta}$ under the assumption of rotational symmetry. One may wonder, however, whether or not this assumption is appropriate in the present context. Visual inspection of Figure 7 indeed reveals that the density contours in the tangent space to the mode $\boldsymbol{\theta}$ could be ellipses rather than circles. We therefore intend to test for rotational symmetry (about an unspecified $\boldsymbol{\theta}$) for the data at hand.

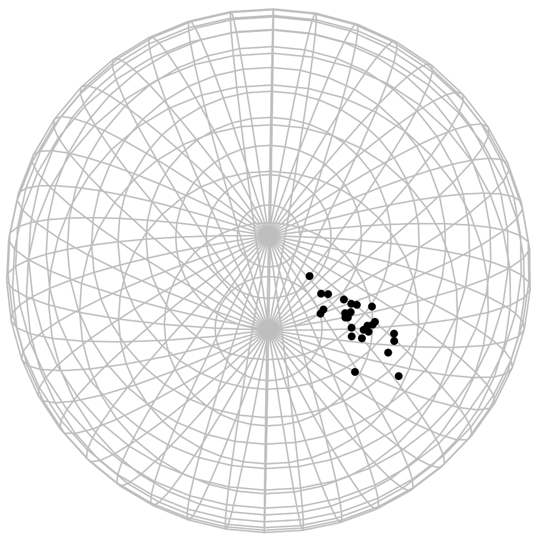

Fig. 7. Paleozoic red-beds data on $\mathcal{S}^2$.

We consider three unspecified-$\boldsymbol{\theta}$ tests of rotational symmetry, namely the tests $\phi_{\dagger}^{\mathrm{sc}}$ and $\phi_{\mathrm{vMF}}^{\mathrm{loc}}$, that are optimal against tangent elliptical and tangent vMF alternatives respectively (but are blind to the other type of alternatives), as well as the hybrid test $\phi_{\mathrm{vMF}}^{\mathrm{hyb}}$ designed to show powers against both types of alternatives. For the data at hand, $\phi_{\dagger}^{\mathrm{sc}}$, $\phi_{\mathrm{vMF}}^{\mathrm{loc}}$, and $\phi_{\mathrm{vMF}}^{\mathrm{hyb}}$, when based on the spherical mean, provide p-values equal to 0.00065, 0.90, and 0.005, respectively. As a consequence, the null hypothesis of rotational symmetry is rejected in favour of tangent elliptical alternatives.

Now, Figure 7 shows that the data are actually highly concentrated. In the vMF parametric model, the maximum likelihood estimator of κ takes the value 69.544. It is unclear that, at the present small sample size ($n = 26$), the three tests above are robust to such a high concentration. To investigate this robustness (and to illustrate the relative behaviours of these tests), we performed the following simulation exercise: we generated 5000 mutually independent random samples of the form $\mathbf{X}_{i;\ell}$, $i = 1, \ldots, n = 26$, $\ell = 0, \ldots, 5$, where $\mathbf{X}_{i;\ell} \sim \mathcal{TE}_3(\boldsymbol{\theta}, g, \boldsymbol{\Lambda}_\ell)$ with location $\boldsymbol{\theta} := (1, 0, 0)'$, shape $\boldsymbol{\Lambda}_\ell := \mathrm{diag}(1+\ell, 1)/(2+\ell)$, and angular function $t \mapsto g(t) := \exp(69.544\, t)$. We therefore matched both the sample size and concentration met in the real data example. The value $\ell = 0$ corresponds to the null of rotational symmetry, whereas $\ell = 1, \ldots, 5$ provide increasingly severe alternatives. We performed, at asymptotic level $\alpha = 5\%$, the tests $\phi^{\mathrm{sc}}_{\dagger}$, $\phi^{\mathrm{loc}}_{\mathrm{vMF}}$, and $\phi^{\mathrm{hyb}}_{\mathrm{vMF}}$, still based on the spherical mean. The resulting rejection frequencies are provided in Figure 8. Clearly, the three tests show null rejection frequencies that are close to the nominal level 5%, hence are robust to the high-concentration/small sample situation we face in the real data example considered.

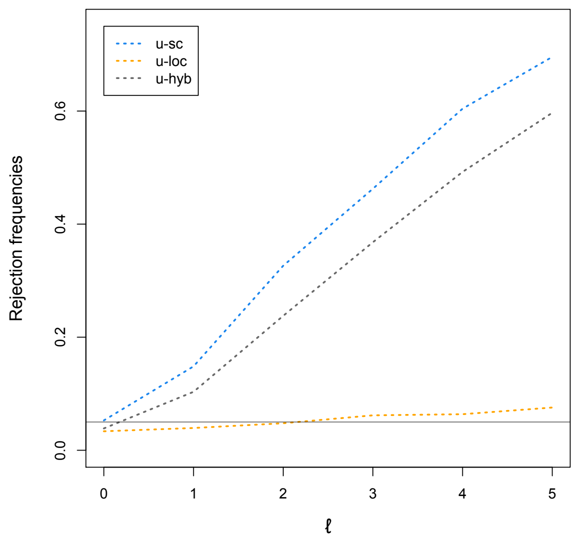

Fig. 8. Rejection frequencies, under tangent elliptical alternatives with vMF angular density, of the unspecified-$\boldsymbol{\theta}$ tests $\phi^{\mathrm{sc}}_{\dagger}$ (u-sc), $\phi^{\mathrm{loc}}_{\mathrm{vMF}}$ (u-loc), and $\phi^{\mathrm{hyb}}_{\mathrm{vMF}}$ (u-hyb). The sample size ($n = 26$) and concentration of the vMF ($\kappa = 69.544$) match those in the Paleozoic red-beds data. All tests are performed at asymptotic level 5%; see Section 6.1 for details.

6.2. Protein structure

We study now the presence of rotational symmetry in the C_α representation of a protein's backbone. Proteins are polypeptide chains built up by amino acids, each of them having a central carbon atom, denoted C_α. During protein synthesis, the carboxyl group of the first amino acid condenses with the amino group of the next, yielding a peptide bond, and this process is repeated as the chain elongates. The final output is a folded three-dimensional structure determined by the backbone, a chain of peptide units that go from one C_α atom to the next. Motivated by the key role of C_α atoms in the protein's backbone, Levitt (1976) proposed a simplified representation of the backbone that employs, sequentially, the C_α atom's positions. Given the coordinates of a C_α atom, Levitt (1976)'s representation encodes the location of the next C_α from the pseudo-bond joining them (the term *pseudo* emphasizes that the atoms are not linked by a single chemical bond but rather by several). Since the distance of pseudo-bonds can be considered constant (around 3.8 Å), the sequence of C_α atoms can be represented as a sequence of vectors in the sphere of radius $r = 3.8$ with the parametrization

$$\mathbf{x} = (\cos(\theta), \sin(\theta)\cos(\tau), \sin(\theta)\sin(\tau)), \quad \theta \in [0, \pi), \quad \tau \in [-\pi, \pi),$$

where the origin is set as the previous C_α atom (θ is not related with the axis of symmetry $\boldsymbol{\theta}$, is the notation used in Levitt (1976)'s representation). This codification is employed in the hidden Markov model of Hamelryck et al. (2006), which considered Kent (1982)'s FB5 non-rotationally symmetric distribution to model dynamically the position of the next C_α atom from the information associated to the former: pseudo-bond direction, amino acid type, and secondary structure label (helix, β-strand, or coil).

In proteins, θ usually lies in $[80°, 150°]$ due to atom clash-avoiding constraints, whereas τ can adopt all values in $[-180°, 180°)$. Thus the vectors $\mathbf{x}$ are in between two meridians in a girdle-like spherical distribution, which might suggest the presence of rotational symmetry around $\boldsymbol{\theta} = (1, 0, 0)$. However, it is evident from Figure 9 that the overall distribution of these spherical vectors is highly non-symmetric. For example, there is a massive non-rotationally symmetric cluster associated to a α-helix conformation (around $(50°, 90°)$). Yet, a less evident question to answer is whether there are particular protein features associated with rotational symmetry of the pseudo-bond directions, or, on the contrary, whether non-rotational symmetry is a systematic and persistent pattern in pseudo-bonds. In order to address this inquiry, we extracted the pseudo-bond directions of the C_α atoms from the top500 dataset (Word et al., 1999), consisting of 500 high precision and non-redundant protein structures, using the `Bio.PDB` module (Hamelryck and Manderick, 2003). The covariates for each direction are its associated Amino Acid (AA; 20 kinds), its associated Secondary Structure (SS; 7 possible labels), and its depth in the protein backbone. This depth is standardized so that 1 represents the most central C_α atom and 0 stands both for the initial and final C_α atoms of the backbone.

When $\boldsymbol{\theta} = (1, 0, 0)$ is specified, rotational symmetry is consistently not present in any of the C_α atoms related to individual data features. Specifically, both $\phi_{\boldsymbol{\theta}}^{\mathrm{loc}}$ and $\phi_{\boldsymbol{\theta}}^{\mathrm{sc}}$ reject rotational symmetry of C_α directions associated to: any of the 20 AAs, any of the 7 SS labels, and any of the blocks of C_α's with depths within $[d_i, d_{i+1})$, $d_i = \frac{i-1}{20}$, $i = 1, \ldots, 21$. The p-values for $\phi_{\boldsymbol{\theta}}^{\mathrm{sc}}$ and $\phi_{\boldsymbol{\theta}}^{\mathrm{loc}}$ strongly reject the null hypothesis, being the largest p-value of the two tests, in all subgroups, of order 10^{-31}. We inspect next the association of C_α directions with respect to the transitions of amino acids. To that aim, we partitioned the data into 20×20 subgroups for the transitions $\mathrm{AA}_i \to \mathrm{AA}_{i+1}$, and we tested rotational symmetry on them. The results from both tests are not coherent, since both are looking for different deviations from the null hypothesis that are present in the data. Precisely, at level $\alpha = 0.05$, $\phi_{\boldsymbol{\theta}}^{\mathrm{sc}}$ does not reject for 2 pairs of amino acids (Figure 10, left plot), and $\phi_{\boldsymbol{\theta}}^{\mathrm{loc}}$ does the same for 27 pairs (Figure 10, central plot). Careful visual inspection revealed the presence of multimodality patterns on the multivariate signs that leaded to non-rejections for $\phi_{\boldsymbol{\theta}}^{\mathrm{loc}}$ (e.g. the signs for G$\to$T, with $n = 579$, are antipodally bimodal), even if the data showed clear non-rotationally symmetric patterns. This evidences the practical necessity of accounting for a test that is consistent against *both* location and scatter deviations, such as $\phi_{\boldsymbol{\theta}}^{\mathrm{hyb}}$. The test $\phi_{\boldsymbol{\theta}}^{\mathrm{hyb}}$ consistently rejects rotational symmetry for any transition of amino acids (Figure 10, right plot), except for the transitions of C (*Cysteine*) to M (*Methionine*, p-value$= 0.013$) and W (*Tryptophan*, p-value$= 0.198$), both extremely rare (less than 0.05% of the analysed transitions). We conclude then that rotational symmetry is emphatically not associated to particular amino acids transitions, except

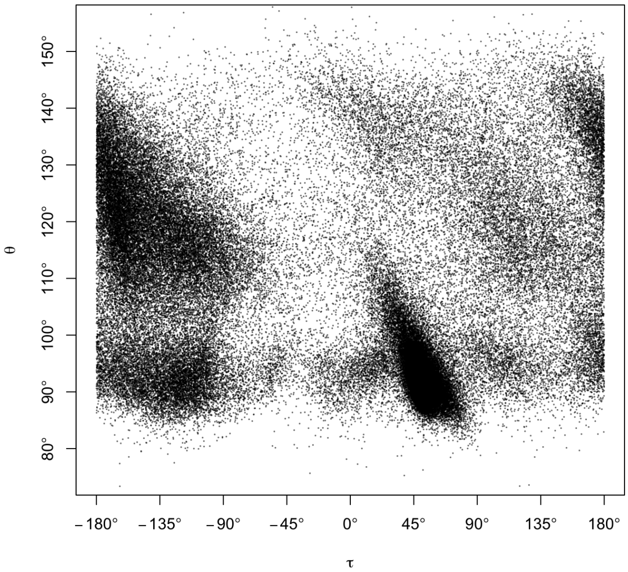

Fig. 9. Scatterplot of the pseudo-angles (θ, τ) forming the spherical band around $\boldsymbol{\theta} = (1, 0, 0)$, at colatitudes (if $\boldsymbol{\theta}$ is regarded as North pole) between 80° and 150°. Sample size is $n = 107778$.

for two transitions from *Cysteine*, for which the significance of the test is more questionable, given the p-values and sample sizes.

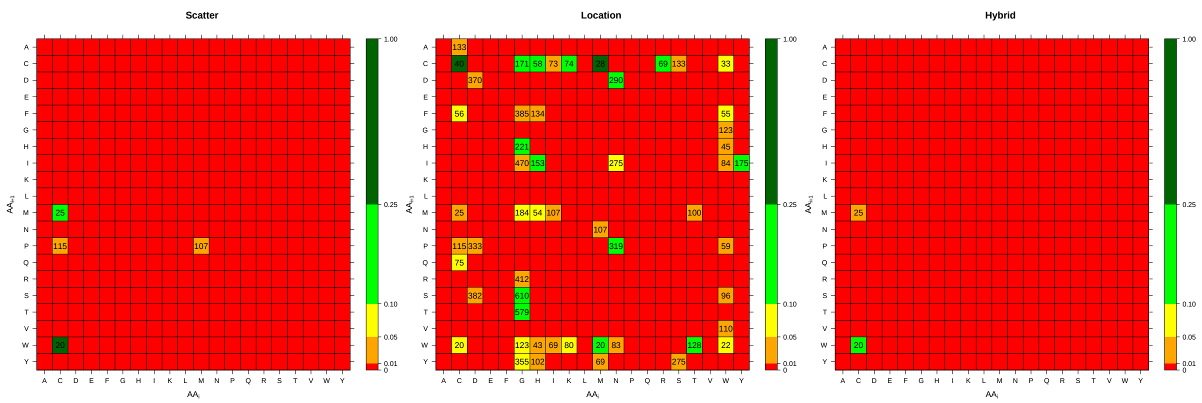

Fig. 10. p-values for testing rotational symmetry on the C$_\alpha$ pseudo-bonds associated to amino acid changes AA$_i$ $\to$AA$_{i+1}$. Left shows the p-values for $\phi^{\mathrm{sc}}_{\boldsymbol{\theta}}$, centre for $\phi^{\mathrm{loc}}_{\boldsymbol{\theta}}$, and right for $\phi^{\mathrm{hyb}}_{\boldsymbol{\theta}}$. Sample size is indicated for the p-values above 0.01.

7. Perspective for future research

As explained in Section 2.1, the random vector $\mathbf{X}$ with values on $\mathcal{S}^{p-1}$ is rotationally symmetric about $\boldsymbol{\theta}$ if and only if, using the notation introduced in (2.1), (i) the random vector $\mathbf{u}_{\boldsymbol{\theta}}(\mathbf{X})$ is uniformly distributed over $\mathcal{S}^{p-2}$ and (ii) $\mathbf{u}_{\boldsymbol{\theta}}(\mathbf{X})$ is independent of $v_{\boldsymbol{\theta}}(\mathbf{X})$. The tests proposed in this paper are designed to detect deviations from rotational symmetry by testing that (i) holds. As a consequence, they will be blind to alternatives of rotational symmetry for which (i) holds but (ii) does not. This could be fixed by testing that the covariance between $\mathbf{u}_{\boldsymbol{\theta}}(\mathbf{X})$ and $v_{\boldsymbol{\theta}}(\mathbf{X})$ is zero, which can be based on a statistic of the form

$$\boldsymbol{\Delta}_{\boldsymbol{\theta}}^{\mathrm{cov}(n)} := \frac{1}{\sqrt{n}} \sum_{i=1}^{n} v_{\boldsymbol{\theta}}(\mathbf{X}_i)\mathbf{u}_{\boldsymbol{\theta}}(\mathbf{X}_i).$$

Since $\boldsymbol{\Delta}_{\boldsymbol{\theta}}^{\mathrm{cov}(n)}$ is asymptotically normal with mean zero and covariance matrix $(p-1)^{-1}\mathrm{E}_{\boldsymbol{\theta},g}[v_{\boldsymbol{\theta}}^2(\mathbf{X}_1)]\mathbf{I}_{p-1}$ under $\mathrm{P}_{\boldsymbol{\theta},g}^{(n)}$, the resulting test would, at asymptotic level α, reject the null hypothesis of rotational symmetry about $\boldsymbol{\theta}$ whenever

$$\frac{p-1}{\sum_{i=1}^{n} v_{\boldsymbol{\theta}}^2(\mathbf{X}_i)} \sum_{i,j=1}^{n} v_{\boldsymbol{\theta}}(\mathbf{X}_i)v_{\boldsymbol{\theta}}(\mathbf{X}_j)\mathbf{u}_{\boldsymbol{\theta}}'(\mathbf{X}_i)\mathbf{u}_{\boldsymbol{\theta}}(\mathbf{X}_j) > \chi^2_{p-1,1-\alpha}.$$

Such a test of course would detect violations of (ii) only and it is natural to design a test that would be able to detect deviations from both (i) and (ii) by considering test statistics that are quadratic forms in $\big((\boldsymbol{\Delta}_{\boldsymbol{\theta}}^{\mathrm{cov}(n)})', (\boldsymbol{\Delta}_{\boldsymbol{\theta};2}^{\mathcal{TE}(n)})'\big)'$ or in $\big((\boldsymbol{\Delta}_{\boldsymbol{\theta}}^{\mathrm{cov}(n)})', (\boldsymbol{\Delta}_{\boldsymbol{\theta};2}^{\mathcal{TM}(n)})'\big)'$, depending on whether tangent elliptical or tangent vMF alternatives are considered. In the spirit of the hybrid test from Section 4, detecting both types of alternatives can be achieved by considering a quadratic form in $\big((\boldsymbol{\Delta}_{\boldsymbol{\theta}}^{\mathrm{cov}(n)})', (\boldsymbol{\Delta}_{\boldsymbol{\theta};2}^{\mathcal{TE}(n)})', (\boldsymbol{\Delta}_{\boldsymbol{\theta};2}^{\mathcal{TM}(n)})'\big)'$. The quadratic form to be used in each case naturally follows from the asymptotic covariance matrix in the (null) joint asymptotic normal distribution of these random vectors.

Another perspective for future research derived from the construction of new distributions is the following. In Section 2.2, we proposed new distributions on the unit sphere $\mathcal{S}^{p-1}$, namely tangent vMF distributions, by imposing that $\mathbf{u}_{\boldsymbol{\theta}}(\mathbf{X}) = \mathbf{u}_{\boldsymbol{\theta}_1;p-2}(\mathbf{X})$ follows its own vMF distribution over $\mathcal{S}^{p-2}$ with location $\boldsymbol{\mu} = \boldsymbol{\theta}_2 \in \mathcal{S}^{p-2}$. In turn, one could specify that $\mathbf{u}_{\boldsymbol{\theta}_2;p-3}(\mathbf{X})$ follows a vMF distribution over $\mathcal{S}^{p-3}$ with location $\boldsymbol{\theta}_3$. Iterating this construction will provide "nested" tangent vMF distributions that are associated with mutually orthogonal directions $\boldsymbol{\theta}_i$, $i = 1, \ldots, p$ (strictly speaking, $\boldsymbol{\theta}_i \in \mathcal{S}^{p-i}$ but they can all be considered embedded in the original unit sphere $\mathcal{S}^{p-1}$). These directions, in some sense, provide analogues of principal directions on the sphere and should therefore be related to the principal nested spheres of Jung et al. (2012). Such distributions provide flexible models on the sphere that are likely to be relevant in various applications of directional statistics.

Acknowledgements

Eduardo García-Portugués acknowledges support from project MTM2016-76969-P from the Spanish Ministry of Economy, Industry and Competitiveness, and ERDF. Davy Paindaveine's research is supported by the IAP research network grant nr. P7/06 of the Belgian government (Belgian Science Policy), the Crédit de Recherche J.0113.16 of the FNRS (Fonds National pour la Recherche Scientifique), Communauté Française de Belgique, and a grant from the National Bank of Belgium. Thomas Verdebout's research is supported by the National Bank of Belgium.

References

Boente, G., Rodriguez, D. and González-Manteiga, W. (2014) Goodness-of-fit test for directional data. *Scand. J. Stat.*, **41**, 259–275.

Boulerice, B. and Ducharme, G. R. (1997) Smooth tests of goodness-of-fit for directional and axial data. *J. Multivariate Anal.*, **60**, 154–175.

Cutting, C., Paindaveine, D. and Verdebout, T. (2017) Testing uniformity on high-dimensional spheres against monotone rotationally symmetric alternatives. *Ann. Statist.*, to appear.

Figueiredo, A. M. S. (2012) Goodness-of-fit for a concentrated von Mises-Fisher distribution. *Comput. Statist.*, **27**, 69–82.

Giné, E. (1975) Invariant tests for uniformity on compact Riemannian manifolds based on Sobolev norms. *Ann. Statist.*, **3**, 1243–1266.

Hallin, M. and Paindaveine, D. (2006a) Parametric and semiparametric inference for shape: the role of the scale functional. *Statist. Decisions*, **24**, 327–350.

— (2006b) Semiparametrically efficient rank-based inference for shape I. Optimal rank-based tests for sphericity. *Ann. Statist.*, **34**, 2707–2756.

Hamelryck, T., Kent, J. T. and Krogh, A. (2006) Sampling realistic protein conformations using local structural bias. *PLoS Comput. Biol.*, **2**, e131.

Hamelryck, T. and Manderick, B. (2003) PDB file parser and structure class implemented in Python. *Bioinformatics*, **19**, 2308–2310.

Ilmonen, P. and Paindaveine, D. (2011) Semiparametrically efficient inference based on signed ranks in symmetric independent component models. *Ann. Statist.*, **39**, 2448–2476.

Jung, S., Dryden, I. L. and Marron, J. S. (2012) Analysis of principal nested spheres. *Biometrika*, **99**, 551–568.

Jupp, P. E. and Spurr, B. D. (1983) Sobolev tests for symmetry of directional data. *Ann. Statist.*, **11**, 1225–1231.

Kent, J. T. (1982) The Fisher-Bingham distribution on the sphere. *J. R. Stat. Soc. Ser. B*, **44**, 71–80.

Kreiss, J. (1987) On adaptive estimation in stationary ARMA processes. *Ann. Statist.*, **15**, 122–133.

Kume, A. and Wood, A. T. (2005) Saddlepoint approximations for the Bingham and Fisher-Bingham normalising constants. *Biometrika*, **92**, 465–476.

Levitt, M. (1976) A simplified representation of protein conformations for rapid simulation of protein folding. *J. Mol. Biol.*, **104**, 59–107.

Ley, C., Swan, Y., Thiam, B. and Verdebout, T. (2013) Optimal R-estimation of a spherical location. *Statist. Sinica*, **23**, 305–333.

Ley, C. and Verdebout, T. (2014) Simple optimal tests for circular reflective symmetry about a specified median direction. *Statist. Sinica*, **14**, 1319–1340.

— (2017a) *Modern Directional Statistics*. Chapman and Hall/CRC.

— (2017b) Skew-rotationally-symmetric distributions on the unit sphere and related efficient inferential procedures. *J. Multivariate Anal.*, to appear.

Magnus, J. R. and Neudecker, H. (2007) *Matrix Differential Calculus with Applications in Statistics and Econometrics*. Wiley Series in Probability and Statistics: Probability and Statistics. Chichester: John Wiley & Sons.

Mardia, K. V. and Jupp, P. E. (2000) *Directional Statistics*. Wiley Series in Probability and Statistics. Chichester: John Wiley & Sons, second edn.

Meintanis, S. and Verdebout, T. (2016) Le Cam maximin tests for symmetry of circular data based on the characteristic function. Submitted.

Paindaveine, D. (2008) A canonical definition of shape. *Statist. Probab. Lett.*, **78**, 2240–2247.

Paindaveine, D. and Verdebout, T. (2015) Optimal rank-based tests for the location parameter of a rotationally symmetric distribution on the hypersphere. In *Mathematical Statistics and Limit Theorems: Festschrift in Honor of Paul Deheuvels* (eds. M. Hallin, D. Mason, D. Pfeifer and J. Steinebach), 249–270. Springer.

— (2016) On high-dimensional sign tests. *Bernoulli*, **22**, 1745–1769.

Pewsey, A. (2002) Testing circular symmetry. *Canad. J. Statist.*, **30**, 591–600.

Rayleigh, L. (1919) On the problem of random vibrations and random flights in one, two and three dimensions. *Phil. Mag.*, **37**, 321–346.

Schach, S. (1969) Nonparametric symmetry tests for circular distributions. *Biometrika*, **56**, 571–577.

Tyler, D. E. (1987) Statistical analysis for the angular central Gaussian distribution on the sphere. *Biometrika*, **74**, 579–589.

van der Vaart, A. W. (1998) *Asymptotic Statistics*. Cambridge: Cambridge Univ. Press.

Watson, G. S. (1983) *Statistics on Spheres*. New York: Wiley.

Word, J. M., Lovell, S. C., LaBean, T. H., Taylor, H. C., Zalis, M. E., Presley, B. K., Richardson, J. S. and Richardson, D. C. (1999) Visualizing and quantifying molecular goodness-of-fit: small-probe contact dots with explicit hydrogen atoms. *J. Mol. Biol.*, **285**, 1711–1733.

A. Proofs of the main results

The lemmas given in Appendix B are used to prove the main results.

Proof (Theorem 2.1). Consider first the case $\mathbf{X} \sim \mathcal{TE}_p(\boldsymbol{\theta}_0, g, \mathbf{\Lambda})$, with $\boldsymbol{\theta}_0 := (1, 0, \ldots, 0)' \in \mathbb{R}^p$. Clearly, $\mathbf{X} = (V, (1-V^2)^{1/2}\mathbf{U}')'$, with $V := v_{\boldsymbol{\theta}_0}(\mathbf{X}) = X_1$ and $\mathbf{U} := \mathbf{u}_{\boldsymbol{\theta}_0}(\mathbf{X}) = (X_2, \ldots, X_p)'/\sqrt{1-X_1^2}$, where we used the notation introduced in (2.1). By definition, $\mathbf{U}$ takes its values in $\mathcal{S}^{p-2}$, with density $\mathbf{u} \mapsto c^{\mathcal{A}}_{p-1,\mathbf{\Lambda}}(\mathbf{u}'\mathbf{\Lambda}^{-1}\mathbf{u})^{-(p-1)/2}$ with respect to σ_{p-2}. Therefore, conditional on $V = v$, $(1-V^2)^{1/2}\mathbf{U}$ takes its values on the hypersphere $\mathcal{S}^{p-2}(r_v) \subset \mathbb{R}^{p-1}$ with radius $r_v := (1-v^2)^{1/2}$. Its density with respect to the surface area measure $\sigma_{p-2,r}$ on $\mathcal{S}^{p-2}(r_v)$ is (recall that V and $\mathbf{U}$ are mutually independent)

$$\mathbf{w} \mapsto c^{\mathcal{A}}_{p-1,\mathbf{\Lambda}}\left(\frac{\mathbf{w}'\mathbf{\Lambda}^{-1}\mathbf{w}}{r_v^2}\right)^{-(p-1)/2} r_v^{-(p-2)},$$

where $r^{-(p-2)}$ is the Jacobian of the radial projection of $\mathcal{S}^{p-2}(r)$ onto $\mathcal{S}^{p-2}$. Since $d\sigma_{p-2,r} = r^{p-2} d\sigma_{p-2}$, the density of $\mathbf{X}$ with respect to the product measure $\mu \times \sigma_{p-2}$ (where μ stands for the Lebesgue measure on $[-1,1]$) is

$$\begin{aligned}\mathbf{x} \mapsto & \, c^{\mathcal{A}}_{p-1,\mathbf{\Lambda}} \big(\mathbf{u}'_{\boldsymbol{\theta}_0}(\mathbf{x}) \mathbf{\Lambda}^{-1} \mathbf{u}_{\boldsymbol{\theta}_0}(\mathbf{x})\big)^{-(p-1)/2} \frac{d\mathrm{P}^V_{\boldsymbol{\theta}_0,g,\mathbf{\Lambda}}}{d\mu}(v_{\boldsymbol{\theta}_0}(\mathbf{x})) \\ & = c^{\mathcal{A}}_{p-1,\mathbf{\Lambda}} \big(\mathbf{u}'_{\boldsymbol{\theta}_0}(\mathbf{x}) \mathbf{\Lambda}^{-1} \mathbf{u}_{\boldsymbol{\theta}_0}(\mathbf{x})\big)^{-(p-1)/2} \omega_{p-1} c_{p,g} (1 - v^2_{\boldsymbol{\theta}_0}(\mathbf{x}))^{(p-3)/2} g(v_{\boldsymbol{\theta}_0}(\mathbf{x})).\end{aligned}$$

The result for $\boldsymbol{\theta} = \boldsymbol{\theta}_0$ then follows from the fact that (see, e.g., page 44 of Watson (1983))

$$\frac{d(\mu \times \sigma_{p-2})}{d\sigma_{p-1}}(\mathbf{x}) = (1 - v^2_{\boldsymbol{\theta}_0}(\mathbf{x}))^{(p-3)/2}.$$

To obtain the result for an arbitrary value of $\boldsymbol{\theta}$, let $\mathbf{X} \sim \mathcal{TE}_p(\boldsymbol{\theta}, g, \mathbf{\Lambda})$ and pick a $p \times p$ orthogonal matrix $\mathbf{O}$ such that $\mathbf{O}\boldsymbol{\theta} = \boldsymbol{\theta}_0$. Since $\mathbf{O}\mathbf{\Gamma}_{\boldsymbol{\theta}} = \mathbf{\Gamma}_{\boldsymbol{\theta}_0}$, we have that $\mathbf{O}\mathbf{X} \sim \mathcal{TE}_p(\boldsymbol{\theta}_0, g, \mathbf{\Lambda})$. Therefore, the result for $\boldsymbol{\theta} = \boldsymbol{\theta}_0$ implies that the density of $\mathbf{X}$ with respect to σ_{p-1} is

$$\begin{aligned}\mathbf{x} \mapsto & \, |\det \mathbf{O}| \, \omega_{p-1} c^{\mathcal{A}}_{p-1,\mathbf{\Lambda}} c_{p,g} g(v_{\boldsymbol{\theta}_0}(\mathbf{O}\mathbf{x})) \big(\mathbf{u}'_{\boldsymbol{\theta}_0}(\mathbf{O}\mathbf{x}) \mathbf{\Lambda}^{-1} \mathbf{u}_{\boldsymbol{\theta}_0}(\mathbf{O}\mathbf{x})\big)^{-(p-1)/2} \\ & = \omega_{p-1} c^{\mathcal{A}}_{p-1,\mathbf{\Lambda}} c_{p,g} g(v_{\boldsymbol{\theta}}(\mathbf{x})) \big(\mathbf{u}'_{\boldsymbol{\theta}}(\mathbf{x}) \mathbf{\Lambda}^{-1} \mathbf{u}_{\boldsymbol{\theta}}(\mathbf{x})\big)^{-(p-1)/2},\end{aligned}$$

as was to be proved. □

Proof (Theorem 2.3). Lemma B.3 readily entails that

$$\log \frac{d\mathrm{P}^{\mathcal{TE}(n)}_{\boldsymbol{\theta}_n,g,\mathbf{\Lambda}_n}}{d\mathrm{P}^{(n)}_{\boldsymbol{\theta},g}} = \log \frac{d\mathrm{P}^{\mathcal{TE}(n)}_{\boldsymbol{\theta}_n,g,\mathbf{\Lambda}_n}}{d\mathrm{P}^{(n)}_{\boldsymbol{\theta}_n,g}} + \log \frac{d\mathrm{P}^{(n)}_{\boldsymbol{\theta}_n,g}}{d\mathrm{P}^{(n)}_{\boldsymbol{\theta},g}} = \log \frac{d\mathrm{P}^{\mathcal{TE}(n)}_{\boldsymbol{\theta}_n,g,\mathbf{\Lambda}_n}}{d\mathrm{P}^{(n)}_{\boldsymbol{\theta}_n,g}} + \mathbf{t}'_n \mathbf{\Delta}^{(n)}_{\boldsymbol{\theta},g;1} - \frac{1}{2} \mathbf{t}'_n \mathbf{\Gamma}_{\boldsymbol{\theta},g;11} \mathbf{t}_n + o_{\mathrm{P}}(1)$$

as $n \to \infty$ under $\mathrm{P}^{(n)}_{\boldsymbol{\theta},g}$. Therefore, we only need to show that

$$L_n := \log \frac{d\mathrm{P}^{\mathcal{TE}(n)}_{\boldsymbol{\theta}_n,g,\mathbf{\Lambda}_n}}{d\mathrm{P}^{(n)}_{\boldsymbol{\theta}_n,g}} = (\overset{\circ}{\mathrm{vech}}\, \mathbf{L}_n)' \mathbf{\Delta}^{\mathcal{TE}(n)}_{\boldsymbol{\theta};2} - \frac{1}{2} (\overset{\circ}{\mathrm{vech}}\, \mathbf{L}_n)' \mathbf{\Gamma}^{\mathcal{TE}}_{\boldsymbol{\theta};22} (\overset{\circ}{\mathrm{vech}}\, \mathbf{L}_n) + o_{\mathrm{P}}(1)$$

as $n \to \infty$ under $\mathrm{P}^{(n)}_{\boldsymbol{\theta},g}$. First note that Theorem 2.1 gives

$$L_n = -\frac{n}{2} \log \big(\det \mathbf{\Lambda}_n\big) - \frac{p-1}{2} \sum_{i=1}^n \log \big(\mathbf{U}'_{i,\boldsymbol{\theta}_n} \mathbf{\Lambda}_n^{-1} \mathbf{U}_{i,\boldsymbol{\theta}_n}\big) =: L_{n,1} + L_{n,2}, \tag{A.21}$$

say. Since $\log(\det(\mathbf{I}_{p-1} + \mathbf{A})) = \mathrm{tr}[\mathbf{A}] - \frac{1}{2}\mathrm{tr}[\mathbf{A}^2] + o(\|\mathbf{A}\|^2)$ as $\|\mathbf{A}\| \to 0$, we have that

$$L_{n,1} = -\frac{n}{2} \log \big(\det(\mathbf{I}_{p-1} + n^{-1/2} \mathbf{L}_n)\big) = \frac{1}{4} \mathrm{tr}[\mathbf{L}_n^2] + o(1) \tag{A.22}$$

as $n \to \infty$ (recall that $\mathrm{tr}[\mathbf{L}_n] = 0$). Now, write

$$\begin{aligned}L_{n,2} &= -\frac{p-1}{2} \sum_{i=1}^n \log \big(1 + \mathbf{U}'_{i,\boldsymbol{\theta}_n} (\mathbf{\Lambda}_n^{-1} - \mathbf{I}_{p-1}) \mathbf{U}_{i,\boldsymbol{\theta}_n}\big) \\ &= -\frac{p-1}{2} \sum_{i=1}^n \log \big(1 + \mathrm{tr}[\mathbf{U}_{i,\boldsymbol{\theta}_n} \mathbf{U}'_{i,\boldsymbol{\theta}_n} (\mathbf{\Lambda}_n^{-1} - \mathbf{I}_{p-1})]\big) \\ &=: -\frac{p-1}{2} \sum_{i=1}^n \log \big(1 + T_{i,n}\big).\end{aligned}$$

Using (9)–(10) in pages 218–219 from Magnus and Neudecker (2007), $T_{i,n} = -n^{-1/2}\mathbf{U}'_{i,\boldsymbol{\theta}_n}\mathbf{L}_n\mathbf{U}_{i,\boldsymbol{\theta}_n} + n^{-1}\mathbf{U}'_{i,\boldsymbol{\theta}_n}\mathbf{L}_n^2\mathbf{U}_{i,\boldsymbol{\theta}_n} + R_{i,n}$, where (due to the uniform boundedness of the $\mathbf{U}_{i,\boldsymbol{\theta}_n}$'s) $\max_{i=1,\ldots,n} R_{i,n} = O_{\mathrm{P}}(n^{-3/2})$ as $n\to\infty$ under $\mathrm{P}^{(n)}_{\boldsymbol{\theta},g}$. Using the fact that $\log(1+x) = x - \frac{1}{2}x^2 + o(x^2)$ as $x\to 0$, it follows that

$$
\begin{aligned}
L_{n,2} &= -\frac{p-1}{2}\sum_{i=1}^n \log\left(1 - \frac{1}{\sqrt{n}}\mathbf{U}'_{i,\boldsymbol{\theta}_n}\mathbf{L}_n\mathbf{U}_{i,\boldsymbol{\theta}_n} + \frac{1}{n}\mathbf{U}'_{i,\boldsymbol{\theta}_n}\mathbf{L}_n^2\mathbf{U}_{i,\boldsymbol{\theta}_n} + R_{i,n}\right)\\
&= -\frac{p-1}{2}\sum_{i=1}^n \left\{ - \frac{1}{\sqrt{n}}\mathbf{U}'_{i,\boldsymbol{\theta}_n}\mathbf{L}_n\mathbf{U}_{i,\boldsymbol{\theta}_n} + \frac{1}{n}\mathbf{U}'_{i,\boldsymbol{\theta}_n}\mathbf{L}_n^2\mathbf{U}_{i,\boldsymbol{\theta}_n} - \frac{1}{2n}(\mathbf{U}'_{i,\boldsymbol{\theta}_n}\mathbf{L}_n\mathbf{U}_{i,\boldsymbol{\theta}_n})^2\right\} + o_{\mathrm{P}}(1)
\end{aligned}
$$

as $n\to\infty$ under $\mathrm{P}^{(n)}_{\boldsymbol{\theta},g}$. Using Lemma B.2, the law of large numbers for triangular arrays then yields

$$
\begin{aligned}
L_{n,2} &= \left(\frac{p-1}{2\sqrt{n}}\sum_{i=1}^n \mathbf{U}'_{i,\boldsymbol{\theta}_n}\mathbf{L}_n\mathbf{U}_{i,\boldsymbol{\theta}_n}\right) - \frac{p-1}{2}\,\mathrm{E}\Big[\mathbf{U}'_{1,\boldsymbol{\theta}_n}\mathbf{L}_n^2\mathbf{U}_{1,\boldsymbol{\theta}_n} - \frac{1}{2}(\mathbf{U}'_{1,\boldsymbol{\theta}_n}\mathbf{L}_n\mathbf{U}_{1,\boldsymbol{\theta}_n})^2\Big] + o_{\mathrm{P}}(1)\\
&= \frac{p-1}{2\sqrt{n}}(\operatorname{vec}\mathbf{L}_n)'\sum_{i=1}^n \operatorname{vec}(\mathbf{U}_{i,\boldsymbol{\theta}_n}\mathbf{U}'_{i,\boldsymbol{\theta}_n})\\
&\quad - \frac{p-1}{2}(\operatorname{vec}\mathbf{L}_n)'\left[\frac{1}{p-1}\mathbf{I}_{(p-1)^2} - \frac{1}{2(p^2-1)}(\mathbf{I}_{(p-1)^2} + \mathbf{K}_{p-1} + \mathbf{J}_{p-1})\right](\operatorname{vec}\mathbf{L}_n) + o_{\mathrm{P}}(1)
\end{aligned}
$$

as $n\to\infty$ under $\mathrm{P}^{(n)}_{\boldsymbol{\theta},g}$. Applying Lemma $(iii_{\mathcal{TE}})$ in B.4, and using the identities $\mathbf{K}_{p-1}(\operatorname{vec}\mathbf{A}) = \operatorname{vec}(\mathbf{A}')$ and $(\operatorname{vec}\mathbf{A})'(\operatorname{vec}\mathbf{B}) = \mathrm{tr}[\mathbf{A}'\mathbf{B}]$ (which implies that $(\operatorname{vec}\mathbf{L}_n)'(\operatorname{vec}\mathbf{I}_{p-1}) = \mathrm{tr}[\mathbf{L}_n] = 0$, hence that $\mathbf{J}_{p-1}(\operatorname{vec}\mathbf{L}_n) = \mathbf{0}$), we obtain

$$
L_{n,2} = \frac{p-1}{2\sqrt{n}}(\operatorname{vec}\mathbf{L}_n)'\sum_{i=1}^n \operatorname{vec}\left(\mathbf{U}_{i,\boldsymbol{\theta}}\mathbf{U}'_{i,\boldsymbol{\theta}} - \frac{1}{p-1}\mathbf{I}_{p-1}\right) - \frac{p}{2(p+1)}\mathrm{tr}[\mathbf{L}_n^2] + o_{\mathrm{P}}(1) \tag{A.23}
$$

as $n\to\infty$ under $\mathrm{P}^{(n)}_{\boldsymbol{\theta},g}$. Plugging (A.22)–(A.23) in (A.21) then provides

$$
L_n = \frac{p-1}{2\sqrt{n}}(\operatorname{vec}\mathbf{L}_n)'\sum_{i=1}^n \operatorname{vec}\left(\mathbf{U}_{i,\boldsymbol{\theta}}\mathbf{U}'_{i,\boldsymbol{\theta}} - \frac{1}{p-1}\mathbf{I}_{p-1}\right) - \frac{p-1}{4(p+1)}\mathrm{tr}[\mathbf{L}_n^2] + o_{\mathrm{P}}(1),
$$

as $n\to\infty$ under $\mathrm{P}^{(n)}_{\boldsymbol{\theta},g}$, which, by using the definition of $\mathbf{M}_p$ and the matrix identities above, yields (2.7). Finally, the CLT ensures that, under $\mathrm{P}^{(n)}_{\boldsymbol{\theta},g}$, $\boldsymbol{\Delta}^{\mathcal{TE}(n)}_{\boldsymbol{\theta};2} \overset{\mathcal{D}}{\rightsquigarrow} \mathcal{N}\big(\mathbf{0},\boldsymbol{\Gamma}^{\mathcal{TE}}_{\boldsymbol{\theta};22}\big)$ with

$$
\mathbf{M}_p\left(\frac{p-1}{4(p+1)}(\mathbf{I}_{(p-1)^2} + \mathbf{K}_{p-1} + \mathbf{J}_{p-1}) - \frac{1}{4}\mathbf{J}_{p-1}\right)\mathbf{M}'_p = \frac{p-1}{4(p+1)}\mathbf{M}_p\big(\mathbf{I}_{(p-1)^2} + \mathbf{K}_{p-1}\big)\mathbf{M}'_p = \boldsymbol{\Gamma}^{\mathcal{TE}}_{\boldsymbol{\theta};22},
$$

where we used the fact that $\mathbf{M}_p(\operatorname{vec}\mathbf{I}_{p-1}) = 0$ (see (v) in Lemma 4.2 of Paindaveine (2008)). □

Proof (Theorem 2.4). First note that

$$
\log\frac{d\mathrm{P}^{\mathcal{TM}(n)}_{\boldsymbol{\theta}_n,g,\boldsymbol{\delta}_n}}{d\mathrm{P}^{(n)}_{\boldsymbol{\theta},g}} = \log\frac{d\mathrm{P}^{\mathcal{TM}(n)}_{\boldsymbol{\theta}_n,g,\boldsymbol{\delta}_n}}{d\mathrm{P}^{(n)}_{\boldsymbol{\theta}_n,g}} + \log\frac{d\mathrm{P}^{(n)}_{\boldsymbol{\theta}_n,g}}{d\mathrm{P}^{(n)}_{\boldsymbol{\theta},g}} = \log\frac{d\mathrm{P}^{\mathcal{TM}(n)}_{\boldsymbol{\theta}_n,g,\boldsymbol{\delta}_n}}{d\mathrm{P}^{(n)}_{\boldsymbol{\theta}_n,g}} + \mathbf{t}'_n\boldsymbol{\Delta}^{(n)}_{\boldsymbol{\theta},g;1} - \frac{1}{2}\mathbf{t}'_n\boldsymbol{\Gamma}_{\boldsymbol{\theta},g;11}\mathbf{t}_n + o_{\mathrm{P}}(1).
$$

In the parametrization adopted in Theorem 2.4, recall that $\boldsymbol{\delta}_n$ corresponds to a skewness direction $\boldsymbol{\mu}_n := \boldsymbol{\delta}_n/\|\boldsymbol{\delta}_n\| = \mathbf{d}_n/\|\mathbf{d}_n\|$ and a skewness intensity $\kappa_n := \|\boldsymbol{\delta}_n\| = n^{-1/2}\|\mathbf{d}_n\|$. From Theorem 2.2, we then readily obtain

$$
G_n := \log\frac{d\mathrm{P}^{\mathcal{TM}(n)}_{\boldsymbol{\theta}_n,g,\boldsymbol{\delta}_n}}{d\mathrm{P}^{(n)}_{\boldsymbol{\theta}_n,g}} = n\big(\log(c_{p-1,n^{-1/2}\|\mathbf{d}^{(n)}\|}) - \log(c_{p-1,0})\big) + \big(\mathbf{d}^{(n)}\big)'\frac{1}{\sqrt{n}}\sum_{i=1}^n \mathbf{U}_{i,\boldsymbol{\theta}_n}.
$$

Lemma A.1 in Cutting et al. (2017) implies that

$$n\big(\log(c_{p-1,n^{-1/2}\|\mathbf{d}^{(n)}\|}) - \log(c_{p-1,0})\big) = -\frac{1}{2(p-1)}\,\|\mathbf{d}^{(n)}\|^2 + o(1)$$

as $n\to\infty$, which, by using $(iii_{\mathcal{TM}})$ in Lemma B.4, yields

$$\begin{aligned} G_n &= (\mathbf{d}^{(n)})'\frac{1}{\sqrt{n}}\sum_{i=1}^n \mathbf{U}_{i,\boldsymbol{\theta}_n} - \frac{1}{2(p-1)}\,\|\mathbf{d}^{(n)}\|^2 + o_{\mathrm{P}}(1)\\ &= (\mathbf{d}^{(n)})'\bigg[\frac{1}{\sqrt{n}}\sum_{i=1}^n \mathbf{U}_{i,\boldsymbol{\theta}} - \frac{\mathcal{I}_p(g)}{p-1}\boldsymbol{\Gamma}'_{\boldsymbol{\theta}}\mathbf{t}_n\bigg] - \frac{1}{2(p-1)}\,\|\mathbf{d}^{(n)}\|^2 + o_{\mathrm{P}}(1)\end{aligned}$$

as $n\to\infty$ under $\mathrm{P}^{(n)}_{\boldsymbol{\theta},g}$. Therefore,

$$\begin{aligned}\log\frac{d\mathrm{P}^{\mathcal{TM}(n)}_{\boldsymbol{\theta}_n,g,\boldsymbol{\delta}_n}}{d\mathrm{P}^{(n)}_{\boldsymbol{\theta},g}} =&\, \mathbf{t}'_n\boldsymbol{\Delta}^{(n)}_{1,\boldsymbol{\theta}} + (\mathbf{d}^{(n)})'\frac{1}{\sqrt{n}}\sum_{i=1}^n \mathbf{U}_{i,\boldsymbol{\theta}}\\ &- \frac{1}{2}\bigg(\mathbf{t}'_n\boldsymbol{\Gamma}_{\boldsymbol{\theta},g;11}\mathbf{t}_n + \frac{2\mathcal{I}_p(g)}{p-1}(\mathbf{d}^{(n)})'\boldsymbol{\Gamma}'_{\boldsymbol{\theta}}\mathbf{t}_n + \frac{1}{p-1}\,\|\mathbf{d}^{(n)}\|^2\bigg) + o_{\mathrm{P}}(1),\end{aligned}$$

as $n\to\infty$ under $\mathrm{P}^{(n)}_{\boldsymbol{\theta},g}$, which establishes the result. □

B. Required lemmas

Lemma B.1. *For any $\boldsymbol{\theta}\in\mathcal{S}^{p-1}$ and $g\in\mathcal{G}$, under $\mathrm{P}^{(n)}_{\boldsymbol{\theta},g}$:*

(i) $\mathrm{E}[\mathbf{U}_{1,\boldsymbol{\theta}}] = \mathbf{0}$,

(ii) $\mathrm{E}[\mathbf{U}_{1,\boldsymbol{\theta}}\mathbf{U}'_{1,\boldsymbol{\theta}}] = \frac{1}{p-1}\mathbf{I}_{p-1}$,

(iii) $\mathrm{E}[\mathrm{vec}\,(\mathbf{U}_{1,\boldsymbol{\theta}}\mathbf{U}'_{1,\boldsymbol{\theta}})\mathrm{vec}\,(\mathbf{U}_{1,\boldsymbol{\theta}}\mathbf{U}'_{1,\boldsymbol{\theta}})'] = \frac{1}{p^2-1}\big(\mathbf{I}_{(p-1)^2} + \mathbf{K}_{p-1} + \mathbf{J}_{p-1}\big)$.

Proof (Lemma B.1). The result is a direct consequence of Lemma A.2 in Paindaveine and Verdebout (2016). □

Lemma B.2. *For any $\boldsymbol{\theta}\in\mathcal{S}^{p-1}$, $g\in\mathcal{G}$, and any bounded sequence $(\mathbf{t}_n)$ in $\mathbb{R}^p$ such that $\boldsymbol{\theta}_n = \boldsymbol{\theta} + n^{-1/2}\mathbf{t}_n\in\mathcal{S}^{p-1}$ for any n, we have that, as $n\to\infty$ under $\mathrm{P}^{(n)}_{\boldsymbol{\theta},g}$:*

(i) $\mathrm{E}[\mathbf{U}_{1,\boldsymbol{\theta}_n}] = o(1)$,

(ii) $\mathrm{E}[\mathbf{U}_{1,\boldsymbol{\theta}_n}\mathbf{U}'_{1,\boldsymbol{\theta}_n}] = \frac{1}{p-1}\mathbf{I}_{p-1} + o(1)$,

(iii) $\mathrm{E}[\mathrm{vec}\,(\mathbf{U}_{1,\boldsymbol{\theta}_n}\mathbf{U}'_{1,\boldsymbol{\theta}_n})\mathrm{vec}\,(\mathbf{U}_{1,\boldsymbol{\theta}_n}\mathbf{U}'_{1,\boldsymbol{\theta}_n})'] = \frac{1}{p^2-1}\left(\mathbf{I}_{(p-1)^2} + \mathbf{K}_{p-1} + \mathbf{J}_{p-1}\right) + o(1)$.

Proof (Lemma B.2). All expectations in this proof are under $\mathrm{P}^{(n)}_{\boldsymbol{\theta},g}$ and all convergences are as $n\to\infty$. For *(i)* first note that, letting $\mathbf{Z}_{1,\boldsymbol{\theta}} := \boldsymbol{\Gamma}'_{\boldsymbol{\theta}}\mathbf{X}_1$ and $d_{1,\boldsymbol{\theta}} := \|\mathbf{Z}_{1,\boldsymbol{\theta}}\|$, we have

$$\begin{aligned}\|\mathbf{U}_{1,\boldsymbol{\theta}_n} - \mathbf{U}_{1,\boldsymbol{\theta}}\| &\le \left\|\frac{\mathbf{Z}_{1,\boldsymbol{\theta}_n}}{d_{1,\boldsymbol{\theta}_n}} - \frac{\mathbf{Z}_{1,\boldsymbol{\theta}_n}}{d_{1,\boldsymbol{\theta}}}\right\| + \left\|\frac{\mathbf{Z}_{1,\boldsymbol{\theta}_n}}{d_{1,\boldsymbol{\theta}}} - \frac{\mathbf{Z}_{1,\boldsymbol{\theta}}}{d_{1,\boldsymbol{\theta}}}\right\|\\ &\le \left|\frac{1}{d_{1,\boldsymbol{\theta}_n}} - \frac{1}{d_{1,\boldsymbol{\theta}}}\right|\|\mathbf{Z}_{1,\boldsymbol{\theta}_n}\| + \frac{1}{d_{1,\boldsymbol{\theta}}}\,\|\mathbf{Z}_{1,\boldsymbol{\theta}_n} - \mathbf{Z}_{1,\boldsymbol{\theta}}\|\\ &\le \frac{|d_{1,\boldsymbol{\theta}_n} - d_{1,\boldsymbol{\theta}}|}{d_{1,\boldsymbol{\theta}}} + \frac{1}{d_{1,\boldsymbol{\theta}}}\,\|\mathbf{Z}_{1,\boldsymbol{\theta}_n} - \mathbf{Z}_{1,\boldsymbol{\theta}}\|\\ &\le \frac{2\|\mathbf{Z}_{1,\boldsymbol{\theta}_n} - \mathbf{Z}_{1,\boldsymbol{\theta}}\|}{d_{1,\boldsymbol{\theta}}},\end{aligned}$$

which implies that $\|\mathbf{U}_{1,\boldsymbol{\theta}_n} - \mathbf{U}_{1,\boldsymbol{\theta}}\| = o_{\mathrm{P}}(1)$. Uniform integrability follows because $\|\mathbf{U}_{1,\boldsymbol{\theta}_n} - \mathbf{U}_{1,\boldsymbol{\theta}}\| \leq 2$ almost surely, hence

$$\mathrm{E}[\|\mathbf{U}_{1,\boldsymbol{\theta}_n} - \mathbf{U}_{1,\boldsymbol{\theta}}\|^2] = o(1). \tag{B.24}$$

Since $\|\mathrm{E}[\mathbf{U}_{1,\boldsymbol{\theta}_n}]\|^2 = \|\mathrm{E}[\mathbf{U}_{1,\boldsymbol{\theta}_n} - \mathbf{U}_{1,\boldsymbol{\theta}}]\|^2 \leq \big(\mathrm{E}[\|\mathbf{U}_{1,\boldsymbol{\theta}_n} - \mathbf{U}_{1,\boldsymbol{\theta}}\|]\big)^2 \leq \mathrm{E}[\|\mathbf{U}_{1,\boldsymbol{\theta}_n} - \mathbf{U}_{1,\boldsymbol{\theta}}\|^2]$, the result then follows from *(i)* in Lemma B.1. For proving *(ii)*, we have that, since *(ii)* in Lemma B.1 entails that

$$\left\|\mathrm{vec}\left(\mathrm{E}[\mathbf{U}_{1,\boldsymbol{\theta}_n}\mathbf{U}'_{1,\boldsymbol{\theta}_n}] - \frac{1}{p-1}\mathbf{I}_{p-1}\right)\right\|^2 = \big\|\mathrm{E}[\mathrm{vec}\,(\mathbf{U}_{1,\boldsymbol{\theta}_n}\mathbf{U}'_{1,\boldsymbol{\theta}_n}) - \mathrm{vec}\,(\mathbf{U}_{1,\boldsymbol{\theta}}\mathbf{U}'_{1,\boldsymbol{\theta}})]\big\|^2,$$

it is enough to show that

$$\mathrm{E}[\|\mathrm{vec}\,(\mathbf{U}_{1,\boldsymbol{\theta}_n}\mathbf{U}'_{1,\boldsymbol{\theta}_n}) - \mathrm{vec}\,(\mathbf{U}_{1,\boldsymbol{\theta}}\mathbf{U}'_{1,\boldsymbol{\theta}})\|^2] = o(1). \tag{B.25}$$

This follows from (B.24), the fact that $\|\mathrm{vec}(\mathbf{U}_{1,\boldsymbol{\theta}_n}\mathbf{U}'_{1,\boldsymbol{\theta}_n}) - \mathrm{vec}(\mathbf{U}_{1,\boldsymbol{\theta}}\mathbf{U}'_{1,\boldsymbol{\theta}})\|^2 = \mathrm{tr}[(\mathbf{U}_{1,\boldsymbol{\theta}_n}\mathbf{U}'_{1,\boldsymbol{\theta}_n} - \mathbf{U}_{1,\boldsymbol{\theta}}\mathbf{U}'_{1,\boldsymbol{\theta}})^2] = 2(1 - (\mathbf{U}'_{1,\boldsymbol{\theta}_n}\mathbf{U}_{1,\boldsymbol{\theta}})^2) = \|\mathbf{U}_{1,\boldsymbol{\theta}_n} - \mathbf{U}_{1,\boldsymbol{\theta}}\|^2$, and the arguments in the proof of *(i)*. For *(iii)*, we proceed as above and use that *(iii)* in Lemma B.1 entails that it is sufficient to show that

$$w_n := \mathrm{E}[\|\mathrm{vec}\,(\mathbf{U}_{1,\boldsymbol{\theta}_n}\mathbf{U}'_{1,\boldsymbol{\theta}_n})\mathrm{vec}\,(\mathbf{U}_{1,\boldsymbol{\theta}_n}\mathbf{U}'_{1,\boldsymbol{\theta}_n})' - \mathrm{vec}\,(\mathbf{U}_{1,\boldsymbol{\theta}}\mathbf{U}'_{1,\boldsymbol{\theta}})\mathrm{vec}\,(\mathbf{U}_{1,\boldsymbol{\theta}}\mathbf{U}'_{1,\boldsymbol{\theta}})'\|^2] = o(1).$$

Since $w_n \leq 2(w_{1n} + w_{2n})$, with

$$\begin{aligned} w_{1n} &:= \mathrm{E}[\|(\mathrm{vec}\,(\mathbf{U}_{1,\boldsymbol{\theta}_n}\mathbf{U}'_{1,\boldsymbol{\theta}_n}) - \mathrm{vec}\,(\mathbf{U}_{1,\boldsymbol{\theta}}\mathbf{U}'_{1,\boldsymbol{\theta}}))\mathrm{vec}\,(\mathbf{U}_{1,\boldsymbol{\theta}_n}\mathbf{U}'_{1,\boldsymbol{\theta}_n})'\|^2], \\ w_{2n} &:= \mathrm{E}[\|\mathrm{vec}\,(\mathbf{U}_{1,\boldsymbol{\theta}}\mathbf{U}'_{1,\boldsymbol{\theta}})(\mathrm{vec}\,(\mathbf{U}_{1,\boldsymbol{\theta}_n}\mathbf{U}'_{1,\boldsymbol{\theta}_n}) - \mathrm{vec}\,(\mathbf{U}_{1,\boldsymbol{\theta}}\mathbf{U}'_{1,\boldsymbol{\theta}})')\|^2], \end{aligned}$$

and since $\mathbf{U}_{1,\boldsymbol{\theta}_n}$ and $\mathbf{U}_{1,\boldsymbol{\theta}}$ are bounded almost surely, the result follows from (B.25). □

LEMMA B.3. *Fix $\boldsymbol{\theta} \in \mathcal{S}^{p-1}$, $g \in \mathcal{G}_a$, and let $(\mathbf{t}_n)$ be a bounded sequence in $\mathbb{R}^p$ such that $\boldsymbol{\theta}_n := \boldsymbol{\theta} + n^{-1/2}\mathbf{t}_n \in \mathcal{S}^{p-1}$ for any n. Then,*

$$\log \frac{d\mathrm{P}^{(n)}_{\boldsymbol{\theta}_n,g}}{d\mathrm{P}^{(n)}_{\boldsymbol{\theta},g}} = \mathbf{t}'_n\boldsymbol{\Delta}^{(n)}_{\boldsymbol{\theta},g;1} - \frac{1}{2}\mathbf{t}'_n\boldsymbol{\Gamma}_{\boldsymbol{\theta},g;11}\mathbf{t}_n + o_{\mathrm{P}}(1),$$

as $n \to \infty$ under $\mathrm{P}^{(n)}_{\boldsymbol{\theta},g}$, where $\boldsymbol{\Delta}^{(n)}_{\boldsymbol{\theta},g;1}$ and $\boldsymbol{\Gamma}_{\boldsymbol{\theta},g;11}$ are as in Theorems 2.3 and 2.4.

PROOF (LEMMA B.3). This follows from Proposition 2.2 in Ley et al. (2013). □

LEMMA B.4. *For any $\boldsymbol{\theta} \in \mathcal{S}^{p-1}$, $g \in \mathcal{G}_a$, and any bounded sequence $(\mathbf{t}_n)$ in $\mathbb{R}^p$ such that $\boldsymbol{\theta}_n := \boldsymbol{\theta} + n^{-1/2}\mathbf{t}_n \in \mathcal{S}^{p-1}$ for any n, we have that, as $n \to \infty$ under $\mathrm{P}^{(n)}_{\boldsymbol{\theta},g}$:*

$(i_{\mathcal{TM}})$ $\frac{1}{\sqrt{n}}\sum_{i=1}^n \Big(\mathbf{U}_{i,\boldsymbol{\theta}_n} - \mathbf{U}_{i,\boldsymbol{\theta}} - \mathrm{E}[\mathbf{U}_{i,\boldsymbol{\theta}_n}]\Big) = o_{\mathrm{P}}(1)$,

$(ii_{\mathcal{TM}})$ $\frac{1}{\sqrt{n}}\sum_{i=1}^n \mathrm{E}[\mathbf{U}_{i,\boldsymbol{\theta}_n}] = -\frac{\mathcal{I}_p(g)}{p-1}\boldsymbol{\Gamma}'_{\boldsymbol{\theta}}\mathbf{t}_n + o(1)$,

$(iii_{\mathcal{TM}})$ $\frac{1}{\sqrt{n}}\sum_{i=1}^n (\mathbf{U}_{i,\boldsymbol{\theta}_n} - \mathbf{U}_{i,\boldsymbol{\theta}}) = -\frac{\mathcal{I}_p(g)}{p-1}\boldsymbol{\Gamma}'_{\boldsymbol{\theta}}\mathbf{t}_n + o_{\mathrm{P}}(1)$,

$(i_{\mathcal{TE}})$ $\frac{1}{\sqrt{n}}\sum_{i=1}^n \Big(\mathbf{U}_{i,\boldsymbol{\theta}_n}\mathbf{U}'_{i,\boldsymbol{\theta}_n} - \mathbf{U}_{i,\boldsymbol{\theta}}\mathbf{U}'_{i,\boldsymbol{\theta}} - \mathrm{E}[\mathbf{U}_{i,\boldsymbol{\theta}_n}\mathbf{U}'_{i,\boldsymbol{\theta}_n}] + \frac{1}{p-1}\mathbf{I}_{p-1}\Big) = o_{\mathrm{P}}(1)$,

$(ii_{\mathcal{TE}})$ $\frac{1}{\sqrt{n}}\sum_{i=1}^n \Big(\mathrm{E}[\mathbf{U}_{i,\boldsymbol{\theta}_n}\mathbf{U}'_{i,\boldsymbol{\theta}_n}] - \frac{1}{p-1}\mathbf{I}_{p-1}\Big) = o(1)$,

$(iii_{\mathcal{TE}})$ $\frac{1}{\sqrt{n}}\sum_{i=1}^n \big(\mathbf{U}_{i,\boldsymbol{\theta}_n}\mathbf{U}'_{i,\boldsymbol{\theta}_n} - \mathbf{U}_{i,\boldsymbol{\theta}}\mathbf{U}'_{i,\boldsymbol{\theta}}\big) = o_{\rm P}(1)$.

Proof (Lemma B.4). Throughout this proof, expectations are under $\mathrm{P}^{(n)}_{\boldsymbol{\theta},g}$, convergences are as $n \to \infty$, and superscript $\mathcal{T}$ stands for "$\mathcal{TM}$ (respectively, $\mathcal{TE}$)". For $(i_{\mathcal{TM}})$–$(i_{\mathcal{TE}})$, let $\mathbf{N}^{\mathcal{TM}}_{i,n} := \mathbf{U}_{i,\boldsymbol{\theta}_n} - \mathbf{U}_{i,\boldsymbol{\theta}}$ and $\mathbf{N}^{\mathcal{TE}}_{i,n} := \mathrm{vec}(\mathbf{U}_{i,\boldsymbol{\theta}_n}\mathbf{U}'_{i,\boldsymbol{\theta}_n}) - \mathrm{vec}(\mathbf{U}_{i,\boldsymbol{\theta}}\mathbf{U}'_{i,\boldsymbol{\theta}})$. We have to show that

$$\mathbf{T}^{\mathcal{T}}_n = n^{-1/2}\sum_{i=1}^n (\mathbf{N}^{\mathcal{T}}_{i,n} - \mathrm{E}[\mathbf{N}^{\mathcal{T}}_{i,n}]) = o_{\rm P}(1).$$

Since $\mathrm{E}[\|\mathbf{T}^{\mathcal{T}}_n\|^2] = n^{-1}\sum_{i,j=1}^n \mathrm{E}[(\mathbf{N}^{\mathcal{T}}_{i,n} - \mathrm{E}[\mathbf{N}^{\mathcal{T}}_{i,n}])'(\mathbf{N}^{\mathcal{T}}_{jn} - \mathrm{E}[\mathbf{N}^{\mathcal{T}}_{jn}])] = \mathrm{E}[\|\mathbf{N}^{\mathcal{T}}_{1n} - \mathrm{E}[\mathbf{N}^{\mathcal{T}}_{1n}]\|^2] \leq \mathrm{E}[\|\mathbf{N}^{\mathcal{T}}_{1n}\|^2]$, the result follows from (B.24) for $\mathcal{TM}$, and from (B.25) for $\mathcal{TE}$. For $(ii_{\mathcal{TM}})$–$(ii_{\mathcal{TE}})$, we consider

$$\mathbf{S}^{\mathcal{TM}(n)}_{\boldsymbol{\theta}} := \frac{1}{\sqrt{n}}\sum_{i=1}^n \mathbf{U}_{i,\boldsymbol{\theta}} \quad \text{and} \quad \mathbf{S}^{\mathcal{TE}(n)}_{\boldsymbol{\theta}} := \frac{1}{\sqrt{n}}\sum_{i=1}^n \mathrm{vec}\left(\mathbf{U}_{i,\boldsymbol{\theta}}\mathbf{U}'_{i,\boldsymbol{\theta}} - \frac{1}{p-1}\mathbf{I}_{p-1}\right).$$

By using Lemma B.1, the CLT for triangular arrays implies that, under $\mathrm{P}^{(n)}_{\boldsymbol{\theta}_n,g}$,

$$\begin{pmatrix} \mathbf{S}^{\mathcal{T}(n)}_{\boldsymbol{\theta}} \\ \boldsymbol{\Delta}^{(n)}_{\boldsymbol{\theta}_n,g;1} \end{pmatrix} \overset{\mathcal{D}}{\rightsquigarrow} \mathcal{N}\left(\mathbf{0}, \begin{pmatrix} \boldsymbol{\Sigma}^{\mathcal{T}} & (\mathbf{C}^{\mathcal{T}}_{\boldsymbol{\theta}})' \\ \mathbf{C}^{\mathcal{T}}_{\boldsymbol{\theta}} & \boldsymbol{\Gamma}_{\boldsymbol{\theta},g;11} \end{pmatrix}\right), \tag{B.26}$$

where $\mathbf{C}^{\mathcal{TM}}_{\boldsymbol{\theta}} = \frac{\mathcal{I}_p(g)}{p-1}\boldsymbol{\Gamma}_{\boldsymbol{\theta}}$, $\mathbf{C}^{\mathcal{TE}}_{\boldsymbol{\theta}} = \mathbf{0}$, $\boldsymbol{\Sigma}^{\mathcal{TM}} := \frac{1}{p-1}\mathbf{I}_{p-1}$, and

$$\boldsymbol{\Sigma}^{\mathcal{TE}} := \frac{1}{p^2-1}\left(\mathbf{I}_{(p-1)^2} + \mathbf{K}_{p-1} + \mathbf{J}_{p-1}\right) - \frac{1}{(p-1)^2}\mathbf{J}_{p-1}.$$

By using Lemma B.3, Le Cam's first lemma implies that $\mathrm{P}^{(n)}_{\boldsymbol{\theta}_n,g}$ and $\mathrm{P}^{(n)}_{\boldsymbol{\theta},g}$ are mutually contiguous. Therefore, one can apply Le Cam's third lemma to the joint asymptotic normality results in (B.26), which yields that, under $\mathrm{P}^{(n)}_{\boldsymbol{\theta},g}$,

$$\frac{1}{\sqrt{n}}\sum_{i=1}^n \mathbf{U}_{i,\boldsymbol{\theta}_n} + \frac{\mathcal{I}_p(g)}{p-1}\boldsymbol{\Gamma}'_{\boldsymbol{\theta}}\mathbf{t}_n = \mathbf{S}^{\mathcal{TM}(n)}_{\boldsymbol{\theta}_n} + (\mathbf{C}^{\mathcal{TM}}_{\boldsymbol{\theta}})'\mathbf{t}_n \overset{\mathcal{D}}{\rightsquigarrow} \mathcal{N}\big(\mathbf{0}, \boldsymbol{\Sigma}^{\mathcal{TM}}\big) \tag{B.27}$$

and

$$\frac{1}{\sqrt{n}}\sum_{i=1}^n \mathrm{vec}\left(\mathbf{U}_{i,\boldsymbol{\theta}_n}\mathbf{U}'_{i,\boldsymbol{\theta}_n} - \frac{1}{p-1}\mathbf{I}_{p-1}\right) = \mathbf{S}^{\mathcal{TE}(n)}_{\boldsymbol{\theta}_n} + (\mathbf{C}^{\mathcal{TE}}_{\boldsymbol{\theta}})'\mathbf{t}_n \overset{\mathcal{D}}{\rightsquigarrow} \mathcal{N}\big(\mathbf{0}, \boldsymbol{\Sigma}^{\mathcal{TE}}\big). \tag{B.28}$$

Now, by using Lemma B.2, the CLT for triangular arrays shows that, still under $\mathrm{P}^{(n)}_{\boldsymbol{\theta},g}$,

$$\frac{1}{\sqrt{n}}\sum_{i=1}^n (\mathbf{U}_{i,\boldsymbol{\theta}_n} - \mathrm{E}[\mathbf{U}_{i,\boldsymbol{\theta}_n}]) \overset{\mathcal{D}}{\rightsquigarrow} \mathcal{N}\big(\mathbf{0}, \boldsymbol{\Sigma}^{\mathcal{TM}}\big), \tag{B.29}$$

and

$$\frac{1}{\sqrt{n}}\sum_{i=1}^n \mathrm{vec}\left(\mathbf{U}_{i,\boldsymbol{\theta}_n}\mathbf{U}'_{i,\boldsymbol{\theta}_n} - \mathrm{E}[\mathbf{U}_{i,\boldsymbol{\theta}_n}\mathbf{U}'_{i,\boldsymbol{\theta}_n}]\right) \overset{\mathcal{D}}{\rightsquigarrow} \mathcal{N}\big(\mathbf{0}, \boldsymbol{\Sigma}^{\mathcal{TE}}\big), \tag{B.30}$$

where the expectations are under $\mathrm{P}^{(n)}_{\boldsymbol{\theta},g}$. The result $(ii_{\mathcal{TM}})$ then follows from (B.27) and (B.29), whereas $(ii_{\mathcal{TE}})$ similarly follows from (B.28) and (B.30). Finally, $(iii_{\mathcal{TM}})$–$(iii_{\mathcal{TE}})$ are a direct consequence of $(i_{\mathcal{TM}})$–$(i_{\mathcal{TE}})$ and $(ii_{\mathcal{TM}})$–$(ii_{\mathcal{TE}})$. $\square$